SEISMIC SEQUENCE STRATIGRAPHY DURING THE CRETACEOUS THROUGH THE EARLY PALEOGENE IN THE NORTHERN SCOTIAN BASIN (LAURENTIAN SUBBASIN), OFFSHORE NOVA SCOTIA AND NEWFOUNDLAND, CANADA

By

IKA SULISTYANINGRUM

A thesis submitted to the

Graduate School-New Brunswick

Rutgers, The State University of New Jersey

in partial fulfillment of the requirements

for the degree of

Master of Science

Graduate Program in Geological Sciences

written under the direction of

Dr. Martha Oliver Withjack

and approved by

_____

_____

_____

New Brunswick, New Jersey

January, 2010

ABSTRACT OF THE THESIS

SEISMIC SEQUENCE STRATIGRAPHY DURING THE CRETACEOUS THROUGH THE EARLY PALEOGENE IN THE NORTHERN SCOTIAN BASIN (LAURENTIAN SUBBASIN), OFFSHORE NOVA SCOTIA AND NEWFOUNDLAND, CANADA

By IKA SULISTYANINGRUM

Thesis Director:

Dr. Martha Oliver Withjack

This thesis uses seismic-sequence-stratigraphic analysis to show the stratigraphic development of the northern Nova Scotia passive margin (the Laurentian Subbasin) during the Cretaceous through Paleogene. It documents the interplay of several variables on margin evolution including changes in relative sea-level, sediment supply, and tectonic activity including thermoflexural subsidence and salt movement. Salt structures, basement-involved deformation, and sparse well control impede the interpretation of stratigraphic patterns in the study area. Despite these difficulties, I have identified eight candidate sequence boundaries using seismic-reflection terminations: (1) top-lap and truncation below a discontinuity, and (2) on-lap and down-lap above a discontinuity.

Study of the sequence stratigraphy in the Laurentian Subbasin reveals two significant unconformities, the Jurassic-Cretaceous (Avalon) unconformity and the Cretaceous-Paleogene (KP) unconformity, and seven sequences: three Cretaceous

sequences (Sequences 1, 2, and 3) and four Paleogene sequences (Sequences 4, 5, 6 and 7). Change in relative sea level and sediment-supply directions during the Cretaceous are not well documented. Salt tectonics and thermoflexural subsidence created the accommodation space for the Early Cretaceous sequences. System tracts controlled by relative sea-level change show that sediment supply was from the northwest and depocenters migrated from northeast to southeast during the Paleogene.

Comparison of the Baltimore Canyon Trough with the Laurentian Subbasin shows that these basins in the passive margin of eastern North America have similarities and differences. The similarity includes the presence of clinoform geometries above the KP boundary indicating aggradational-progradational stratigraphic patterns. The differences include the major Jurassic-Cretaceous (JK) unconformity, the presence of salt structures, and the presence of Paleogene sequences. In the Scotian Basin, the JK unconformity is a major angular unconformity (Avalon unconformity) separating gently dipping Cretaceous rocks above from folded Jurassic rocks below. However, the JK unconformity in the Baltimore Canyon Trough generally is a paraconformity separating subparallel beds above and below the unconformity.

ACKNOWLEDGMENTS

First and foremost I would like to thank to my lovely husband, Lutfi Hanafi Dwi Nugroho, for your prayers and continuous support during my school in Rutgers University. His positive support and love allowed the completion of this puzzle of our life.

I would like to thank the Canadian government and TGS/Nopec that provided moderate-to-high seismic resolution 2D seismic data of offshore Nova Scotia, southern Newfoundland, and the French territory of St. Pierre and Miquelon for this research.

Special thank are to my advisor Martha Withjack for countless hours of mentoring and discussion for everything. I would also like to thank Gregory Mountain and Don Montevarde (My adopted father), whose comments and eager assistance. My former colleagues from the Geology Department, I want to thank them for all their help, support, interest and valuable hints. Especially, I am obliged to Triyani (my younger sister), Abang Zulfitriadi, and Hendra.

Table of Contents

	Page
Title page	i
Abstract	ii
Acknowledgements	iv
Table of Contents	v
List of Tables	viii
List of Figures	ix
List of Appendices	xii
I. Introduction	1
II. Background	
II.1. Sequence Stratigraphy	2
II.2. Seismic Stratigraphy	3
II.3. Regional Geologic Setting	5
III. Methods	
III.1. Data Preparation	7
III.2. Data Interpretation and Analysis	8
IV. Observations	
IV.1. Horizon	10
Horizon N1 (Avalon unconformity)	11
Horizon N2	11
Horizon N3	11
Horizon N4 (KP boundary)	12

Horizon N5 12

Horizon N6 12

Horizon N7 13

Horizon N8 13

IV.II. Sequence Stratigraphy 13

Sequence-1 13

Sequence-2 14

Sequence-3 14

Sequence-4 14

Sequence-5 15

Sequence-6 15

Sequence-7 15

V. Interpretation

V.I. Cretaceous Sequences 17

Sequence-1 (Early Cretaceous) 17

Sequence-2 (early Late Cretaceous/Cenomanian) 18

Sequence-3 (Late Cretaceous/Turonian-Maastrichtian) 19

V.II. Paleogene Sequences 20

Sequence-4 (Early Paleocene) 20

Sequence-5 (Middle Paleocene) 21

Sequence-6 (Late Paleocene) 22

Sequence-7 (Early Eocene) 23

VI. Discussion

VI .1. Sediment supply 24

VI .2. Accommodation space 25

VI .3. Relative sea-level 26

VI .4. Sequence stratigraphy on the passive margins; Nova Scotia passive margin (Laurentian Subbasin) and New Jersey passive margin (Baltimore Canyon Trough) 27

V11. Conclusions 30

References 32

Tables Captions 37

Figures Captions 40

Appendices Captions

LIST OF TABLES

Table	Page
1. Seismic Terminations	37
2. Horizons	38
3. Sequence Stratigraphy	39

LIST OF TABLES

Table	Page
1. Seismic Terminations	37
2. Horizons	38
3. Sequence Stratigraphy	39

LIST OF FIGURES

Figure		Page
1.	Map of eastern North America showing the Baltimore Canyon Trough and the Laurentian Subbasin	40
2.	Geographic location of the Laurentian Subbasin	41
3.	Type of seismic reflection terminations and system tracts	43
4.	Location of seismic survey	44
5.	Location of wells data and seismic-lines name	45
6.	Well and seismic correlation	46
7.	Contour map of water bottom in the Laurentian Subbasin	47
8.	Seismic line B showing the Cretaceous and Paleogene sequences	49
9.	Seismic line STP-4 showing the Cretaceous and Paleogene sequences	51
10.	Seismic line STP-3 showing the Cretaceous and Paleogene sequences	53
11.	Seismic line C showing the localized folding	55
12.	Seismic line D showing the water bottom multiples	57
13.	Location of interpreted Horizons N1, N2, N3, and N4	58
14.	Location of interpreted Horizons N5, N6, N7, and N8	59
15.	Seismic line showing the interpreted Horizon N1	60
16.	Contour map of Horizon N1	61
17.	Contour map of Horizon N2	62
18.	Seismic line showing the interpreted Horizon N2	63
19.	Seismic line showing the interpreted Horizon N3	64
20.	Contour map of Horizon N3	65

21.	Seismic line showing the interpreted Horizon N4	66
22.	Contour map of Horizon N4	67
23.	Contour map of Horizon N5	68
24.	Seismic line showing the interpreted Horizon N5	69
25.	Contour map of Horizon N6	70
26.	Seismic line showing the interpreted Horizon N6	71
27.	Contour map of Horizon N7	72
28.	Seismic line showing the interpreted Horizon N7	73
29.	Contour map of Horizon N8	74
30.	Seismic line showing the interpreted Horizon N8	75
31.	Isochron map of Sequence-1	76
32.	Isochron map of Sequence-2	77
33.	Isochron map of Sequence-3	78
34.	Seismic line STP-7 showing the salt movement	80
35.	Isochron map of Sequence-4	81
36.	Seismic line B showing the Paleogene sequences and maximum flooding surfaces	82
37.	Seismic line B showing the Paleogene sequences and cartoon showing progradational-aggradational stratigraphic patterns	83
38.	Isochron map of Sequence-5	84
39.	Isochron map of Sequence-6	85
40.	Isochron map of Sequence-7	86
41.	Flattening seismic line B on top of Sequence-2	88

42. Progradational-downlapping terminations showing the direction of sediment supply for Sequence-4 89
43. Direction of sediment supply on Sequence-4 and Sequence-5 91
44. Clinoform rollover map of Paleogene sequences 92
45. Progradational-downlapping terminations showing the direction of sediment supply for Sequence-5 93
46. Direction of sediment supply on Sequence-6 and Sequence-7 95
47. Generalized illustration of the main geographic and depositional settings on a continental shelf 96
48. Depocenter migrations during the Paleogene 97
49. Graphic showing the tectonic event in the Mesozoic time of Baltimore Canyon Trough and Laurentian Subbasin 98
50. Jurassic and Cretaceous boundary in the Baltimore Canyon Trough and the Laurentian Subbasin 100
51. Salt structure in the Baltimore Canyon Trough and the Laurentian Subbasin 102
52. Clinoform rollover interpreted in the Baltimore Canyon Trough and the Laurentian Subbasin 104

LIST OF APPENDICES

Appendix		Page
1.	Biostratigraphic data	105
2.	Lithostratigraphic data	110
3.	Time to depth conversions	115
4.	Detailed Processing Parameters for Canadian Government Seismic Data	118
5.	Detailed Processing Parameters for TGS/Nopec Seismic Data	122

I. INTRODUCTION

Sequence stratigraphy is the preferred method for examining the sedimentary evolution of passive margins, e.g. the New Jersey margin (Greenlee et al., 1992; Steckler et al., 1999; Miller et al., 1998; Monteverde et al., 2000) and the Scotian Basin of offshore Nova Scotia (Wade and Maclean, 1990; Wade et al., 1995; Pe-Piper and Piper, 2004; Piper et al., 2005) (Fig. 1). Earlier investigations of the New Jersey passive margin analyzed the geometry of the margin through time in response to variations of relative sea-level, subsidence, and rate of sediment supply. Using the backstripping technique, Steckler et al. (1999) and Miller et al. (2006) determined the details of the change in passive-margin growth, e.g., the sediment prograded across the margin creating clinoform geometries and building a new shallower, flatter shelf overlying the earlier ramp structure. However, stratigraphic and sedimentation patterns in the Scotian Basin are less well understood due to the presence of salt structures, basement-involved deformation, and sparse well control (Keen et al., 1990; Shimeld, 2004; Piper, 2005) (Fig. 2). This thesis provides additional information about the stratigraphic development of the Nova Scotia passive margin using 2D seismic data. Specifically, this work presents a sequence-stratigraphic analysis of the Cretaceous to early Paleogene strata in the northern margin of the Scotian Basin e.g., Laurentian Subbasin (Fig. 2). This work defines how changes in relative sea-level, sediment supply and subsidence affected the depositional patterns in the Laurentian Subbasin, offshore eastern Nova Scotia and Newfoundland by answering the following questions:

1. What was the major direction of sediment supply during the Cretaceous and Paleogene?
2. Did the direction of sediment supply change through time?

3. Did relative sea-level change through time?
4. Where were the major depocenters during the Cretaceous and Paleogene?
5. Did the depocenters move through time?
6. Which factor (relative sea-level, accommodation space, sediment supply) had the most effect of margin growth?
7. What was the influence of tectonics (subsidence and uplift) on margin growth?

II. BACKGROUND

II.1. Sequence Stratigraphy

Sequence stratigraphy is the study of rock relationships between laterally associated correlative beds bounded at their tops and bottoms by surfaces of erosion or non-deposition or their correlative conformities (e.g., Mitchum et al., 1977; Vail, 1987; Posamentier et al., 1988; Galloway, 1989; Van Wagoner et al., 1990; Catuneanu, 2006). It provides a method to interpret and reconstruct the relative chronology of sedimentary deposits in basins and to predict their facies. A key concept of sequence stratigraphy is the interplay among variations in eustatic sea level, accommodation space, and sediment supply e.g., Vail, 1987; Van Wagoner et al., 1990; Posamentier and Allen, 1999. Eustatic sea level (global sea level) is the distance between the sea surface and a globally recognized datum, usually the center of the earth. The variation between the amount of ocean-water (glacio-eustacy) and the ocean-basin volume (tectono-eustacy) controls eustatic sea level. Alternatively, relative sea level is the distance between the sea surface and a local datum, usually the top of the basement rock in a sedimentary basin. Eustacy

and the elevation of the sea floor control relative sea level.

Accommodation is the total space available for sediment infilling, as marked by the different in elevation between base level and the depositional surfaces (Jervey, 1988; Posamentier, 1988; Emery and Myers, 1996; Posamentier and Allen, 1999). Base level is the elevation above which the action of waves, nearshore currents and other methods of sea floor erosion can remove and transport sediment. Below base level, sediment will accumulate. Generally if sediment supply remains constant, a rise in base level increases accommodation, whereas a fall in base level decreases accommodation. On many passive margins, the primary control of accommodation is the interplay of thermal tectonic subsidence, sediment supply, and the variation of eustatic sea level (Reynolds, 1991; Emery and Myers, 1996). Additionally, isostatic compensation resulting from sediment loading and sediment compaction creates additional subsidence and adds to the creation of accommodation space (Reynolds, 1991; Emery and Myers, 1996; Catuneanu 2006).

II.2. Seismic Stratigraphy

Seismic stratigraphy, the original technique to extract stratigraphic information using seismic-reflection data, lead to the development of sequence stratigraphy. Seismic stratigraphy involves the analysis of seismic-reflection terminations, i.e., clinoform geometry relationships between strata and stratigraphic surfaces (Fig. 3A). A clinoform is a depositional surface that is inclined to the horizontal as a result of progradation e.g., Rich, 1951; Miller et al., 1998. Clinoform reflections provide the opportunity to study the correlation between sequences and relative sea-level change e.g., Catuneanu, 2002; Catuneanu, 2006.

The fundamental package in stratigraphic analysis is the sequence. A sequence is

a unit bounded by significant subaerial erosional surfaces (Mitchum et al., 1977; Emery and Myers, 1996). In sequence stratigraphy, each sequence is divided into system tracts (especially in the seismic stratigraphy analysis) and is defined by the position and pattern of parasequence and parasequence sets (especially for well and outcrop analysis) e.g., Van Wagoner et al., 1988; Van Wagoner et al., 1990; Catuneanu, 2006. A parasequence is a stratigraphic unit of associated beds and bedsets bounded by flooding surfaces and their correlative surfaces (Van Wagoner et al., 1990; Emery and Myers, 1996; Catuneanu, 2006). Flooding surface is a surface exhibiting evidence of an abrupt increase in water depth. In seismic stratigraphic analysis, the three types of system tracts are: lowstand system tract (LST), transgressive system tract (TST), and highstand system tract (HST) (Fig. 3B). A system tract is a three-dimensional unit of deposition, bounded by surfaces of reflection terminations e.g., onlap, downlap, etc (Brown and Fisher, 1977; Mitchum et al., 1977; Van Wagoner et al., 1988; Emery and Myers, 1996) (Fig. 3B).

The lowstand system tract is characterized by sediments deposited during a period of relative sea-level fall, subsequent still-stand, and the slow initial rise of relative sea-level (Posamentier and Allen, 1999). The early phase of lowstand system tracts create submarine fans during the relative sea-level fall; the late phase creates a lowstand wedge characterized by an onlapping and progradational sequence set that becomes aggradational during the slow rise of relative sea level (Posamentier et al., 1988; Posamentier and Allen, 1999). The transgressive system tract develops when relative sea level begins to rise significantly. It is recognized by retrogradational parasequence sets that onlap onto the sequence boundary in a landward direction and downlap onto the older sediments in the basinward direction (Van Wagoner et al., 1988; Catuneanu, 2006). When the rate of rising relative sea-level is maximal, the rate of accommodation-space creation decreases to a point where it matches

sediment supply. This time, when the parasequences change from retrogradational to aggradational, is when the maximum flooding surface (MFS) is deposited (Emery and Myers, 1996; Catuneanu 2002). This surface separates the transgressive system tract from the overlying highstand system tract. The highstand system tract is the result of a decreasing rate of relative sea-level rise that produces parasequence sets that begin as aggradational and then become progradational. These parasequence sets onlap onto the underlying sequence boundary in the landward direction and prograde and downlap onto the MFS in the basinward direction (Posamentier et al., 1988; Van Wagoner et al., 1988; Van Wagoner et al., 1990) (Fig. 3B).

II.3. Regional Geologic Setting

The Laurentian Subbasin is part of the Scotian Basin, offshore eastern Nova Scotia and Newfoundland that extends from the northeast portion of the Georges Banks Basin to the western portion of the Grand Banks Basin (Fig. 2). The Scotian Basin formed after Late Triassic/Early Jurassic rifting and during the Early-to-Middle Jurassic separation of the North American and African plates (Jansa and Wade, 1975; Wade and MacLean, 1990; MacLean and Wade, 1992; Withjack et al., 1998; Withjack et al., 2005). Two tectonostratigraphic depositional packages distinguished by the rate of extension and basin subsidence are found in the Scotian Basin (MacLean and Wade, 1992). The oldest package consists primarily of continental redbeds (Eurydice Formation) and evaporites (Argo Formation) deposited during rifting in the Late Triassic and Early Jurassic. The red clastic sedimentary rocks of the Eurydice Formation underlie and interfinger with the Argo Formation (Jansa and Wade, 1975; Wade et al., 1995). The Argo Formation consists of thick evaporites, dominated by coarsely crystalline halite interbedded with dolomitic shale and some anhydrite (Wade and MacLean, 1990; MacLean and Wade, 1992; Tanner and

Brown, 2003). The youngest package is a succession of Mesozoic and Cenozoic clastic and carbonate sedimentary rocks deposited during subsidence of the passive margin (Tanner and Brown, 2003). In this thesis, I focus on the youngest tectonostratigraphic depositional package deposited during the drifting stage of the passive margin of Nova Scotia.

Previous researchers (e.g., Jansa and Wade, 1975; Wade and MacLean, 1990, and Wade et al., 1995) analyzed several wells in the Scotian Basin. They determined that the Early Cretaceous is characterized by the thick fluvial-deltaic Missisauga and Logan Canyon Formations, and the Late Cretaceous consists of the transgressive marine shales of the Dawson Canyon Formation. Furthermore, Piper et al. (2005) used seismic stratigraphy, biostratigraphy and radiometric dating to describe the Late Cenozoic stratigraphic evolution of the northern Scotian Basin, located northeast of my study area. They confirmed only thin Oligocene to mid-Miocene strata are present, and they identified a major unconformity of late Miocene age. However, Oligocene and Miocene strata are not present in my study area because the Laurentian Channel eroded away most of the Neogene strata during the Quaternary glaciation (Piper and Aksu, 1987).

III. METHODS

III.1. Data Preparation

The Canadian government and TGS/Nopec provided moderate-to-high resolution 2D seismic data covering 10,000 km of offshore Nova Scotia, southern Newfoundland, and the French territory of St. Pierre and Miquelon (Figs. 2 and 4). The public data provided by the Canadian government was acquired in 1984 –1985 and recently

reprocessed (Appendices 4 and 5). It consists of 29 2D migrated lines, representing 3,100 km of seismic data. The data have an airgun source volume of 4075 m^3., 120 recording channel, a trace length of 8000 ms, a sampling interval of 4 ms, and a streamer length of 3000 m. The proprietary data provided by TGS/NOPEC was acquired in 2002. The data have an airgun source volume of 5240 m^3, 640 recording channel, a trace length of 14336 ms, a sampling interval of 2 ms, a streamer length of 8000 m, and a nominal fold of 106. Processing included resampling, editing, static correction, FK filtering, spherical divergence correction, deconvolution, velocity analysis, and Kirchoff pre stack time migration. I interpreted approximately the top 3000 ms of data for 47 lines using the Kingdom Suite Software Package 8.2 (32-bit) (Fig. 5). Crossing lines show no evidence of misties. Supporting data included lithostratigraphic (Appendix 1) and biostratigraphic data (Appendix 2) derived from well cuttings from four wells: Dauntless D-35, Sachem D-76, Hesper I-52, and Adventure F-80) (Ascoli, 1974; Williams, 1974) (Fig. 5). Check-shot velocity data from the Dauntless D35, Sachem D-76, Hesper I-52, and Adventure F-80 well permitted well-seismic correlation (Fig. 6).

III.2. Data Interpretation and Analysis

The first step of the interpretation was mapping the water bottom to observe the recent surface structures, the direction of recent sediment supply, and to identify sites of erosion (Fig. 7). Where reflections are parallel or subparallel to the water-bottom reflection, missing section may be overlooked if the area of erosion is large compared to the length of the seismic line. The water-bottom reflection also provides a horizon for calculating aggregate thicknesses (isochrons and isopachs), e.g., the total thickness above the Avalon unconformity or the total thickness above the Cretaceous-Paleogene

unconformity. The Laurentian Channel in my study area is approximately 450 m deep (assuming a water velocity of 1.5 km/s) and trends NW-SE (Fig. 7).

The next step was identifying potential sequence boundaries based on seismic-reflection terminations: (1) top-lap and truncation below a discontinuity and (2) on-lap and down-lap above a discontinuity (Fig. 3 and Table 1). Each surface was loop-tied through the seismic grid for internal consistency. I interpreted the first horizon (N1) based on the top-laps and/or erosional truncations that exist throughout in the study area, although several salt structures locally obscure this reflection. The next selected horizon was an undulating reflection with high seismic amplitude (N4). I then identified six other horizons in the study area (N2, N3, N5, N6, N7, and N8) (Figs. 8 and 9). Erosional features in the upper part of seismic data limit the interpretation above Horizon N8. From oldest to youngest, the correlation of the horizon name with the horizon color is as follows: Horizon 1–red, Horizon 2–orange, Horizon 3–pink, Horizon 4–dark blue, Horizon 5–light blue, Horizon 6–purple, Horizon 7–green, Horizon 8–light red (Figs. 8 and 9).

I then correlated the horizons interpreted with the four wells that surround the study area using the Time-Depth Chart tool in the Kingdom Suite Software Package. The well data provide information about the approximately age of the seismic horizons and their lithologies. The correlation of the well and seismic data yielded the following ages for the horizons: Horizon 1-Base Cretaceous (Avalon) unconformity, Horizon 2-Early Cretaceous (Albian), Horizon 3-Late Cretaceous (Cenomanian), Horizon 4-Cretaceous Paleogene Boundary, Horizon 5-Early Paleocene, Horizon 6-Middle Paleocene, Horizon 7-Late Paleocene and Horizon N8-Early Eocene. The last step was preparing contour and isochron maps. Isochron units were named after the underlying sequence boundary. For

example, Sequence-1 is the unit of sedimentary rocks bounded by the Horizon N1 below and Horizon N2 above. Isochron maps display the variation of sediment thickness in two-way-travel time. They are important to understand the dominant locus of deposition, the changing thickness, the sediment-supply direction, and the progradation, aggradation and/or retrogradation cycles that occur during margin growth.

IV. OBSERVATIONS

The quality of the 2D seismic data in the Laurentian Subbasin is good, especially above 2.5 seconds two-way travel-time. Clinoform geometries associated with stratigraphic sequences based on reflection terminations are well-defined: (1) toplap and truncation are present below a discontinuity, and (2) onlap and downlap are present above a discontinuity, e.g., seismic line B (Fig. 8). In some areas, however, interpretation of the seismic data in the Laurentian Subbasin is challenging because reflection geometries are deformed by salt structures, e.g., seismic line STP-3 and STP-4 (Figs. 9 and 10), faults with normal separation, e.g., seismic line STP-3 and STP-4 (Figs. 9 and 10), and erosion-related incised valleys, e.g., seismic line C (Fig. 11). The signal-to-noise ratio is high; however, water-bottom multiples are common below 1.5 seconds, e.g., seismic line D (Fig.12).

I interpreted eight candidate sequence boundaries (N1 to N8, oldest to the youngest) with different seismic characteristics. Two major unconformities, the base Cretaceous (Avalon) unconformity and the Cretaceous-Paleogene unconformity, have strong seismic reflection and exist in every seismic line in the study area. Contour maps of the horizons and a series of isochron maps for the individual sequences also have distinctive geometries and seismic characteristics.

IV.I. Horizons

Table 2 shows the ages and seismic characteristics (e.g., seismic terminations, continuity, and reflection amplitudes) of the eight mapped horizons.

Horizon N1 (Avalon unconformity)

The first horizon, N1, correlates with the Avalon unconformity based on correlation with the Dauntless D-35 and Sachem D-76 wells (Ascoli, 1974; Williams, 1974). It is associated with onlap, toplap and/or erosional terminations, suggesting that N1 is a potential sequence boundary. Seismic data show the erosional truncations of the tilted reflections below the Avalon unconformity and the horizontal reflections above the unconformity. Thus, this horizon is an angular unconformity (Figs. 13, 14 and 15). Horizon N1 exists throughout the study area (Fig. 16). It is a relatively continuous reflection and has a high amplitude. It deepens in the southeast direction with a maximum depth of about 3 seconds in the study area. Several salt structures and faults deform the unconformity (Figs. 9 and 10). In the northwest part of the study area, salt movement produced local uplift, erosion and minor faults with normal separation (Figs. 9 and 10). In general, the slope of the unconformity is steeper in the southeast than in the northwest.

Horizon N2

Horizon N2 also exists throughout the study area (Fig. 17). Downlapping terminations and erosional truncations identify N2 as a potential sequence boundary (Fig. 18). Horizon N2 is relatively discontinuous with low-to-moderate amplitude (Table 2). In general, horizon N2 parallels horizon N1 (Fig. 8).

Horizon N3

Horizon N3 is a moderate-to-high-amplitude reflection and is more continuous than horizon N2 (Table 2, Fig. 19). Onlap and erosional terminations indicate that horizon N3 is a potential sequence boundary. It exists over the entire study area, and generally deepens toward the southeast part of the basin (Fig. 20). In the northwest,

horizon N3 is eroded and cut by normal faults associated with underlying salt movement (Fig. 9).

Horizon N4 (Cretaceous-Paleogene boundary)

Horizon N4 has a high amplitude, is continuous in the study area, and produces an undulating reflection indicating a rough or irregular surface (Table 2, Figs. 21 and 22). Erosional truncations beneath horizon N4 suggest that it is a potential sequence boundary (Fig. 21). In general, horizon N4 deepens toward the southeast, following horizon N3, e.g. seismic line STP-3 and STP-4 (Figs. 9 and 10). Correlation with the Dauntless D-35 and Sachem D-76 wells (Ascoli, 1974; Williams, 1974) indicates that this horizon is associated with the Cretaceous-Paleogene boundary.

Horizon N5

Horizon N5 merges on horizon N4 as shown on line B (Fig. 8). This horizon is found only in the center part of the Laurentian Subbasin (Fig. 23). It has a low-to-moderate amplitude and is discontinuous (Table 2). Onlap and erosional truncations make horizon N5 a potential sequence boundary, as seen in line C (Fig. 24).

Horizon N6

Horizon N6 occurs in the center part of the study area (Fig. 25). Onlap and erosional truncation make horizon N6 a potential sequence boundary, as evidenced on seismic line B (Fig. 26). In general, horizon N6 has a moderate-to-high amplitude and is discontinuous (Table 2).

Horizon N7

Horizon N7 exists only in the central part of the study area (Fig. 27). It has a low-to-moderate amplitude and tends to be discontinuous (Table 2). Onlap indicates that it is a potential sequence boundary (Fig. 28).

Horizon N8

The youngest interpreted horizon in the study area, horizon N8, has a moderate-to-high amplitude and is relatively continuous (Table 2). It is found in the central part of the study area (Fig. 29). As discussed previously, based on the biostratigraphy in the Dauntless D35 well, this horizon is associated with Early Eocene unconformity (Ascoli, 1974; Williams, 1974) (Fig. 30).

IV.2. Sequence Stratigraphy

Table 3 shows the age and the seismic characteristics of the sequences including their internal patterns (amplitude, spacing, continuity), stratigraphic patterns, and system tracts.

Sequence-1

Sequence-1 represents the oldest Cretaceous sedimentary rocks in the Laurentian Subbasin based on correlation of seismic and well data in the study area (Dauntless D-35 and Sachem D-76) (Table 3). It is bounded by the Avalon unconformity (horizon N1) below and horizon N2 above (Figs. 8, 9, and 10) and is characterized by reflections that are parallel to subparallel, closely spaced, relatively continuous, and moderate-to-high amplitude (Table 3). In general, the bottom and top of this sequence consist of higher amplitude, more closely spaced, and more continuous reflections than the middle. In some areas, salt movement has deformed Sequence-1 (Figs. 9 and 10). The overall

thickness of this unit varies from less than 200 ms in the north to over 700 ms in the southern part of the study area (Fig. 31).

Sequence-2

Based on correlation of seismic data with the Dauntless D-35 well, Sequence-2 represents early Late Cretaceous (Cenomanian) sedimentary rocks (Table 3). It is bounded by horizon N2 below and horizon N3 above (Figs. 8, 9 and 10). In general, Sequence-2 consists of reflections which are parallel to subparallel, low amplitude, relatively discontinuous, and widely spaced (Table 3). Progradational and downlapping terminations are present, especially in the southeast part of study area (Fig. 8). The thickness of Sequence-2 varies from less than 10 ms to over 250 ms on line 1281B-105 and thins significantly toward the southeast (Fig. 32).

Sequence-3

Sequence-3 is associated with Late Cretaceous (Turonian-Maastrichtian) sedimentary rocks based on the correlation of seismic data with the Dauntless D-35 well (Table 3). It consists of reflections that are parallel to subparallel, relatively continuous, closely spaced, and high amplitude (Table 3). The erosional limit of this sequence is in the northwest part of the study area (Figs. 9 and 33). Sequence-3 thins above underlying salt structures, e.g., seismic line STP-7 (Fig. 34). In general, the thickness of Sequence-3 varies from less than 20 ms to over 400 ms in the southern part of the study area represented by line B (Figs. 8 and 33).

Sequence-4

Sequence-4 consists of early Paleocene sedimentary rocks based on correlation of the seismic data and the Dauntless D-35 well (Table 3). Sequence-4 only exists in the

central part of the study area (Fig. 35), and is characterized by reflections which are low-to-high amplitude, discontinuous to continuous, and moderately spaced (Table 3). Prograding clinoforms display sigmoid geometries that are present in the upper part of the seismic data (Figs. 36 and 37). The thickness of this sequence varies from less than 5 ms to over 200 ms, becoming thinner toward the southeast (Fig. 35).

Sequence-5

Sequence-5 consists of middle Paleocene sedimentary rocks based on correlation of the seismic data and the Dauntless D-35 well (Table 3). It exists only in the central part of the Laurentian Subbasin (Fig. 38). Reflections in Seqence-5 are low-to-high amplitude, discontinuous, and moderately spaced (Table 3). Sequence-5 is thin in the northwest, thickens to the southeast, and then thins in the southeast (Fig. 38). The thickness of this sequence varies on line STP-4 from less than 15 ms to over 350 ms (Fig. 38).

Sequence-6

Sequence-6 consists of late Paleocene sedimentary rocks based on correlation of the seismic data and the Dauntless D-35 well (Table 3). Onlapping and downlapping terminations are present in the southeast part of the study area, e.g., seismic line 1281B-105 (Fig. 8). This sequence is characterized by divergent reflections that thicken toward the southeast, have moderate-to-high amplitudes, and are widely spaced (Table 3). The relative thickness of this sequence on line STP 3 varies from less than 50 ms to over 500 ms (Fig. 39).

Sequence-7

The last identified sequence is Sequence-7, consisting of Early Eocene sedimentary rocks based on correlation of the seismic data and the Dauntless D-35 well

(Table 3). It consists of reflections that are parallel to subparallel, relatively continuous, closely spaced, and have hummocky patterns (Table 3, Figs. 8, 9, and 10). This sequence thickens toward the southeast, varying from less than 10 ms to over 500 ms in the southeast portion (Fig. 40).

V. INTERPRETATION

The sequence stratigraphy of the Laurentian Subbasin reflects the interplay of several variables: (1) relative sea-level variations which influence the geometry of clinoform reflections, sequences, systems tracts, and the creation of disconformities, (2) tectonic events, including the thermoflexural subsidence of the continental crust across the margin which provides accommodation space that increases toward the oceanic crust (south to southeast offshore Nova Scotia), (3) primary direction of sediment supply, and (4) salt movement in the northeast part of the subbasin which modifies the direction of sediment transport and accommodation space.

V.I. Cretaceous Sequences

Sequence-1 (Early Cretaceous)

Sequence-1 overlies a large angular unconformity (Avalon unconformity), separating relatively flat and undeformed Cretaceous rocks above from folded and tilted Jurassic rocks below. This geometry suggests that Jurassic sedimentary rocks were deposited, folded, uplifted and eroded before the formation of the Avalon unconformity. This angular unconformity represents a major relative sea-level fall and sub-aerial erosion in the Late Jurassic and/or Early Cretaceous in the study area. Based on an assumption that the average velocity of sediment is 3 km/s, the projection of the beds above the unconformity predicts that approximately 1.5 - 2 km of sub-aerial erosion occurred during this time (Fig. 15).

The deposition of Sequence-1 is marked by the initiation of onlapping beds above the Avalon unconformity (Fig. 9). The onlapping beds illustrate that transgression occurred when relative sea-level rose during the deposition of Sequence-1. The relatively uniformly changing thickness of Sequence-1 reflects relative tectonic quiescence (e.g., no salt movement) during its deposition (Fig. 31). This sequence thickens towards the south-southeast reflecting an increasing accommodation space toward the oceanic crust.

The lithologic information in the Dauntless D-35 and Sachem D-76 wells, located in the southwest part of the Laurentian Subbasin (Fig. 31), show that sandstone is an important sedimentary rock in Sequence-1. Ascoli (1990), using benthic and/or planktonic foraminifera (in the Dauntless D-35 and Sachem D-76 wells), suggests that the water depth during the deposition of Sequence-1 (dominated by the Missisauga Formation) varied from 30-200 m with an inner neritic to outer neritic environment. However, the exact distribution of the different sedimentary facies in Sequence-1 is unknown due to sparse well data in the study area. Moreover, the correlation of seismic character and the sedimentary facies is unpredictable and impedes interpretation of the distribution of sedimentary facies throughout the study area.

Sequence-2 (early Late Cretaceous/Cenomanian)

Sequence-2 thins abruptly toward the southeast (Fig. 32). Local thickness variations in Sequence-2 reflect folding after the deposition of Sequence-1. This folding modified the accommodation space during the deposition of Sequence-2 by creating isolated depocenters in the center portion of the study area. Flattening on top of Sequence-2 illustrates reflection terminations onlapping the monoclinal structure

suggesting that the folding occurred before the deposition of Sequence-2 (Fig. 41). A possible explanation for the cause of the folding is salt movement associated with differential sediment loading and/or tectonic activity in the Laurentian Subbasin.

Reflections downlapping onto Horizon N2 are associated with progradational wedges (Fig. 41) that reflect the direction of sediment supply and variation of accommodation space. The progradational and aggradational reflection geometries in Sequence-2 illustrate that sediment came from the west and that relative sea-level was higher than relative sea-level in Sequence-1, suggesting that relative sea-level increased from the Early Cretaceous to the Late Cretaceous in the Laurentian Subbasin. The limited analysis of Cenomanian planktonic foraminifera in the Dauntless D-35 well indicates that the paleoenvironment was inner neritic to outer neritic, dominated by the deposition of alternating shale and sandstone (Logan Canyon Formation) (Ascoli, 1990; MacLean & Wade, 1993). The isopach map suggests the southeastern portion of the study area might be associated with a deeper water (outer neritic) environment dominated by shale deposition, whereas the northwestern portion might be correlated with a shallower water/inner neritic environment dominated by sandstone deposition.

Sequence-3 (Late Cretaceous /Turonian-Maastrichtian)

Sequence-3 generally thickens from east to west. Thickness variations in the northeast part of the study area are likely associated with salt movement (Fig. 33). Thickness variations and onlapping terminations indicate that the salt movement occurred during the deposition of Sequence-3, e.g., seismic line STP-7 (Fig. 34).

The absence of progradational and aggradational patterns prevents the interpretation of relative sea level during the deposition of Sequence-3. However,

reflections in Sequence-3 are parallel and continuous. This type of reflection geometry, coupled with regional lithologic information from Dauntless D-35 well, suggests that this sequence was deposited in a deep marine environment. Furthermore, based on lithostratigraphic data from the Dauntless D-35 and Sachem D-76 wells, Sequence-3 is dominated by marine shale (Dawson Canyon and Wyandot Formations), indicating that the deposition of this sequence was in a deep marine environment (MacLean and Wade, 1993).

V.II. Paleocene Sequences

Sequence-4 (Early Paleocene)

Sequence-4 consists of Early Paleocene sedimentary rocks characterized by progradational-aggradational sedimentary patterns. It is bounded by the underlying Cretaceous/Paleogene (KP) unconformity. Sequence-4 was preserved in a small area in the Laurentian Subbasin because erosion occurred in the northern part of study area. Based on the biostratigraphic and lithostratigraphic data from several regional wells in the Laurentian Subbasin, the KP boundary separates the Wyandot Formation beneath from the Banquereau Formation above, and it correlates with a hiatus at the top of Wyandot Formation (Ascoli, 1976; Barss et al., 1979; Doeven, 1983). Furthermore, the KP boundary correlates with horizon N4 characterized by a rough or irregular seismic signature caused by prograding or downlapping reflections (Figs. 36, and 37). Wade and MacLean (1990) propose that prograding and downlapping terminations created the local scouring that built the KP boundary unconformity. Another explanation is that an

extremely condensed section loaded by sedimentary rocks above the KP boundary creating sediment-load fractures (Wade and MacLean, 1990).

A lowstand system track and highstand system track are present in Sequence-4 in the southeast portion of the study area, separated by a maximum flooding surface indicated by downlapping reflections (Figs. 36 and 37). The different system tracts illustrate that relative sea-level fluctuated during Sequence-4 deposition. For example, the highstand system track is the result of a decreasing rate of relative sea level rise and increasing rate of sediment supply that produced parasequence sets that began as aggradational and then became progradational (Figs. 36 and 37) (Van Wagoner et al., 1988). Moreover, based on the downlapping terminations in the highstand system track, the sediment supply direction was from the northwest to southeast (Figs. 42 and 43).

Shale dominates Sequence-4, e.g., the Banquereau Formation, suggesting that the regional paleoenvironment was inner neritic to outer neritic. This interpretation is supported by benthic and/or planktonic foraminifera analysis from the well data in the study area (Wade et al., 1995; Ascoli, 1990). Furthermore, the geometry of the isopach map shows that sediments were deposited in a localized deltaic lobe suggesting that the dominant direction of the river system that provided the sediment for Sequence-4 was from the northwest direction.

Sequence-5 (Middle Paleocene)

The reflection terminations for this sequence show a clear separation of lowstand system track and highstand system track (Figs. 36 and 37). Highstand system track is characterized by downlapping terminations atop the maximum flooding surface that separates the lowstand system tract and highstand system tract (Figs. 36 and 37). For

example, the sedimentary succession deposited during the period of relative sea-level fall and slow initial rise of relative sea level in the lowstand system track has progradational patterns supported by the downlapping and onlapping terminations (Figs. 36 and 37) (Posamentier and Allen, 1999). The downlapping terminations in the highstand system track show that the direction of sediment supply was from the northwest.

The isochron map of Sequence-5 shows that the major depocenter for this sequence is in the northeast portion of the Laurentian Subbasin indicated by the thickest preserved sedimentary rock (Fig. 38). Furthermore, the geometry of this isochron map suggests that a dominant fluvial network controlled the sediment transport of Sequence-5 and it is possibly associated with the channel previously identified with Sequence-4 (Fig. 43). Based on the isochron maps of Sequence-4 and Sequence-5, the margin growth during the Early to Middle Paleocene was progradational, accompanied by a localized delta lobe shift toward the southeast (Fig. 43)

Sequence-6 (Late Paleocene)

Sequence-6 thickens toward the southeast (Fig. 39). The identification of a lowstand system track and a highstand system track in the southeastern part of the study area, e.g., seismic line 1281B-105 (Fig. 36) indicates that relative sea level fluctuated during the deposition of Sequence-6. For example, onlapping terminations in the lowstand system tract suggest an increasing relative sea-level during the initial deposition of Sequence-6.

Clinoform geometries in Sequence-4 to Sequence-6 suggest that margin growth during the Early Paleocene to Late Paleocene had aggradational-progradational

stratigraphic patterns (Fig. 44). Downlapping terminations suggest that the direction of sediment supply of Sequence-6 was similar to the previous sequences (Sequence-4 and Sequence-5) (Figs. 45 and 46). Thus, the northwest sourced sediment appeared to feed an offshore depocenter and tended to bypass the coastal plain, resulting in thin sedimentary deposits in the northern part of the Laurentian Subbasin (Figs. 45, 46 and 47).

Sequence-7 (Early Eocene)

The last sequence interpreted in the Laurentian Subbasin is Sequence-7 (Early Eocene sequence). The Laurentian Channel eroded the upper part of the sedimentary rocks in the Laurentian Subbasin hindering further interpretation of younger sediments. System tracks are not apparent in Sequence-7 because of the limitation of seismic data caused by significant erosion of the upper part of this sequence (Figs. 9 and 11). The isochron map of Sequence-7 shows that the depocenter was in the southeast part of the Laurentian Subbasin and has the same geometry as Sequence-6. The direction of sediment supply in Sequence-7 was probably the same as previous sequences (Sequence-4, 5 and 6) but no significant downlapping terminations are present. A river system dominated the point source of sediment supply as indicated by the localized delta lobe geometry in the isochron map of Sequence-7.

VI. DISCUSSION

The seven identified sequences reveal the evolution of progradational-aggradational margin growth from the Cretaceous to the Paleocene in the Laurentian Subbasin. Seismic terminations and isochron maps of those sequences provide evidence for: (1) the major direction of sediment supply in the Cretaceous to Paleocene (2) depocenter migrations during the Paleogene, (3) changing relative sea levels, and (4) salt movement modifying the accommodation space during the early Late Cretaceous.

VI.1. Sediment Supply

Seismic sequence stratigraphy reveals the direction of sediment supply by identifying progradational-downlapping terminations especially in the highstand system tracks. No significant downlapping terminations are identified in the Cretaceous sequences, Sequence-1 and Sequence-3. However, Sequence-2 shows downlapping-terminations or sediment-progradations, indicating the sediment supply from the west to east. The absence of progradational-downlapping termination in Sequence-1 may be due to insufficient accommodation space during its deposition. For Sequence-3, the lack of progradational-downlapping terminations may reflect deep marine paleoenvironment with clinoform geometries presents in the landward or northwest direction.

Increasing and decreasing rates of sediment supply can affect sequence thicknesses, the degree of progradation, aggradation and retrogradation, and the expression of lithofacies and biofacies (Reynolds et al., 1991). Based on the isochron maps of the Cretaceous sequences deposition was continuous across the entire study area, indicating that the total subsidence rate matched or exceeded the rate of sediment supply during the Cretaceous. Progradational-downlapping terminations are present in the Paleogene

sequences, Sequences 4, 5 and 6, providing evidence of the sediment-supply direction from the northwest to southeast (Figs. 43 and 46). The isochron maps of the Paleogene sequences show that the sedimentary rocks accumulated in a localized depocenter in the southeastern portion of the study area, suggesting that the dominant sediment-supply direction and available accommodation space controlled the sediment deposition in the Laurentian Subbasin during the Paleogene.

Progradational and aggradational patterns in the Paleogene reveal changes in margin growth. For example, generally the sediment deposition in the northeast portion of the Laurentian Subbasin is thicker than in the southwest portion especially above the KP boundary (Fig. 44). This condition suggests that margin growth in the northeast portion is faster than in the southwest portion.

VI.2. Accommodation Space

The series of isochron maps show the spatial distribution of sedimentary rocks that accumulated during the Early Cretaceous to the Paleocene. Significant depocenters in the Early Cretaceous are not visible in the Laurentian Subbasin because the initial subsidence after the Avalon uplift (Late Jurassic- Early Cretaceous) required a significant time to create accommodation space. Salt movement is not documented during the deposition in the Early Cretaceous Sequence-1, but is documented during the deposition of the Late Cretaceous Sequence-2 and Sequence-3. Salt movement and/or sediment loading modified the accommodation space during the deposition of these sequences by creating localized depocenters in the southwest portion of the study area (Sequence-2) and by creating several anticlinal structures in the northeast portion of the study area (Sequence-3).

Depocenters are well documented in the Laurentian Subbasin during the Paleogene. The integration of the Paleogene isochron maps reveals that the isolated depocenters (localized accommodation space) migrated toward the southeast (Figs. 35, 38, 39, 40 and 48). Moreover, the isochron maps of the Paleogene sedimentary rocks show a persistent thickening of sequences toward the oceanic crust, suggesting that the accommodation space increased toward the southeast (Sequence-4 and Sequence-5). However, in Sequence-6 and Sequence-7, the sediment source in the northwest fed an offshore depocenter and tended to bypass the coastal plain, resulting in thin sedimentary deposits in the northern part of the Laurentian Subbasin followed by the thickening sequence toward the southeast.

VI.3. Relative Sea Level

Cretaceous relative sea-level in the Laurentian Subbasin cannot be well documented because of a scarcity of reflection terminations in Sequence-1 and Sequence-3. However, limited analysis of reflection terminations in Sequence-2, coupled with regional lithologic information, suggest that relative sea level rose in the Laurentian Subbasin during the deposition of Early Cretaceous, Sequence-1, to Late Cretaceous, Sequence-2 and Sequence-3. Based on the lithostratigraphic analysis from several wells in the Laurentian Subbasin (Ascoli, 1976), Sequence-1 (Missisauga Formation) is characterized by thick fluvial-deltaic sequence (illustrated as parallel reflections on the seismic data) suggesting that relative sea level was low in the Early Cretaceous. In Sequence-2 (Logan Canyon Formation) progradational patterns initially appear in the southeast portion of the Laurentian Subbasin, suggesting that relative sea-level rose during Sequence-2 deposition. In the Late Cretaceous, Sequence 3 consists of

transgressive marine shale (Dawson Canyon Formation) and chalk and marl (Wyandot Formation), suggesting that relative sea level increased during Sequence-3 deposition. The clinoform geometries above the KP boundary document the changing relative sea-level in the Laurentian Subbasin during the deposition of Paleogene sequences. Furthermore, the progradational-aggradational terminations indicate that relative sea level rose in the Laurentian Subbasin during the deposition of Sequence-4 to Sequence-7 (Fig. 44).

VI.4. Sequence Stratigraphy on Passive Margins; Comparison of the Laurentian Subbasin and the Baltimore Canyon Trough

Sequence stratigraphic studies reveal the evolution of passive margin growth, e.g. Scotian Basin (Wade et al., 1995; Piper et al., 2004) and the New Jersey margin (Greenlee et al., 1992; Steckler et al., 1998; Miller et al., 1998; Monteverde et al., 2000). The New Jersey passive margin (Baltimore Canyon Trough) is a typical classic and well-studied passive margin. However, the Scotian Basin (Lautentian Subbasin) is less well understood. Both passive margins formed during the breakup of Pangea in the Early to Middle Jurassic. This thesis suggests that the tectonic history of the Laurentian Subbasin basin is likely more complicated than the Baltimore Canyon Trough. For example, major uplift and erosion occurred in the Laurentian Subbasin in the Late Jurassic and/or Early Cretaceous, but not in the Baltimore Canyon Trough (Fig. 49).

The Base Cretaceous unconformity or Avalon unconformity is an angular unconformity separating relatively flat and undeformed Cretaceous rocks above from folded and tilted Jurassic rocks below. This unconformity is possibly linked to the initiation of seafloor spreading between Iberia and the Grand Banks (Wade and

MacLean, 1990) just north of the study area. The Jurassic and Cretaceous boundary in the Baltimore Canyon Trough generally is a paraconformity although locally there some truncations and missing section showed by USG multichannel seismic line 25 (Fig. 50) (Poag, 1987). The possible explanation why this boundary was not impacted by the initiation of seafloor spreading between Iberia and the Grand Banks is that the location of the Baltimore Canyon Trough is far from the tectonic location.

Another difference between the Laurentian Subbasin and the Baltimore Canyon Trough is the presence of salt structures in the Laurentian Subbasin. Salt structures modified the accommodation space in the Laurentian Subbasin (Fig. 51). However, only one feature in the Baltimore Canyon Trough is a possible salt structure (Fig. 51) (Grow et al., 1988). This salt structure did not significantly impact the accommodation space and deposition in the Baltimore Canyon Trough.

Comparisons of seismic profiles from the Laurentian Subbasin and seismic profiles from Baltimore Canyon Trough indicate that clinoform geometries are present in both areas, especially above the Cretaceous-Paleogene boundary. Aggradational and progradational patterns dominate the stratigraphic patterns on both passive margins during the Paleogene (Fig. 52) suggesting that relative sea level variations and subsidence controlled the accommodation space during Paleogene deposition. However, the presence of Paleogene sequences is different on both passive margins. Thick Paleocene sedimentary rocks are present in the Laurentian Subbasin. However, thin Paleocene sedimentary rocks are present in the New Jersey passive margin. Several possibilities that create those differences are the interplay between accommodation space, variations of sediment supply, and subsidence. For example, one possibility is that the rate of

subsidence creating the accommodation space was slower than the rate of sediment supply producing the thin Paleocene section on the New Jersey passive margin. The rate of subsidence creating accommodation space was high in the Laurentian Subbasin followed by a high rate of sediment supply.

VII. CONCLUSIONS

- This thesis examined the development of the Laurentian Subbasin from Cretaceous through Early Paleogene using seismic sequence stratigraphy. I have identified three Cretaceous sequences (Sequence-1, Sequence-2, and Sequence-3) and four Paleogene sequences (Sequence-4, Sequence-5, Sequence-6 and Sequence-7).
- The Avalon unconformity represents a relative sea-level fall and sub-aerial erosion in the Late Jurassic and/or Early Cretaceous. It is a large angular unconformity, separating relatively flat and undeformed Cretaceous rocks above from the folded and tilted Jurassic rocks below. The presence of this unconformity suggests that Jurassic sedimentary rocks were deposited, folded, uplifted and eroded before and/or during the formation of the Avalon unconformity. Furthermore, onlapping terminations above the Avalon unconformity suggest that an initial rise of relative sea-level occurred during the Early Cretaceous.
- The progradational-downlapping terminations reveal the direction of source-sediment supply in the study area. The seismic-reflection terminations in the Paleogene section suggest that the major direction of sediment supply in the Laurentian Subbasin was from the northwest to southeast. Furthermore, the sediment supply was the major factor controlling the development of margin growth. However, the direction of source sediment supply is unknown in the Cretaceous.

- Clinoform geometries in the Paleogene section document that margin growth in the Laurentian Subbasin has progradational-aggradational patterns. The margin prograded toward the southeast. Furthermore, margin growth developed more rapidly in the northeast than in the southwest as indicated by the greater distance between clinoform points in the northeast than in the southwest (Fig. 46). Moreover, the isochron maps of the Paleogene section document the chronology of localized depocenter migrations from the northwest to the southeast. No significant depocenter is visible in the Laurentian Subbasin during the Cretaceous section, Sequence-1 and Sequence-3. However, localized depocenter is visible in the central portion of my study area with northeast trending in the Sequence-2.
- The major differences between the Baltimore Canyon Trough and the Laurentian Subbasin are the presence of a major angular unconformity of Late Jurassic/Early Cretaceous age, the presence of numerous salt structures, and the presence of thick Paleogene sequences in the Laurentian Subbasin. In the study area, the Jurassic-Cretaceous boundary is a major angular unconformity, separating relatively flat and undeformed Cretaceous rocks above from folded and tilted Jurassic rocks below. However, the Jurassic-Cretaceous boundary in the Baltimore Canyon Trough is a paraconformity separating parallel beds above and below the unconformity. Salt structures affected the interplay of the sequence stratigraphic variables in the Laurentian Subbasin but not significantly in the Baltimore Canyon Trough.

REFERENCES

Ascoli, P., 1976, Foraminiferal and ostracod biostratigraphy of the Mesozoic-Cenozoic, Scotian Shelf, Atlantic Canada; Maritime Sediments, Special Publication no. 1, p. 653-771.

Ascoli, P., 1990, Foraminiferal, ostracod and calpionellid zonation and correlation of 42 selected wells from the North Atlantic margin of North America, Bulletin of Canadian Petroleum Geology, v. 38, no. 4, p. 485-492.

Barss, M.S., Bujak, J.P., and Williams, G.L., 1979, Palynological zonation and correlation of sixty-seven wells, eastern Canada: Geological Survey of Canada, Paper 78-24, p. 118.

Brown, L.F., and Fisher, W.L., 1977, Seismic stratigraphic interpretation of depositional systems: examples from Brazilian rift and pull-apart basins. In: C.E. Payton, Editor, Seismic Stratigraphy—Applications to Hydrocarbon Exploration, American Association of Geologists Memoir vol. 26 (1977), pp. 213–248.

Catuneanu, O., 2002, Sequence stratigraphy of clastic systems: concepts, merits and pitfalls, Journal of African Earth Sciences, v. 35, p. 1-43.

Catuneanu, O., 2006, Principles of sequence stratigraphy, Elsevier, New York, 375p.

Doevan, P.H., 1983, Cretaceous nannofossil stratigraphy and paleoecology of the Canadian Atlantic Margin: Geological Survey of Canada, Bulletin 356, p. 70.

Emery, D., and Myers, K., 1996, Sequence stratigraphy, Oxford, Blackwell Science, 297p

Galloway, W.E., 1989, Genetic stratigraphic sequences in basin analysis; I, Architecture and genesis of flooding-surface bounded depositional units: AAPG Bulletin, vol. 73, no. 2, p. 125-142.

Greenlee, S.M., Devlin, W.J., Miller, K.G., Mountain, G.S., and Flemings, P.B., 1992, Integrated sequence stratigraphy of Neogene deposits, New Jersey continental shelf and slope: comparison with the Exxon model; Geological Society of America Bulletin, v. 104, p. 1403-1411.

Grow, J.A., Klitgord, K.D., and Schlee, J.S., 1988, Structure and evolution of Baltimore Canyon Trough: The Geology of North America, v.1-2: The Atlantic Continental Margin, p.269-290.

Hardy, I.A., 1975, Lithostratigraphy of the Banquereau Formation of the Scotian Shelf; in Offshore Geology of Eastern Canada, Volume 2, Regional Geology, ed. W.J.M.

van der Linden and J.A.Wade; Geologycal survey of Canada, Paper 74-30, v. 2, p. 163-174.

Jansa, L. F., and J. A. Wade, 1975, Geology of the continental margin off Nova Scotia and Newfoundland, in W. J. M. van der Linden and J. A. Wade, eds., Offshore geology of eastern Canada, v. 2: Regional geology: Geological Survey of Canada Paper 74-30, p. 51–106.

Jervey, M.T., 1988, Quantitative geological modeling of siliciclastic rock sequences and their seismic expression: in Wilgus, et al, (eds.), Sea-Level changes: an integrated approach, SEPM Special Publication No. 42, p. 47-69.

Klitgord, K. D., D. R. Hutchinson, and H. Schouten, 1988, U.S. Atlantic Continental margin; Structural and tectonic framework, in R. E. Sheridan, and J. A. Grow, eds., The Atlantic Continental Margin, U.S.: Geological Society of America, The Geology of North America, v. 1-2.

Keen, C.E., Kay, W.A., and Roest, W.R., 1990, Crustal Anatomy of a Transform Continental Margin, Tectonophysics, v. 173, p. 527-544.

MacLean, B.C., and J.A. Wade, 1992, Petroleum geology of the continental margin south of the islands of St. Pierre and Miquelon, offshore Eastern Canada: Bulletin of Canadian Petroleum Geology, v. 40, p. 222-253.

MacLean, B.C., and Wade, J.A. 1993. Seismic markers and stratigraphic picks in Scotian Basin wells. Atlantic Geoscience Centre, Geological Survey of Canada.

Miller, et al, 1998. Cenozoic Global Sea Level, Sequences, and the New Jersey Transect: Results from Coastal Plain and Continental Slope Drilling. Geophysics 36: 569-601.

Mitchum, R.M., Vail, P.R., and Thompson, S., III, 1977a, Seismic stratigraphy and global changes of sea level, Part 2: the depositional sequence as a basic unit for stratigraphic analysis, *in,* Payton, C.E., editor, Seismic stratigraphy – applications to hydrocarbon exploration, American Association of Petroleum Geologists Memoir 26, p. 53-62.

Mountain, G.S., Miller, K.G., Blum, P., Alm, P.-G., Aubrey, M.-P., Burckle, L.H., Christensen, B.A., Compton, J., Damuth, J.E., Deconinck, J.-F., de Verteuil, L., Fulthorpe, C.S., Gartner, S., Guerin, G., Hesselbo, S.P., Hoppie, B., Katz, M.E., Kotake, N., Lorenzo, J.M., McCracken, S., McHugh, C.M., Quayle, W.C., Saito, Y., Snyder, S.W., ten Kate, W.G., Urbat, M., Van Fossen, M.C., Vecsei, A., 1994, New Jersey continental slope and rise, Proc. Ocean Drill. Program, Initial Reports, V.150, College Station, TX (Ocean Drilling Program).

Monteverde, D.H., Miller, K.G., and Mountain, G.S., 2000, Correlation of offshore

seismic profiles with onshore New Jersey Miocene sediments, Sedimentary Geology, v.134, p.111-127

Olsen, P. E., 1997, Stratigraphic record of the early Mesozoic breakup of Pangea in the Laurasia-Gondwana rift system: Annual Review of Earth and Planetary Sciences, v. 25, p. 337-401.

Olsen, P.E., P.M. Hanshaw, R.W. Schlische, P.J.W. Gore, 1989, Sedimentation and basin analysis in siliciclastic rock sequences; Volume 2, Tectonic, depositional, and paleoecological history of early Mesozoic rift basins, eastern North America: Field trips for the 28th international geological congress, Am. Geophys. Union, Washington, DC, United States, p. 174.

Piper, D.J.W and Aksu, A.E., 1987, The Source and Origin of the 1929 Grand Banks Turbidity Current Inferred from Sediment Budgets: Geo-Marine Letters, v.7, p. 177-182.

Pe-Piper, G. and Piper, D. J. W., 2004, The effects of strike-slip motion along the Cobequid-Chedabucto-southwest Grand Banks fault system on the Cretaceous-Tertiary evolution of Atlantic Canada: Canadian Journal of Earth Sciences, v. 41, p. 799-808.

Piper, D.J.W., Macdonald, A.W.A., Ingram, S., Williams, G.L., and McCall, C., 2005, Late Cenozoic architecture of the St. Pierre Slope: Canadian Journal of Earth Sciences, v. 42, p. 1987–2000.

Poag, C.W., 1987, The New Jersey Transect: Stratigraphic Framework and Depositional History of a Sediment-Rich Passive Margin: Initial Report of the Deep Sea Drilling Project, v. XCV, p. 763-817.

Posamentier, H.W., and Allen, G.P., 1999, Siliciclastic sequences stratigraphy – concepts and applications: Society for Sedimentary Geology, SEPM Concepts in Sedimentology and Paleontology 7, 210p.

Posamentier, H.W., M.T. Jervey, and P.R. Vail, 1988, Eustatic controls on clastic deposition I -- Conceptual framework, in Sea Level Changes: An Integrated Approach, edited by C. K. Wilgus, B. S. Hastings, C. G. St. C. Kendall, H. W. Posamentier, C. A. Ross, and J. C. Van Wagoner, Society of Economic Paleontologists and Mineralogists, Special Publication, 42, p.109-124.

Reynolds, D.J., Steckler, M.S., and Coakley, B.J., 1991, The role of sediment load in sequence stratigraphy; the influence of flexural isostasy and compaction: Journal of Geophysical Research, v. 96, p. 6931-6949.

Rich, J.L. 1951. Three critical environments of deposition, and criteria for recognition of rocks deposited in each of them. Geological Society of America Bulletin 62: 1-20.

Steckler, M.S., G.S. Mountain, K.G. Miller, and N. Christie-Blick. 1999, Reconstruction of Tertiary progradation and clinoform development on the New Jersey passive margin by 2-D backstripping. Marine Geology 154: 399-420.

Steckler, M.S. and A.B. Watts, 1978, Subsidence of the Atlantic-type continental margin off New York, Earth Planet. Sci. Lett. 4, p. 1-13.

Shimeld, J., 2004, A comparison of salt tectonic subprovinces beneath the Scotian Slope and Laurentian Fan: Concepts, applications and case studies for the 21st century, Gulf Coast Society Section of the Society of Economic Paleontologists and Mineralogists, 24th Annual Bob F. Perkins Research Conference, extended abstracts volume, Houston.

Tanner, L.H. and Brown, D.E., 2003, Tectonostratigraphy of the Orpheus Graben, Scotian Basin, Offshore Eastern Canada, and Its Relationship to the Fundy Rift Basin: The Great Rift Valleys of Pangea in Eastern North America.

Vail, P.R., 1987, Seismic stratigraphy interpretation using sequence stratigraphy. Part 1: seismic stratigraphy interpretation procedure, in: Bally, A.W. (Ed.), Atlas of seismic stratigraphy, vol. 1, American Association of Petroleum Geologists, Studies in Geology, 27, p.1–10.

Van Wagoner, J.C., Mitchum, R.M., Jr., Campion, K.M., and Rahmanian, V.D., 1990, Siliciclastic sequence stratigraphy in well logs, core, and outcrop: concepts for high-resolution correlation of time and facies: American Association of Petroleum Geologists Methods in Exploration Series 7, 55p.

Van Wagoner, J.C., Posamentier, H.W., Michum, R.M., Vail, P.R., Sarg, J.F., Loutit, T.S., and Hardenbol, J., 1988, An overview of the fundamentals of sequence stratigraphy and key definitions, *in*, Wilgus, C.K., Hastings, B.S., Kendall, C.G.St.C., Posamentier, H., Ross, C.A., and Van Wagoner, J., Ross, C.A., editors, Sea-level changes: an integrated approach, Society of Economic Paleontologists and Mineralogists, Special Publication 42, p.39-48

Wade, J. A. and MacLean, B. C., 1990, Aspects of the geology of the Scotian Basin from recent seismic and well data; the geology of the southeastern margin of Canada: Geological Society of America Special Pub.

Wade, J. A., MacLean, B. C., and Williams, G. L., 1995, Mesozoic and Cenozoic Stratigraphy, Eastern Scotian Shelf - New Interpretations: Canadian Journal of Earth Sciences, v. 32, p. 1462-1473.

Withjack, M. O., Schlische, R. W., and Olsen, P. E., 1998, Diachronous rifting, drifting, and inversion on the passive margin of central eastern North America: An analog for other passive margins: Aapg Bulletin, v. 82, p. 817-835.

Withjack, M.O., and Schlische, R.W., 2005, A review of tectonic events on the passive margin of eastern North America, in Post, P., ed., Petroleum Systems of Divergent Continental Margin Basins: 25th Bob S. Perkins Research Conference, Gulf Coast Section of SEPM, p. 203-235.

Table 1. Types of Reflection Terminations (definitions from Mitchum, 1977; Galloway, 1989; Emery and Myers, 1996)

Truncation: termination of strata against an overlying erosional surface. *Toplap* may develop into truncation, but truncation is more extreme than toplap and implies either the development of erosional relief or the development of an angular unconformity.

Toplap: termination of inclined strata (clinoforms) against an overlying lower angle surface, mainly as a result of nondeposition (sediment bypass), ± minor erosion. Strata lap out in a landward direction at the top of the unit, but the successive terminations lie progressively seaward. The toplap surface represents the proximal depositional limit of the sedimentary unit. In seismic stratigraphy, the *topset* of a deltaic system (delta plain deposits) may be too thin to be "seen" on the seismic profiles as a separate unit (thickness below the seismic resolution). In this case, the topset may be confused with toplap (i.e., *apparent toplap*).

Onlap: termination of low-angle strata against a steeper stratigraphic surface. Onlap may also be referred to as *lapout*, and marks the lateral termination of a sedimentary unit at its depositional limit.

Downlap: termination of inclined strata against a lower-angle surface. Downlap may also be referred to as *baselap*, and marks the base of a sedimentary unit at its depositional limit. Downlap is commonly seen at the base of prograding clinoforms, either in shallow-marine or deep-marine environments. It is uncommon to generate downlap in nonmarine settings, excepting for lacustrine environments. Downlap therefore represents a change from marine (or lacustrine) slope deposition to marine (or lacustrine) condensation or nondeposition.

Table 2. Horizon

No	Horizon	Seismic Characteristics			Age	Representative Lines	Figures
		Seismic Terminations	Continuity	Reflection Amplitudes			
1	N1	Erosional or/and toplap onlap	Continuous	Variable, but generally high	Base Cretaceous (Jurassic/Cretaceous Boundary)	STP 7, STP 5	1, 2, 6, 8, 13, 24, 33
2	N2	Erosional, downlapping	Variable, generally discontinuous	Low to moderate	early Late Cretaceous (Cenomanian)	Line B, Line C	1, 2, 6, 8, 14, 24, 34
3	N3	Erosional	Variable, generally continuous	Moderate to high	Late Cretaceous (Turonian)	Line A, Line C	1, 2, 6, 8, 15, 24, 35
4	N4	Erosional	Continuous	High	Base Paleocene (Cretaceous/Paleogene Boundary)	Line B, STP 4	1, 2, 6, 8, 16, 24, 36
5	N5	Erosional, onlapping	Variable, generally discontinuous	Low to moderate	late Early Paleocene	Line C, STP 21	1, 2, 6, 8, 17, 24, 37
6	N6	Erosional, onlapping	Variable, generally continuous	Moderate to high	Middle Paleocene	Line B	1, 2, 6, 8, 18, 24, 38
7	N7	Onlapping	Variable, generally discontinuous	Low to moderate	Late Paleocene	Line A, Line B	1, 2, 6, 8, 19, 24, 39
8	N8	-	Continuous	Moderate to high	Early Eocene	-	1, 2, 6, 8, 20, 24, 40
9	MFS 1	Downlapping	Variable, generally discontinuous	Low to moderate	Early Paleocene	Line B, STP 4	6, 8, 21, 24
10	MFS 2	Downlapping	Variable, generally discontinuous	Low to moderate	late Early Paleocene	Line B, Line C	6, 8, 22, 24
11	MFS 3	Downlapping	Variable, generally discontinuous	Low to moderate	Late Paleocene	Line A, Line B	6, 8, 23, 24

Table 3. Sequence Stratigraphy

No	Sequence	Sequence Characteristics					Age	Representative Lines	Figures
		Internal Patterns			Stratigraphic Patterns	System Tracts			
		Amplitude	Spacing	Continuity					
1	S1	Parallel to subparallel, moderate to high	Close to moderate	Variable, generally continuous	-	-	Early Cretaceous	Line B, STP 3, Line C, STP 4	1, 2, 3, 7, 24, 25
2	S2	Parallel to subparallel, low	Moderate to wide	Variable, generally discontinuous	Local progradation	-	early Late Cretaceous	Line B, STP 3, Line C, STP 4	1, 2, 3, 7 24, 26
3	S3	Parallel to subparallel, high	Close	Continuous	-	-	Late Cretaceous	Line B, STP 3, Line C, STP 4	1, 2, 3, 24, 27
4	S4	Divergent, parallel to subparallel, high	Moderate to wide	Variable, generally continuous	Progradation, aggradation	LST HST	Early Paleocene	Line B, STP 3, Line C, STP 4	1, 2, 3, 24, 28
5	S5	Divergent, parallel to subparallel, high	Moderate	Variable, generally discontinuous	Progradation, aggradation	LST HST	late Early Paleocene	Line B, STP 3, Line C, STP 4	1, 2, 3, 24, 29
6	S6	Divergent, moderate to high	Wide	Variable, generally continuous	Progradation, aggradation	LST HST	Middle Paleocene	Line B, STP 3, Line C, STP 4	1, 2, 3, 24, 30
7	S7	Parallel to subparallel, (hummocky)	Close to moderate	Variable, generally continuous	-	-	Early Eocene	Line B, STP 3, Line C, STP 4	1, 2, 3, 24, 31

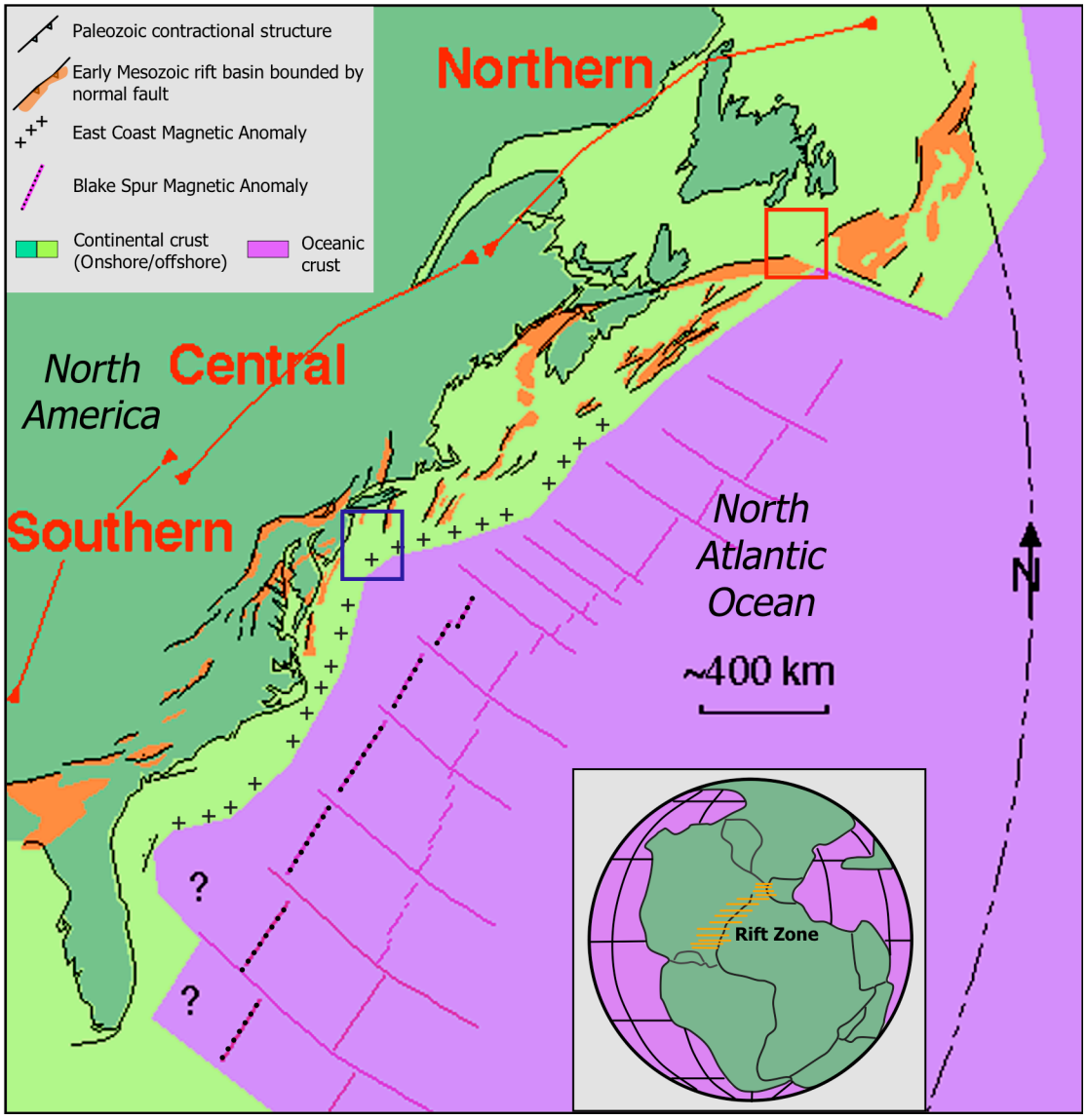

Figure 1. Major Paleozoic structures and early Mesozoic rift basins of eastern North America, and tectonic features of the eastern North Atlantic Ocean (Kiltgord et al., 1988; Olsen et al., 1989). Red box indicates the study area, northern Scotian Basin (Laurentian Subbasin) and blue box indicates the Baltimore Canyon Trough on the New Jersey passive margin. Inset map shows Pangea supercontinent during Late Triassic time (Olsen, 1997) and orange area highlights rift zone between eastern North America, northwest Africa, and Iberia. Modified from Withjack and Schlische (2005).

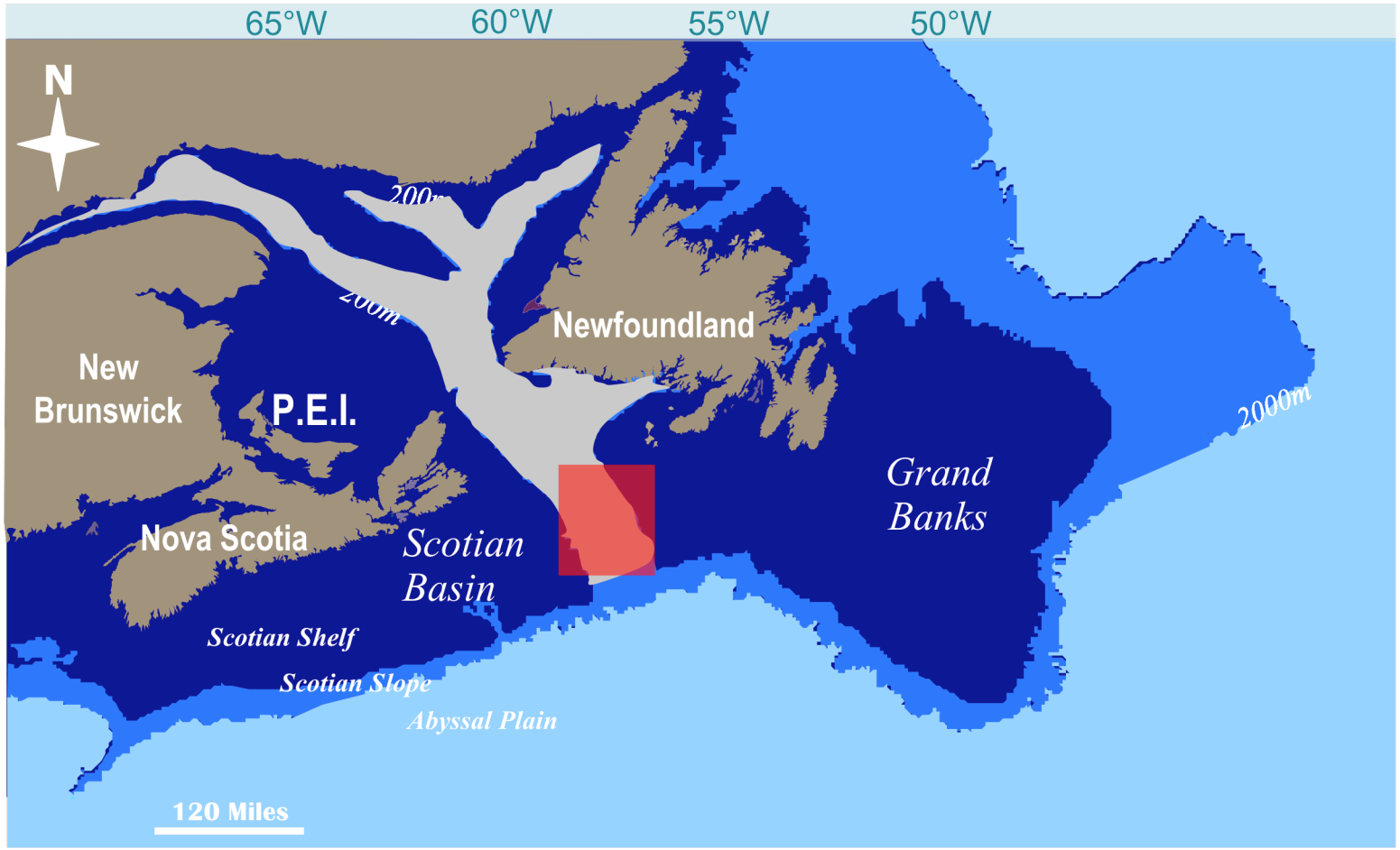

Figure 2. Geographic location of the northern Scotian Basin (Laurentian Subbasin), offshore Nova Scotia and Newfoundland. Light grey color indicates the Laurentian Channel. Red box is the location of the study area. Modified from Archuleta (2006).

Figure 3. (A) Types of seismic-reflection terminations and patterns, modified from Mitchum et al. (1977), Coe and Church (2003), and Monteverde (2008), (B) Sequence stratigraphic depiction of the geometric arrangement of lowstand system tract (LST), transgressive system tract (TST) and highstand systems tracts (HST), modified from van Wagoner et al. (1990).

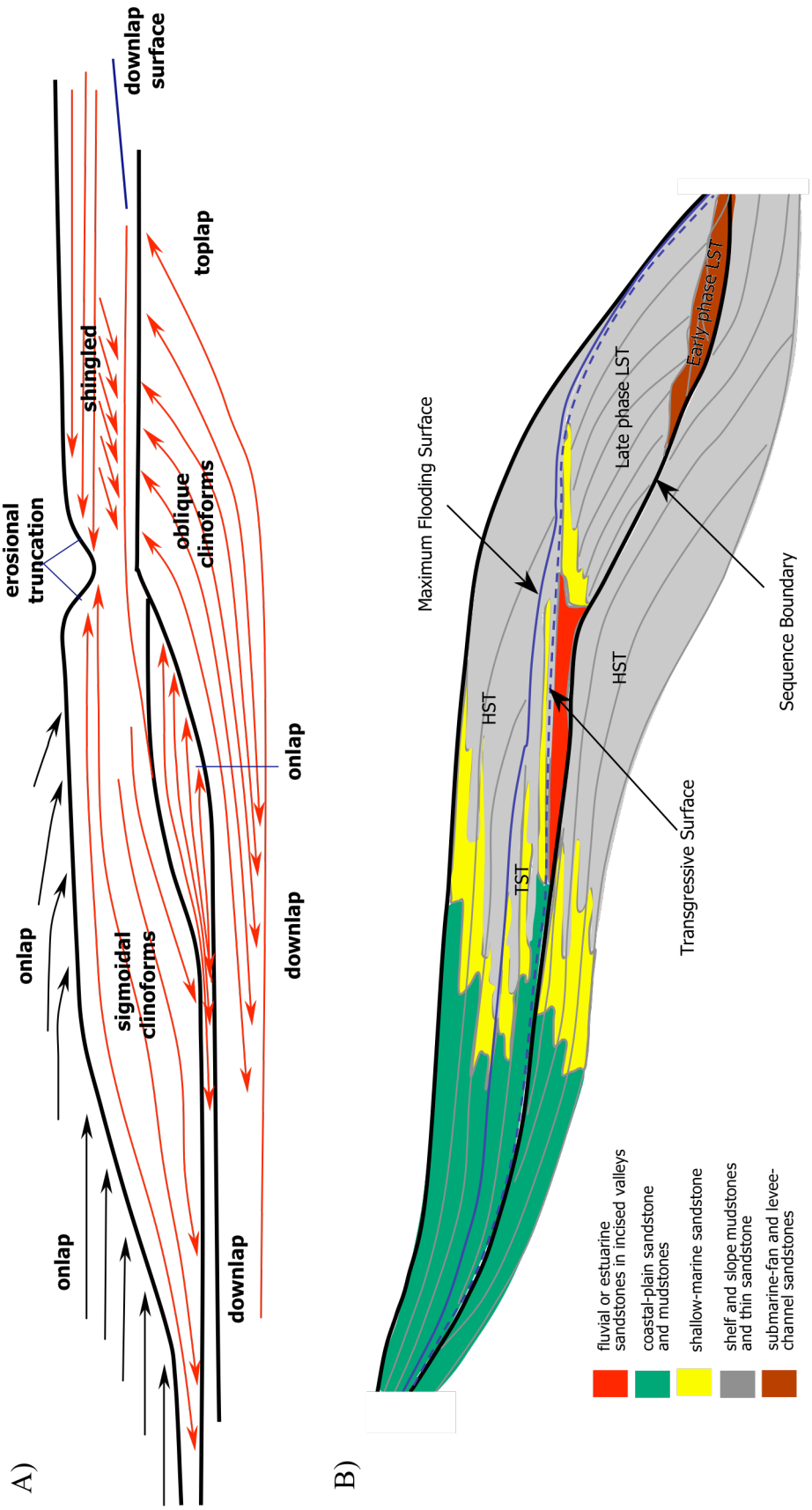
A)
erosional truncation
shingled
downlap surface
toplap
oblique clinoforms
onlap
onlap
sigmoidal clinoforms
downlap
onlap
downlap
B)
Maximum Flooding Surface
HST
TST
HST
Late phase LST
Early phase LST
Transgressive Surface
Sequence Boundary
fluvial or estuarine sandstones in incised valleys
coastal-plain sandstone and mudstones
shallow-marine sandstone
shelf and slope mudstones and thin sandstone
submarine-fan and levee-channel sandstones

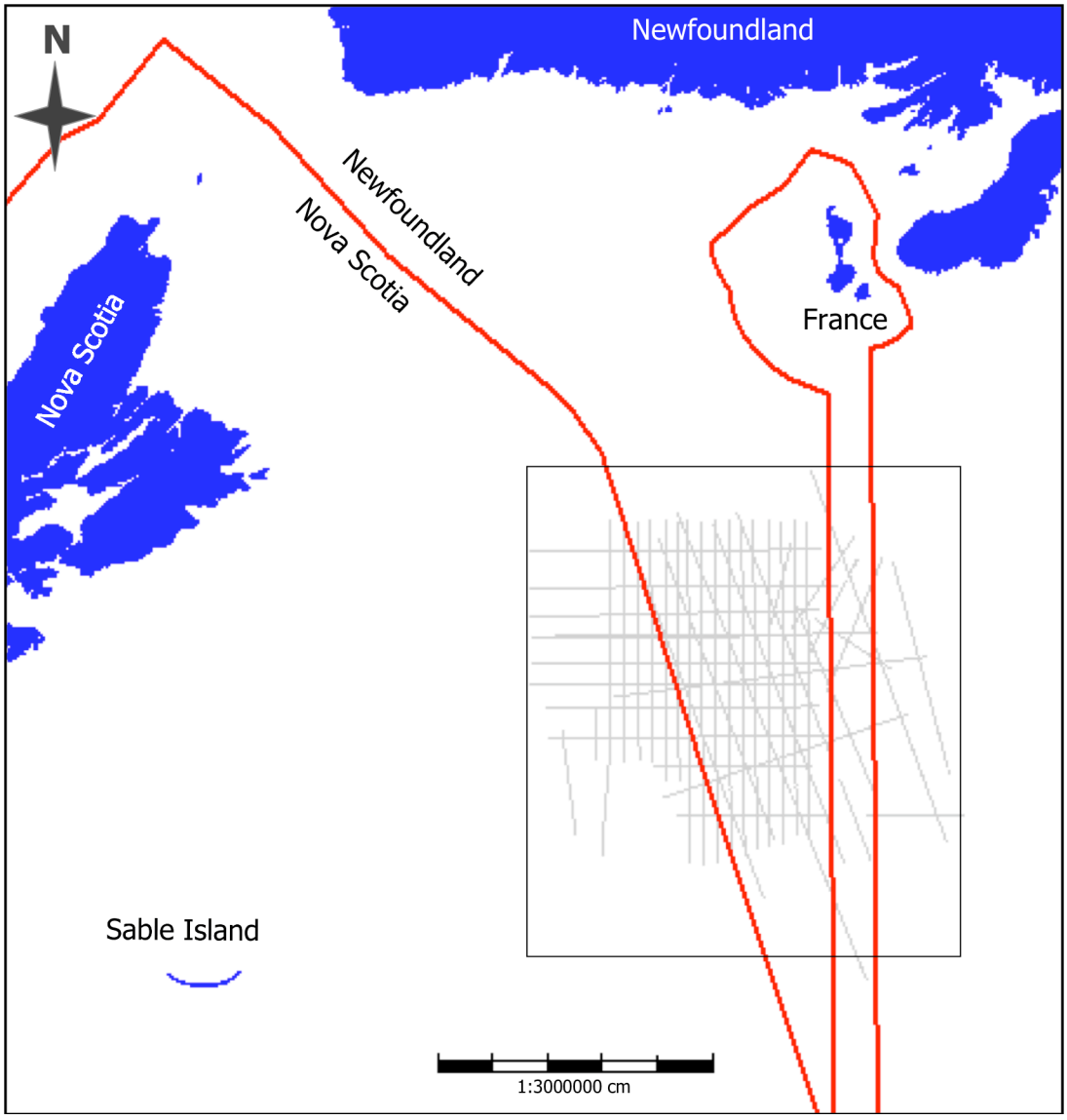

Figure 4. Location of Laurentian Subbasin in offshore Nova Scotia and southern Newfoundland. Red lines indicate province and country boundaries. Black box indicates the location of the study area, and grey lines are seismic lines. See Figure 5 for well locations and names of key seismic lines.

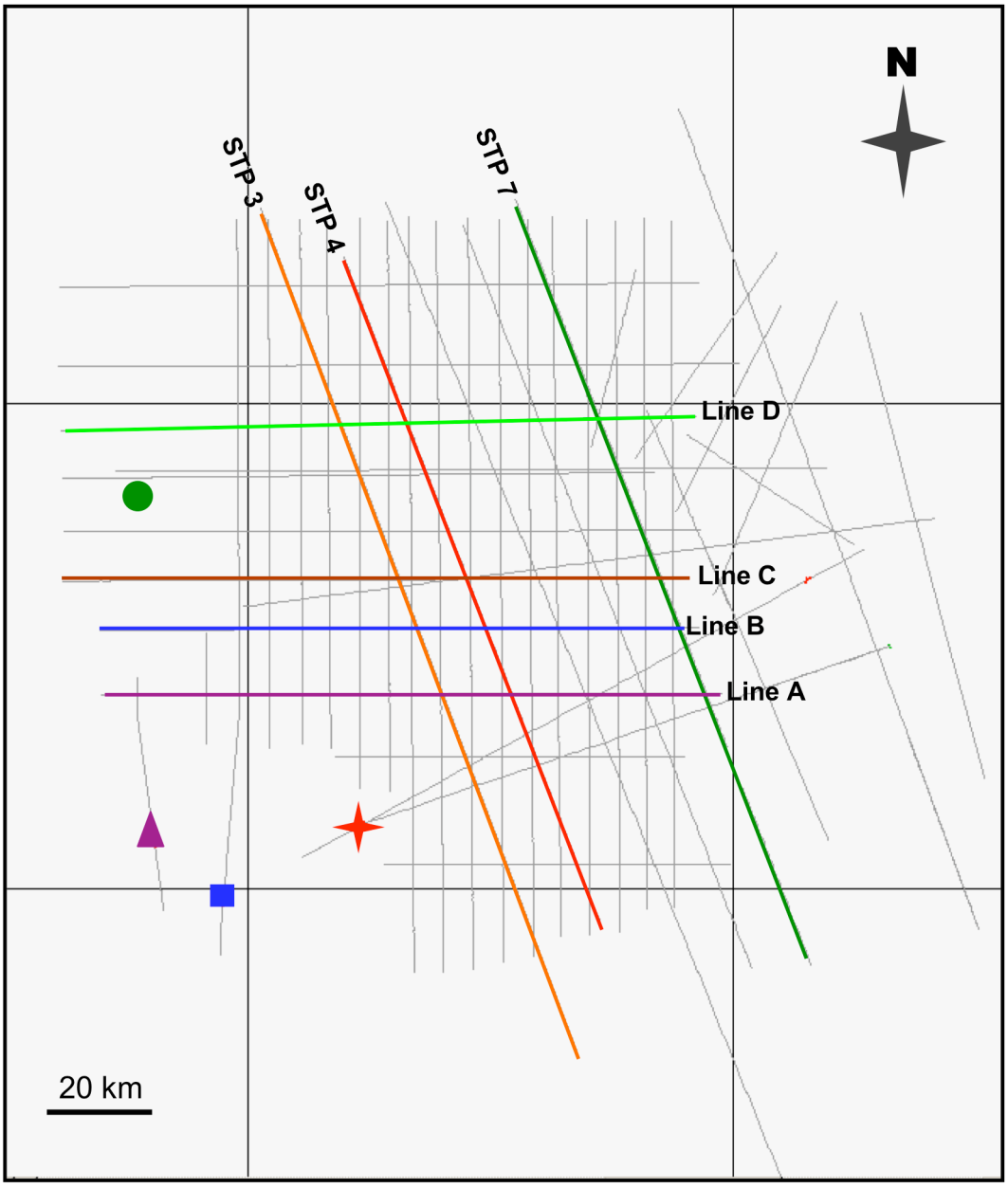

Figure 5. Location of Dauntless D-35 well (red star), Sachem D-76 (blue rectangle), Hesper I-52 (purple triangle), Adventure F-80 (green circle) and seismic line data. Colored lines show locations of six profiles shown elsewhere in this thesis.

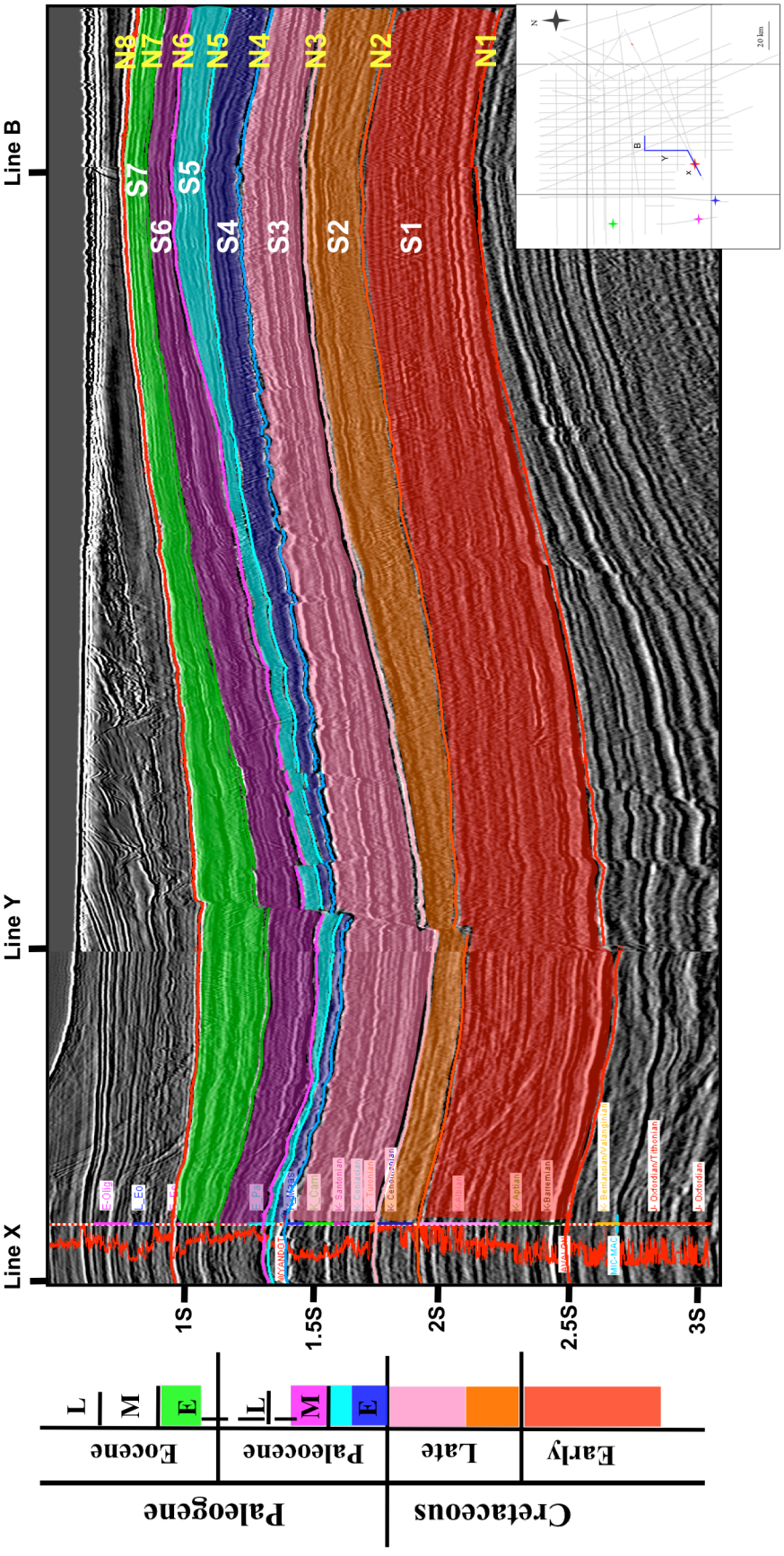

Figure 6. Correlation Dauntless D-35 well and the seismic data. N1-N8 are the interpreted horizons; S-1, S-2, and S-3 are the Cretaceous sequences; S-4, S-5, S-6, and S-7 are the Paleogene sequences. N1 is the Avalon unconformity, N4 is the Cretaceous-Paleogene boundary unconformity, and N8 is the Early Eocene Unconformity. The vertical red line on the seismic section shows the gamma-ray log. The inset map shows the location of the arbitrary seismic lines used to correlate with the well data.

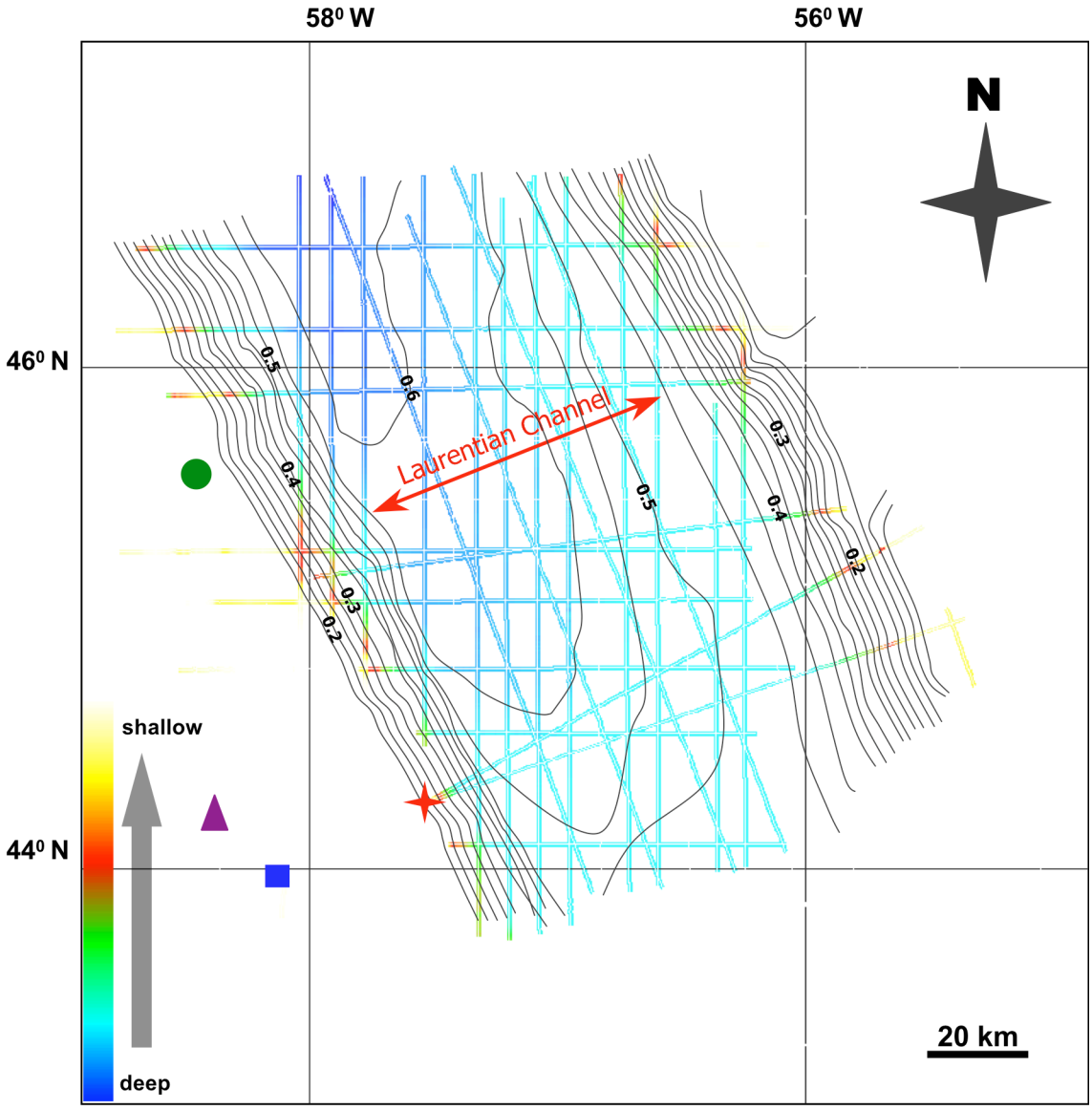

Figure 7. Contour map of water bottom in the Laurentian Subbasin. The contour unit is seconds. The contour map shows the shape of the Laurentian Channel with a depth of approximately 450 m (assuming water velocity is 1500 m/s). The Laurentian Channel formed during the Quaternary glaciation (Piper and Aksu, 1987) and covers mostly the study area. Location of Dauntless D-35 well (red star), Sachem D-76 (blue rectangle), Hesper I-52 (purple triangle), Adventure F-80 (green circle).

Figure 8. Seismic line B, uninterpreted (top) and interpreted (bottom). N1-N8 are the interpreted horizons, N1 is the Avalon unconformity, and N6 is the Cretaceous-Paleogene unconformity. S-1, S-2, and S-3 are the Cretaceous sequences identified in this study; S-4, S-5, S-6, and S-7 are the Paleogene sequences identified in this study. Line drawings of seismic profiles are displayed at approximately 4:1, assuming an average velocity of 3 km/s. See Figure 5 for line location.

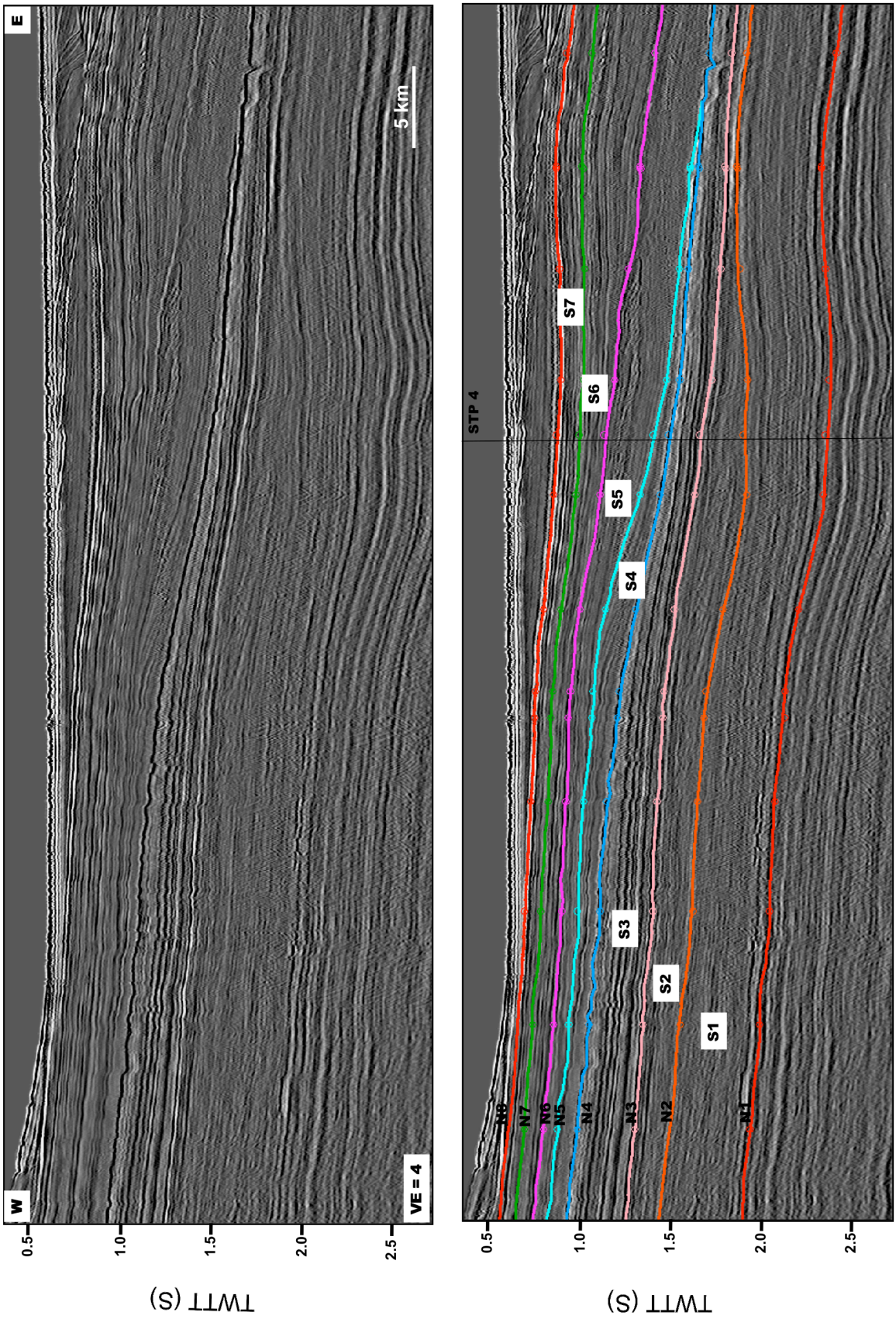
E
W
5 km
VE = 4
TWTT (S)
0.5
1.0
1.5
2.0
2.5
STP 4
S7
S6
S5
S4
S3
S2
S1
N8
N7
N6
N5
N4
N3
N2
N1
TWTT (S)
0.5
1.0
1.5
2.0
2.5

Figure 9. Seismic line STP-4, uninterpreted (top) and interpreted (bottom). N1-N8 are the interpreted horizons, N1 is the Avalon unconformity, and N6 is the Cretaceous-Paleogene unconformity. S-1, S-2, and S-3 are the Cretaceous sequences identified in this study; S-4, S-5, S-6, and S-7 are the Paleogene sequences identified in this study. Sequence boundaries are cut by faults; red lines show faults with normal separation. Line drawings of seismic profiles are displayed at approximately 4:1, assuming an average velocity of 3 km/s. See Figure 5 for line location.

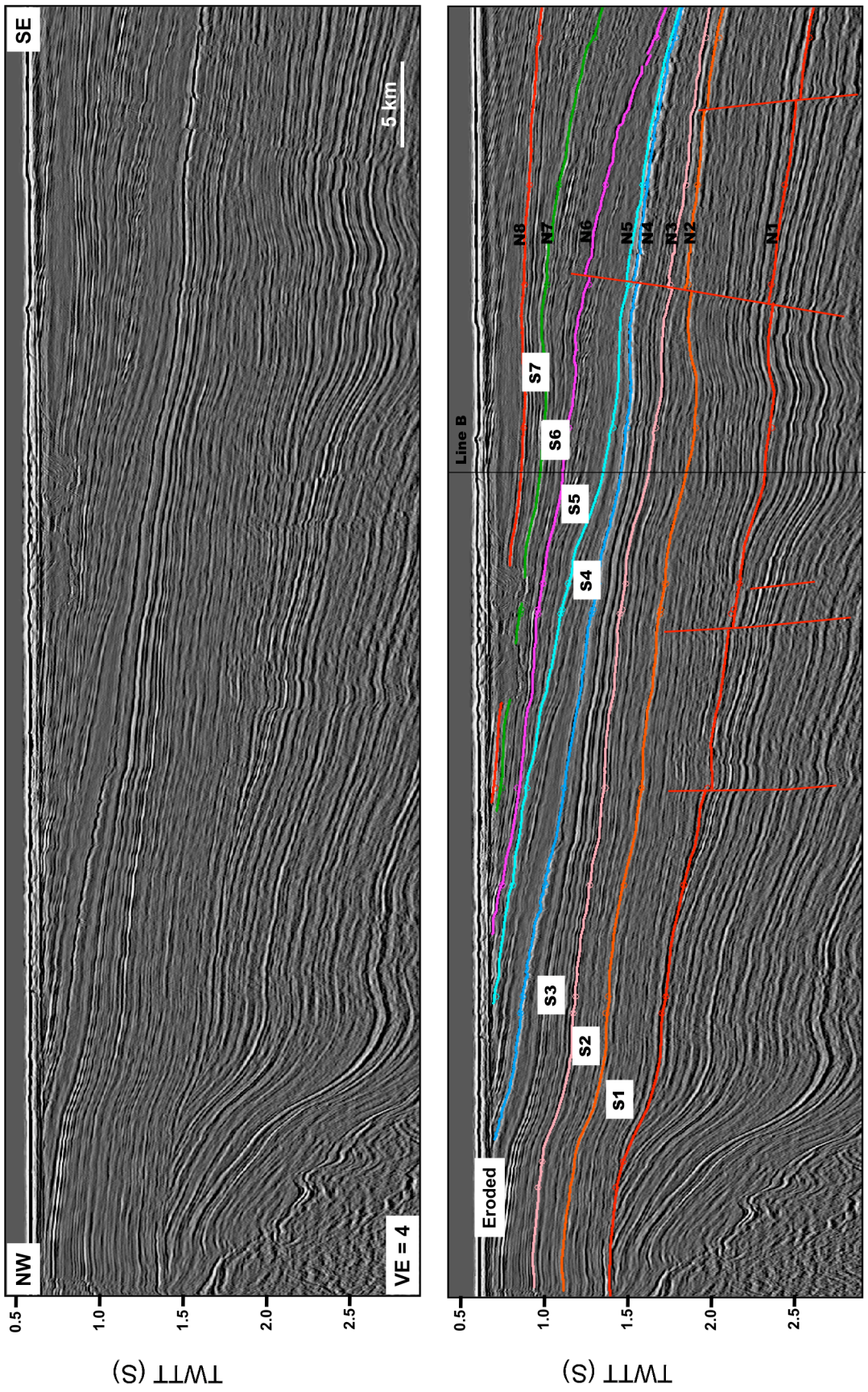
SE
NW
5 km
VE = 4
TWTT (S)
0.5
1.0
1.5
2.0
2.5
Line B
Eroded
S1
S2
S3
S4
S5
S6
S7
N1
N2
N3
N4
N5
N6
N7
N8
TWTT (S)

Figure 10. Seismic line STP-3, uninterpreted (top) and interpreted (bottom). N1-N8 are the interpreted horizons, N1 is the Avalon unconformity, and N6 is the Cretaceous-Paleogene unconformity. S-1, S-2, and S-3 are the Cretaceous sequences identified in this study; S-4, S-5, S-6, and S-7 are the Paleogene sequences identified in this study. Sequence boundaries are cut by faults and deformed by salt structures; red lines show faults with normal separation. Line drawings of seismic profiles are displayed at approximately 4:1, assuming an average velocity of 3 km/s. See Figure 5 for line location.

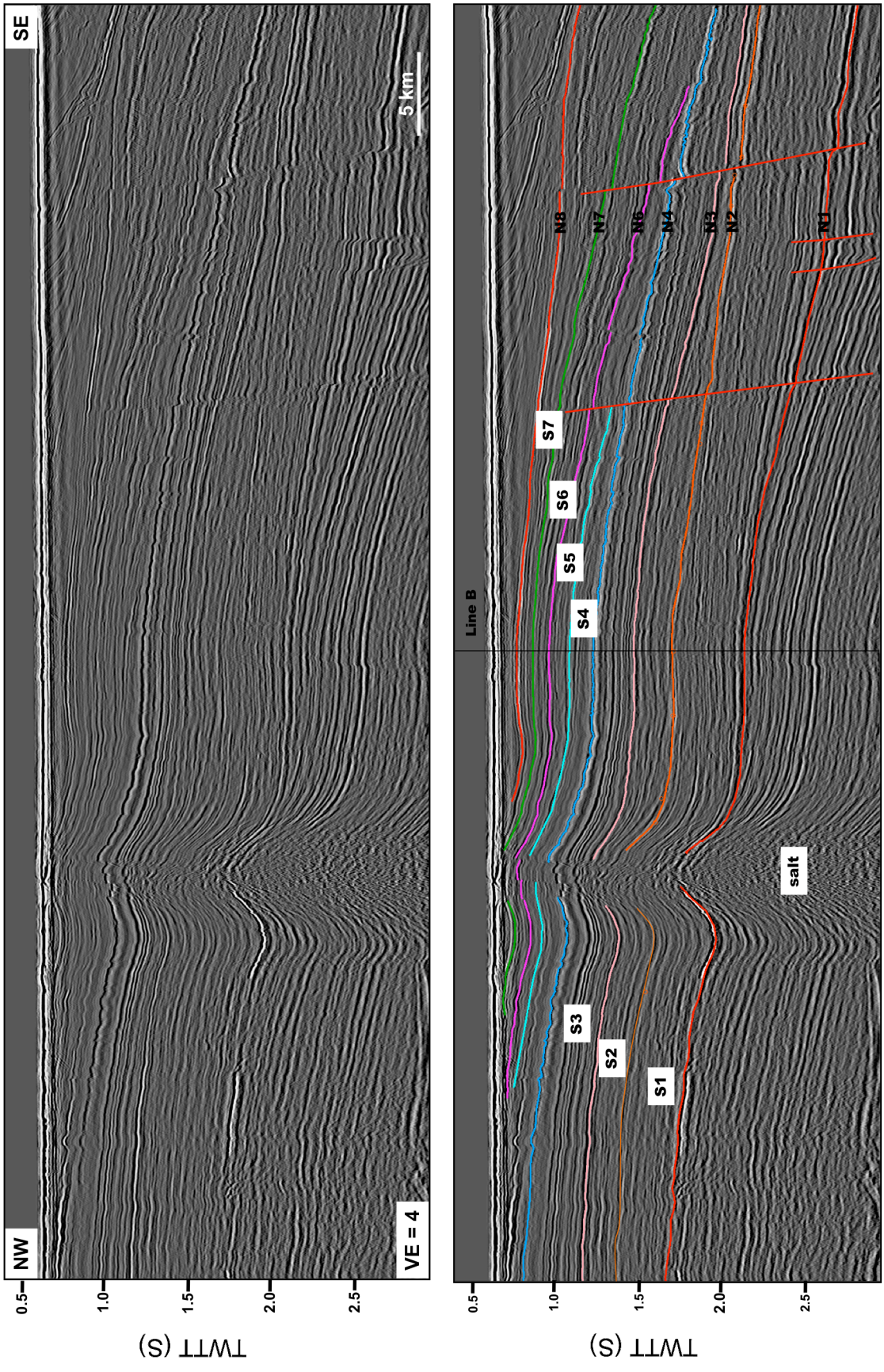
NW
SE
5 km
VE = 4
TWTT (S)
0.5
1.0
1.5
2.0
2.5
Line B
S1
S2
S3
S4
S5
S6
S7
N1
N2
N3
N4
N5
N6
N7
N8
salt

Figure 11. Seismic line C, uninterpreted (top) and interpreted (bottom). Deep-seated salt movement created the folding at depth approximately 2.1 second. Incised valleys are present in the upper part of seismic data. Line drawings of seismic profiles are displayed at approximately 4:1, assuming an average velocity of 3 km/s. See Figure 5 for line location.

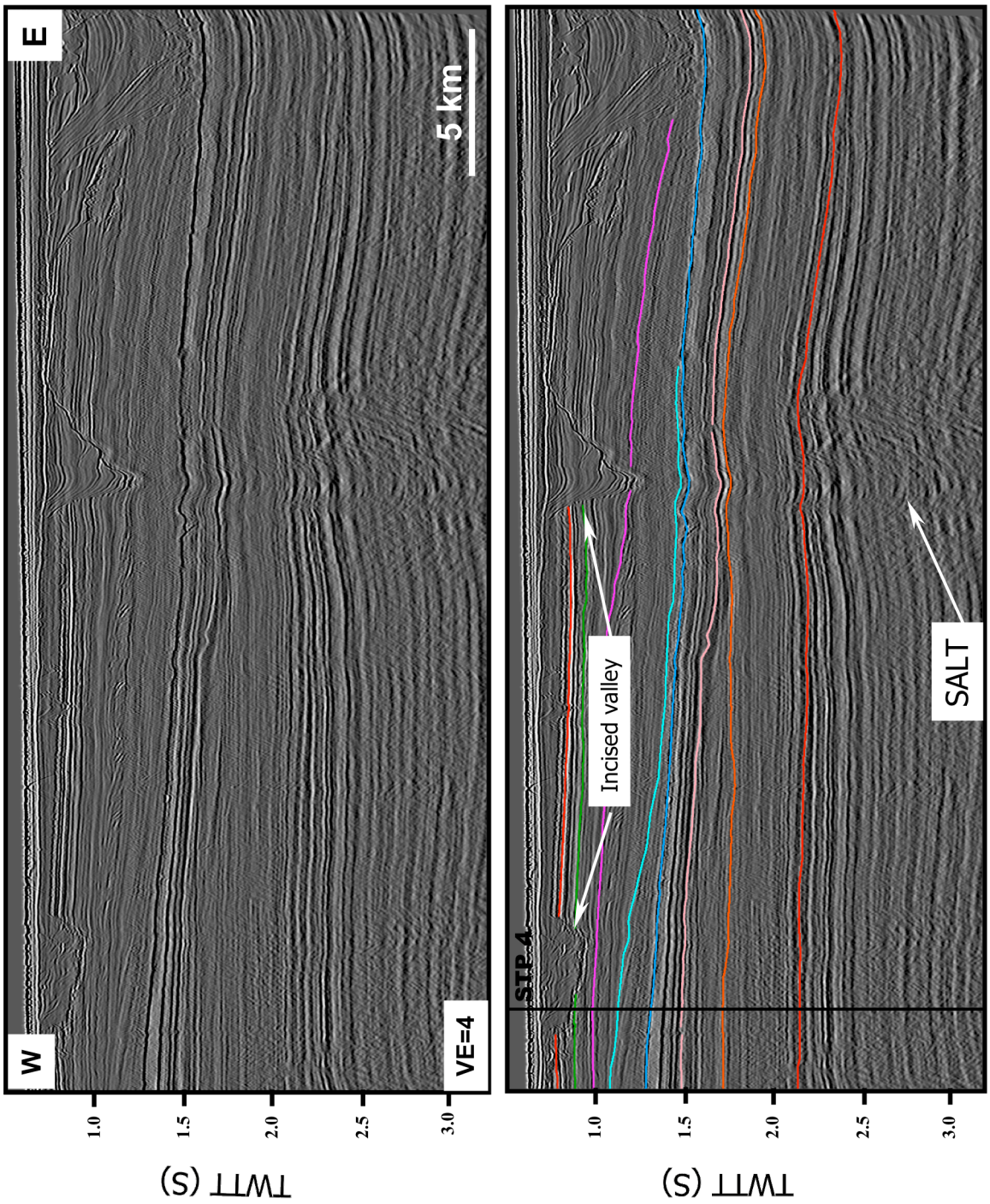
W
E
5 km
VE=4
TWTT (S)
1.0
1.5
2.0
2.5
3.0
STP 4
Incised valley
SALT
TWTT (S)
1.0
1.5
2.0
2.5
3.0

Figure 12. Seismic line D, uninterpreted (top) and interpreted (bottom). N1, N3 and N4 are the interpreted horizons in this study. In general, all the Paleogene sequences have been partially eroded. Yellow lines show the water-bottom multiples. Line drawings of seismic profiles are displayed at approximately 4:1, assuming an average velocity of 3 km/s. See Figure 5 for line location.

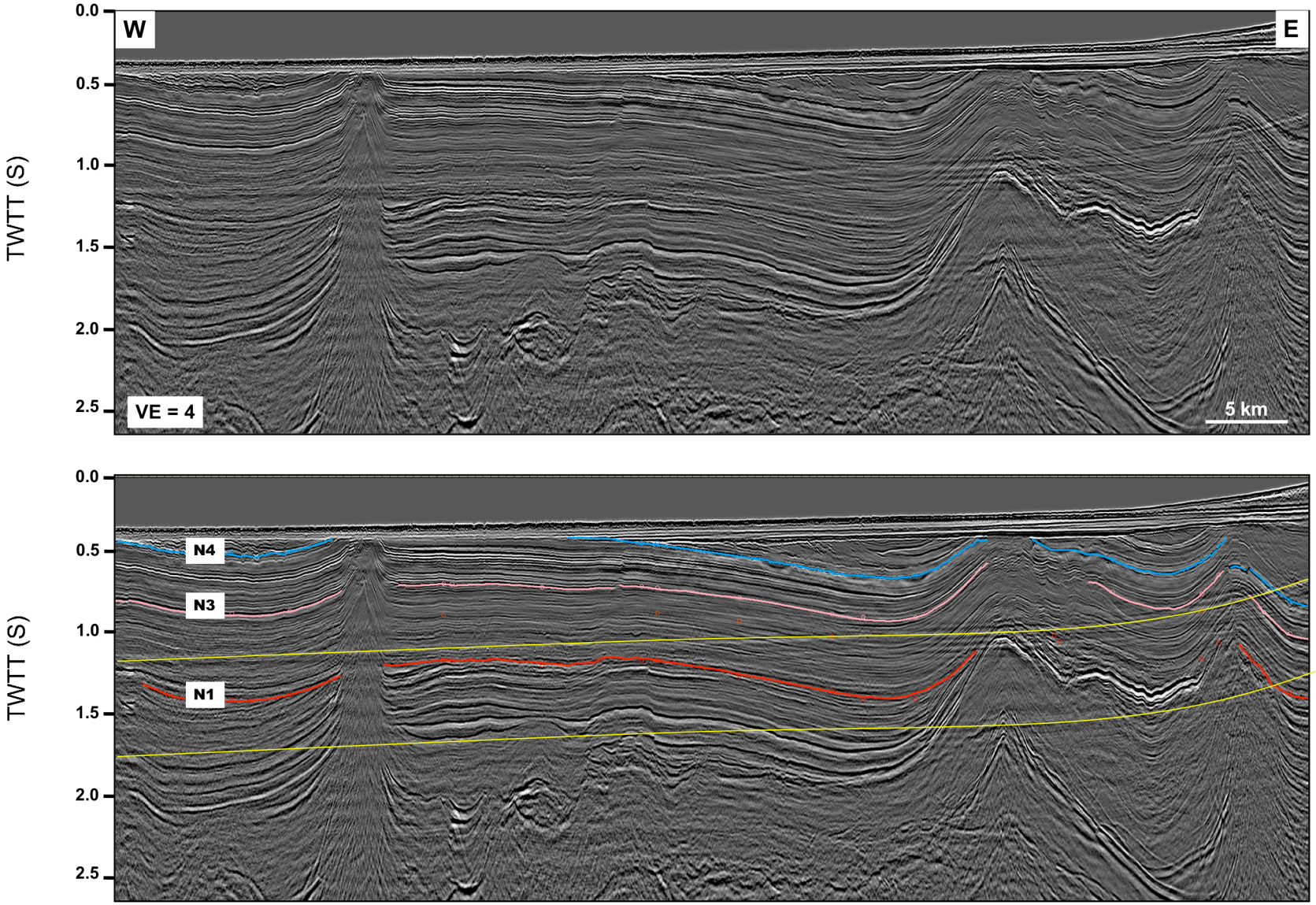
TWTT (S)
0.0
0.5
1.0
1.5
2.0
2.5
W
E
VE = 4
5 km
TWTT (S)
0.0
0.5
1.0
1.5
2.0
2.5
N4
N3
N1

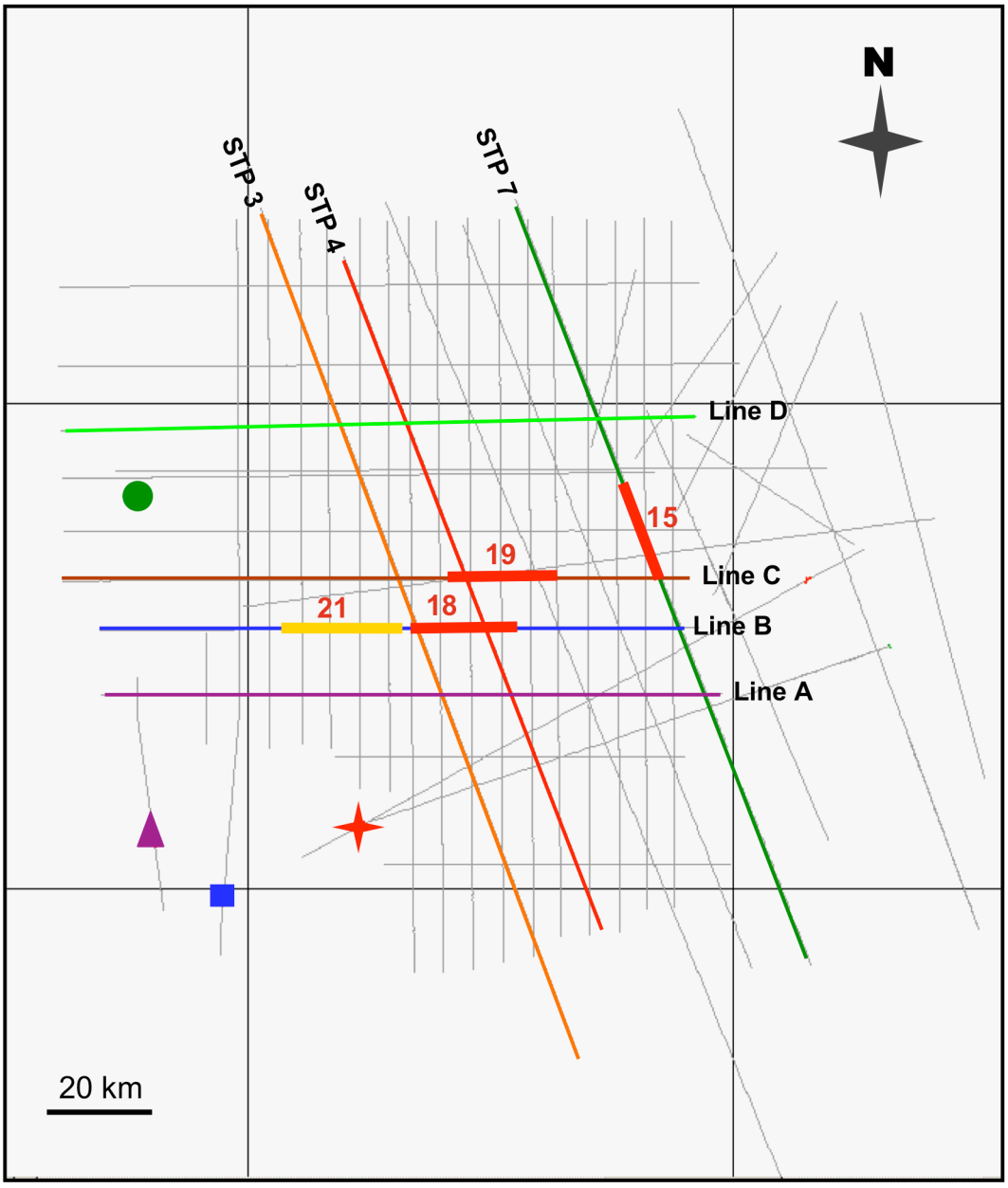

Figure 13. Location of Dauntless D-35 well (red star), Sachem D-76 (blue rectangle), Hesper I-52 (purple triangle), Adventure F-80 (green circle) and seismic data used in this study. Bold red lines are locations of Figures 15, 18 and 19; bold yellow line is the location of figure 21.

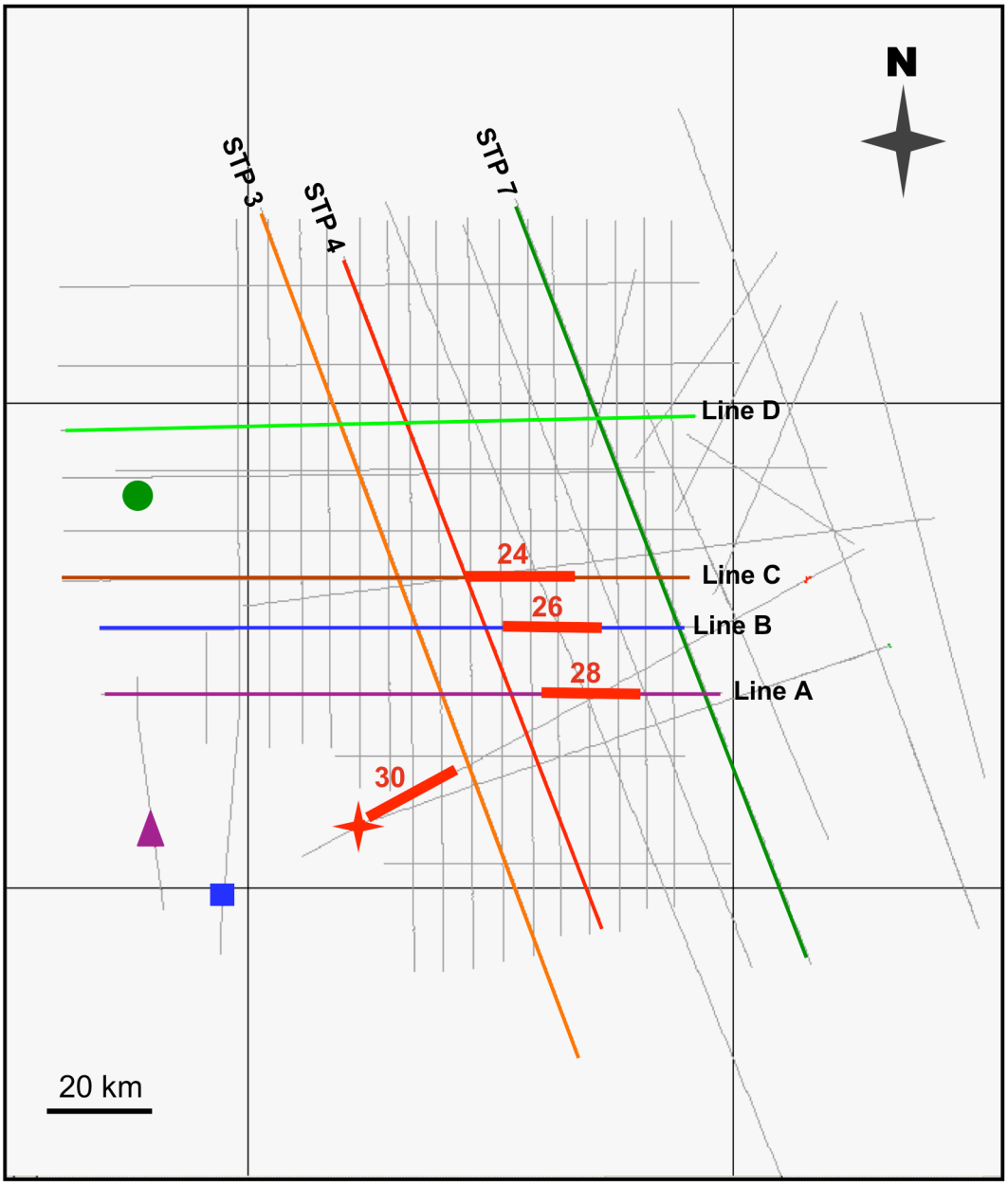

Figure 14. Location of Dauntless D-35 well (red star), Sachem D-76 (blue rectangle), Hesper I-52 (purple triangle), Adventure F-80 (green circle) and seismic data used in this study. Bold red lines are location of Figures 24, 26, 28 and 30.

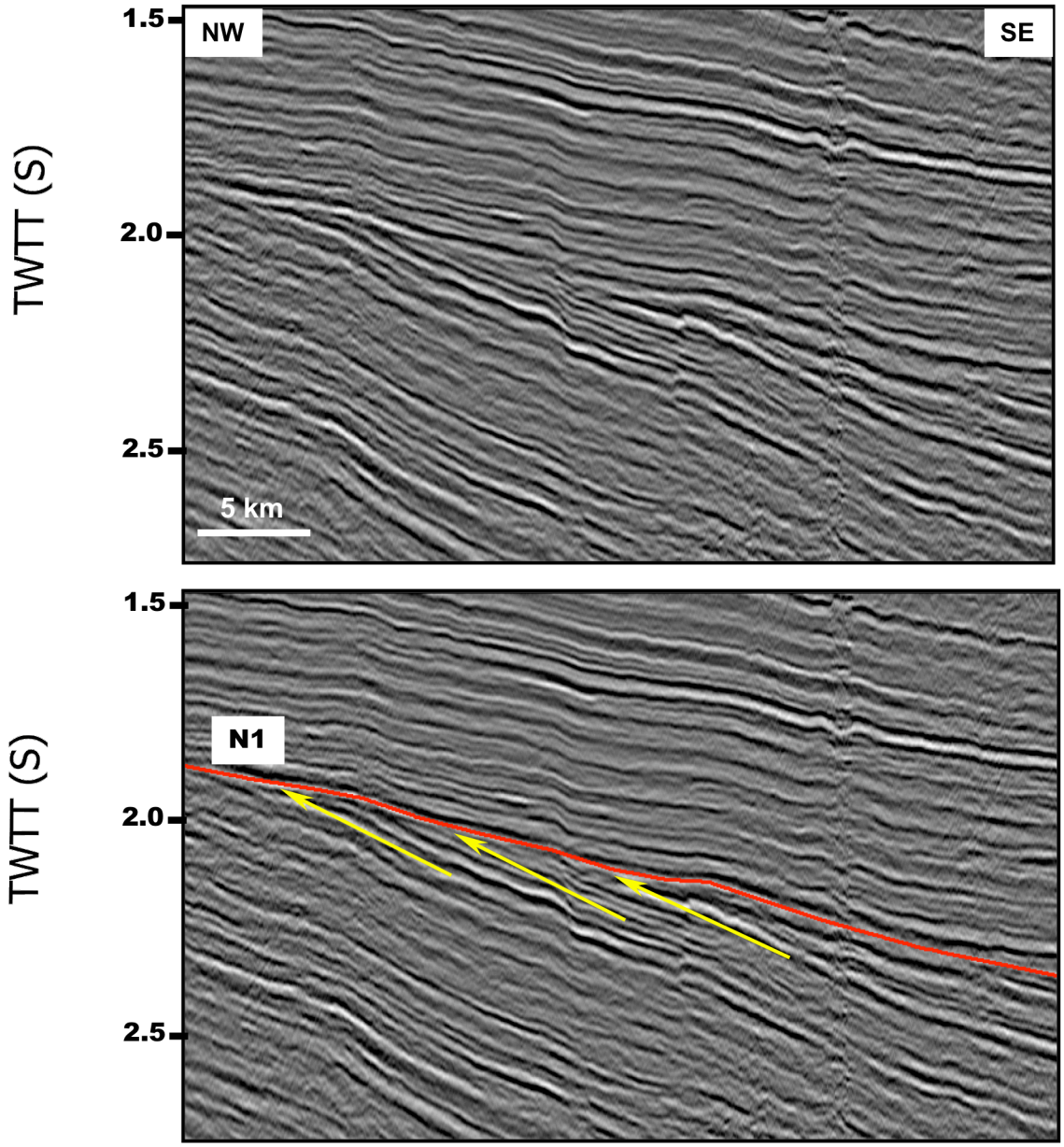

Figure 15. Seismic line STP 7, uninterpreted (top) and interpreted (bottom). Erosional truncation shows that horizon N1 is a potential sequence boundary. Horizon N1 is a major angular unconformity separating relatively flat and undeformed Cretaceous rocks above from folded and tilted Jurassic rocks below. See Figure 13 for location of seismic line.

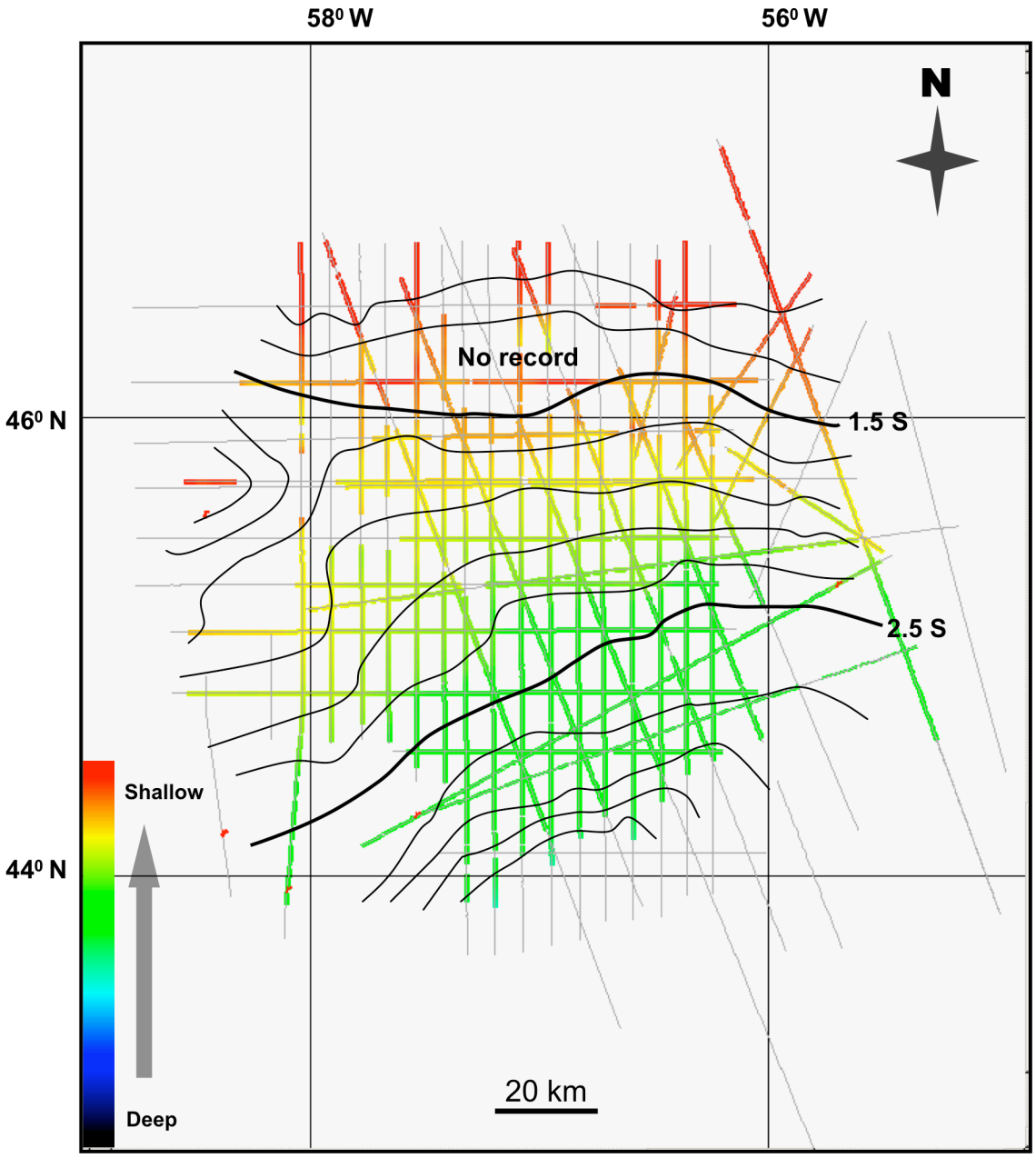

Figure 16. Contour map of Horizon N1. The contours (black lines) represent two-way-travel time. The contour interval is 0.2 second. Horizon N1 exists throughout the study area. In the northern part, salt structures obscure the horizon interpretation producing a no-record zone. Horizon N1 deepens toward the south.

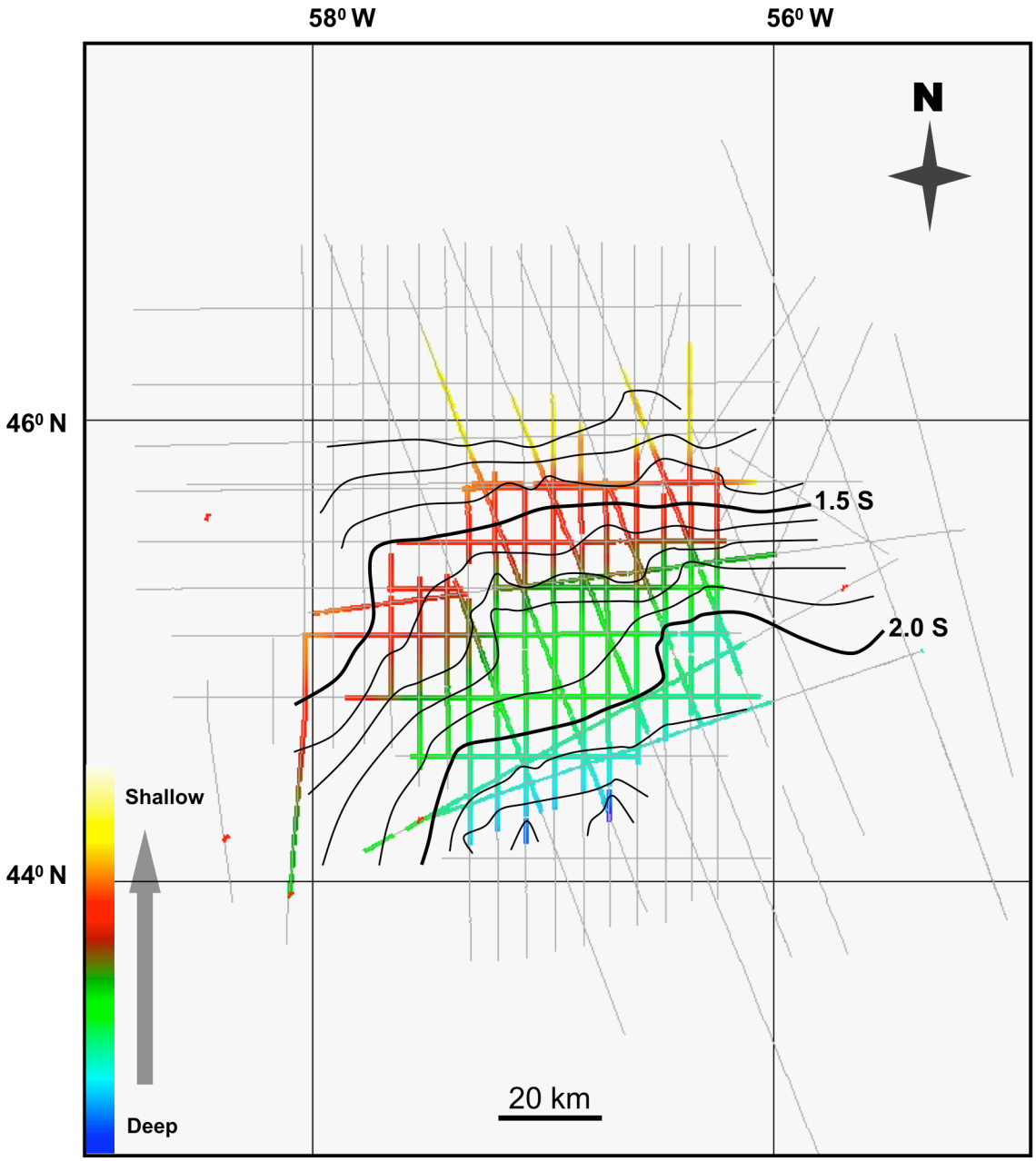

Figure 17. Contour map of Horizon N2. The contours (black lines) represent two-way-travel time. The contour interval is 0.1 second. Horizon N2 exists throughout the study area. Horizon N2 deepens toward the southeast

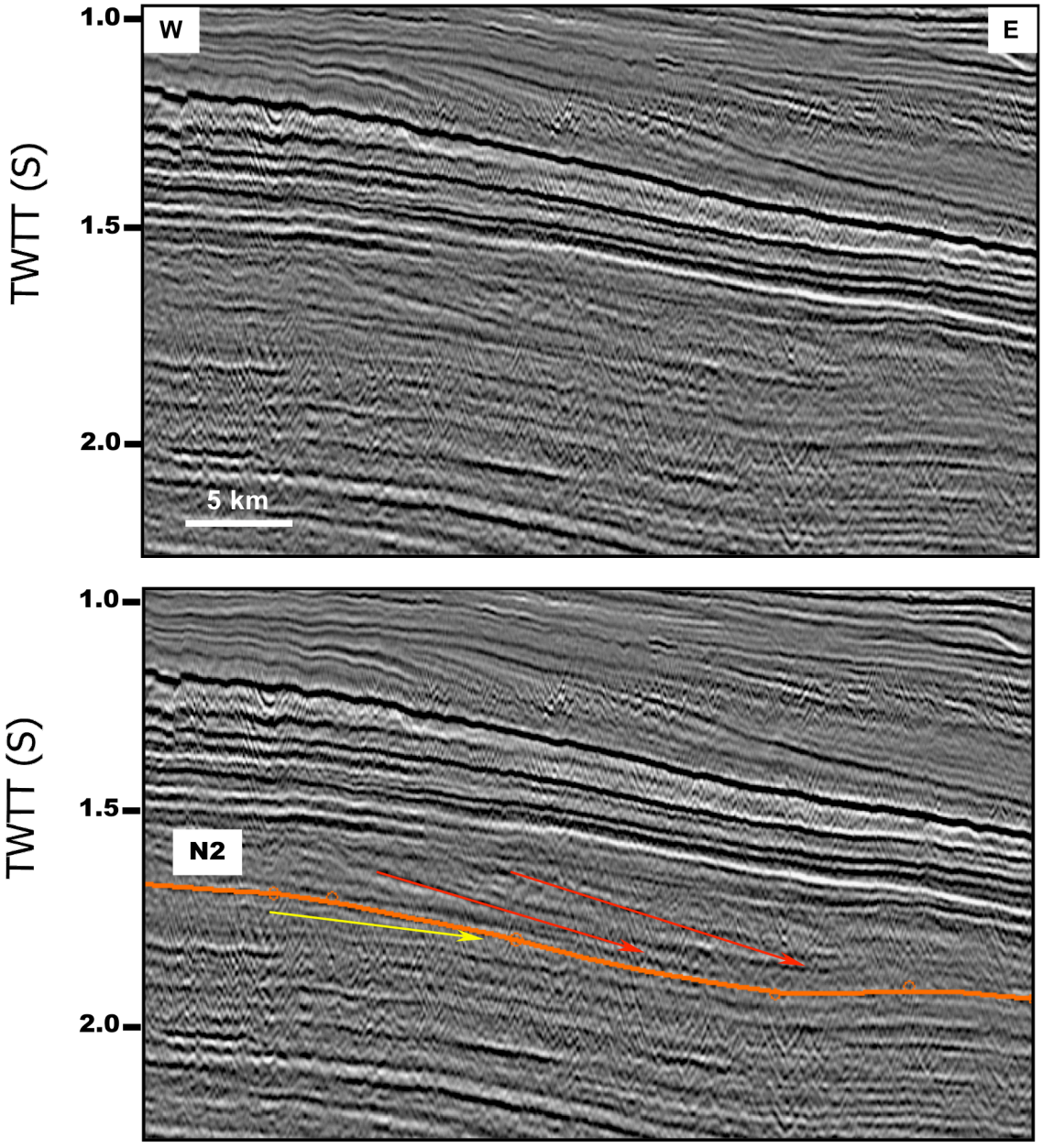

Figure 18. Seismic line B, uninterpreted (top) and interpreted (bottom). Erosional truncation and downlapping terminations show that Horizon N2 is a potential sequence boundary. See Figure 13 for location of seismic line.

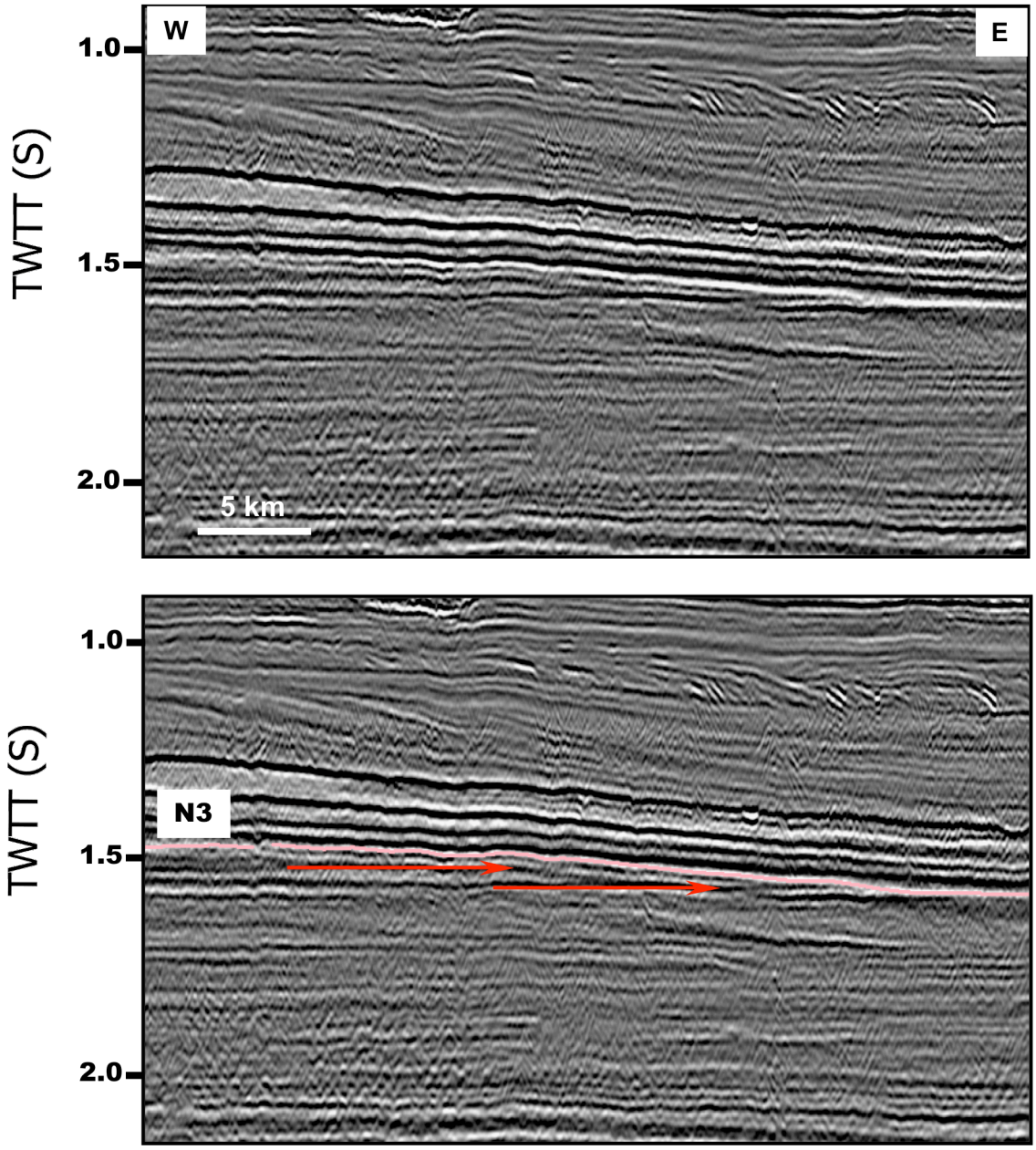

Figure 19. Seismic line C, uninterpreted (top) and interpreted (bottom). Erosional truncations show that Horizon N3 is a potential sequence boundary. See Figure 13 for location of seismic line.

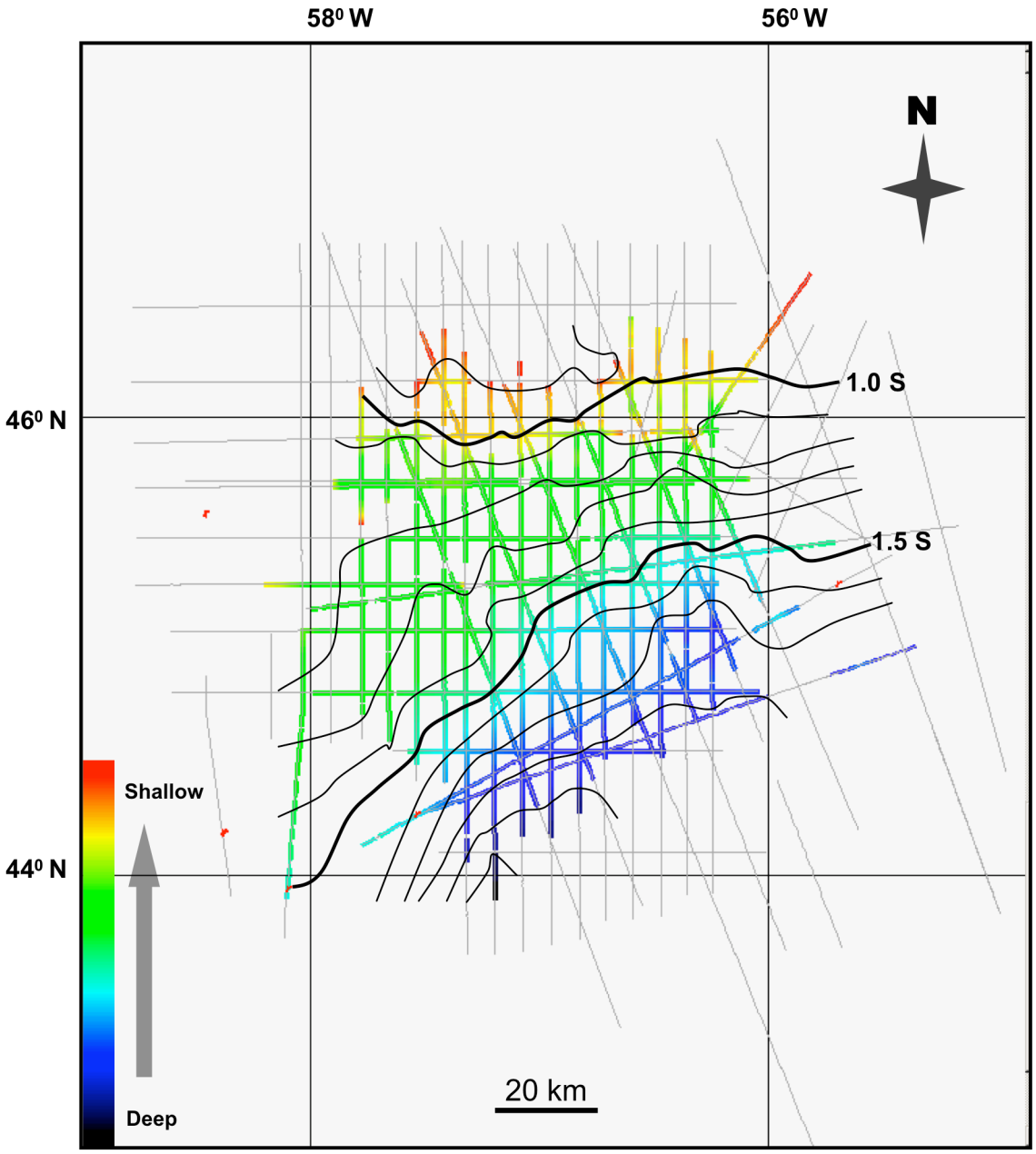

Figure 20. Contour map of Horizon N3. The contours (black lines) represent two-way-travel time. The contour interval is 0.1 second. Horizon N3 exists throughout the study area. Horizon N3 deepens toward the southeast.

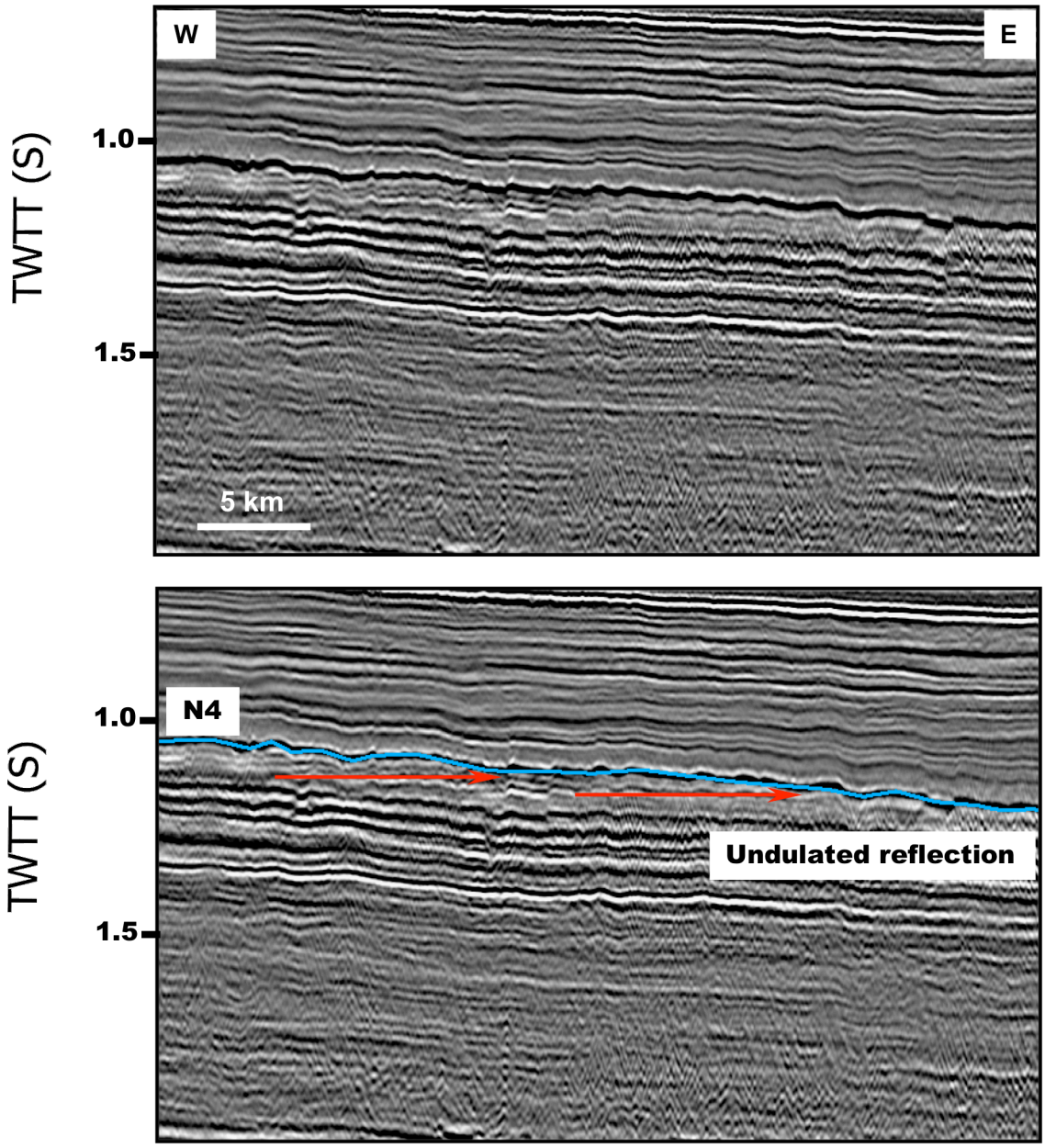

Figure 21. Seismic line B, uninterpreted (top) and interpreted (bottom). Erosional truncations show that horizon N4 is a potential sequence boundary. Horizon N4 is associated with an undulating reflection or irregular surface. See Figure 13 for location of seismic line.

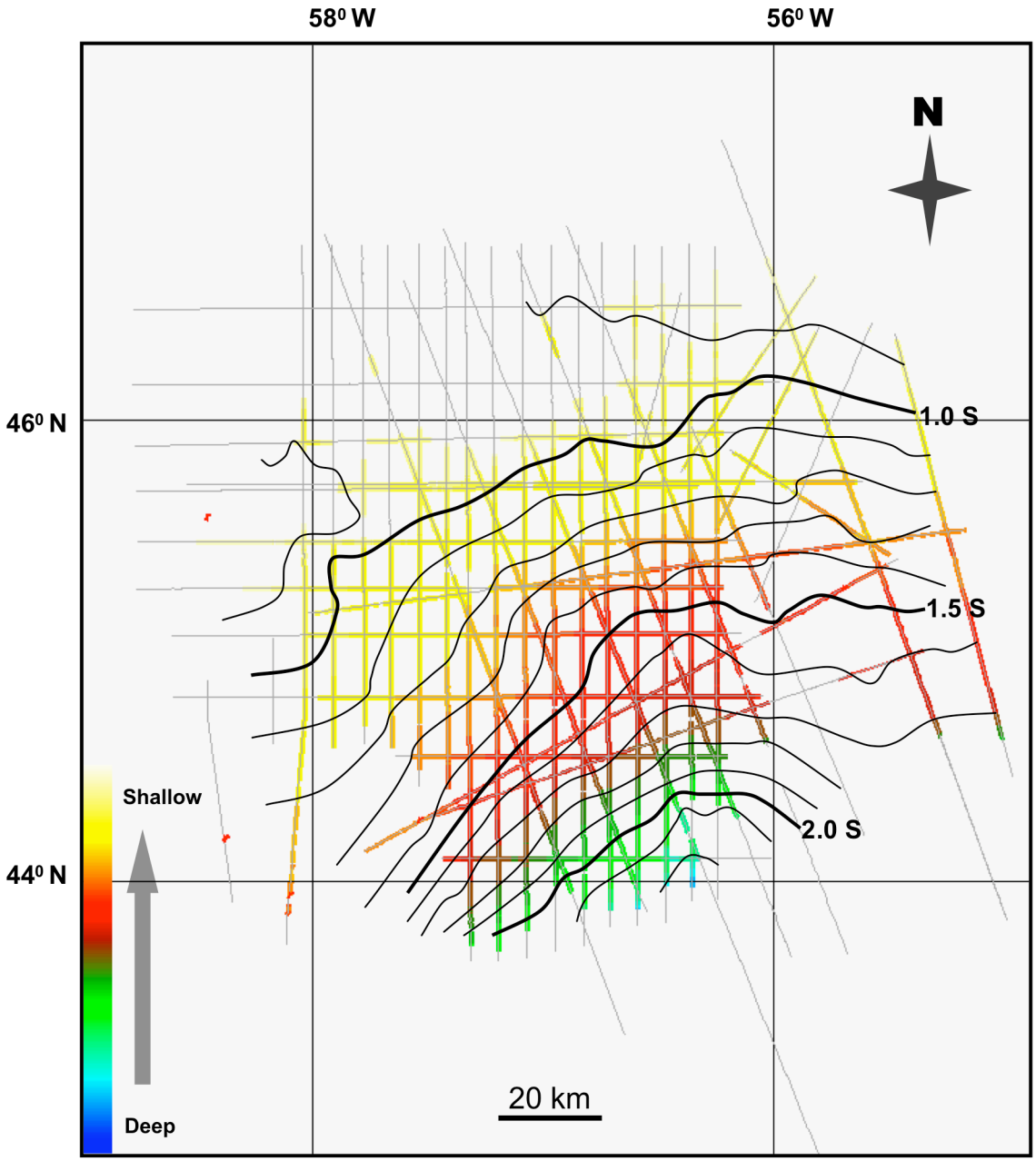

Figure 22. Contour map of Horizon N4. The contours (black lines) represent two-way-travel time. The contour interval is 0.1 second. Horizon N4 exists throughout the study area. Horizon N4 deepens toward the southeast.

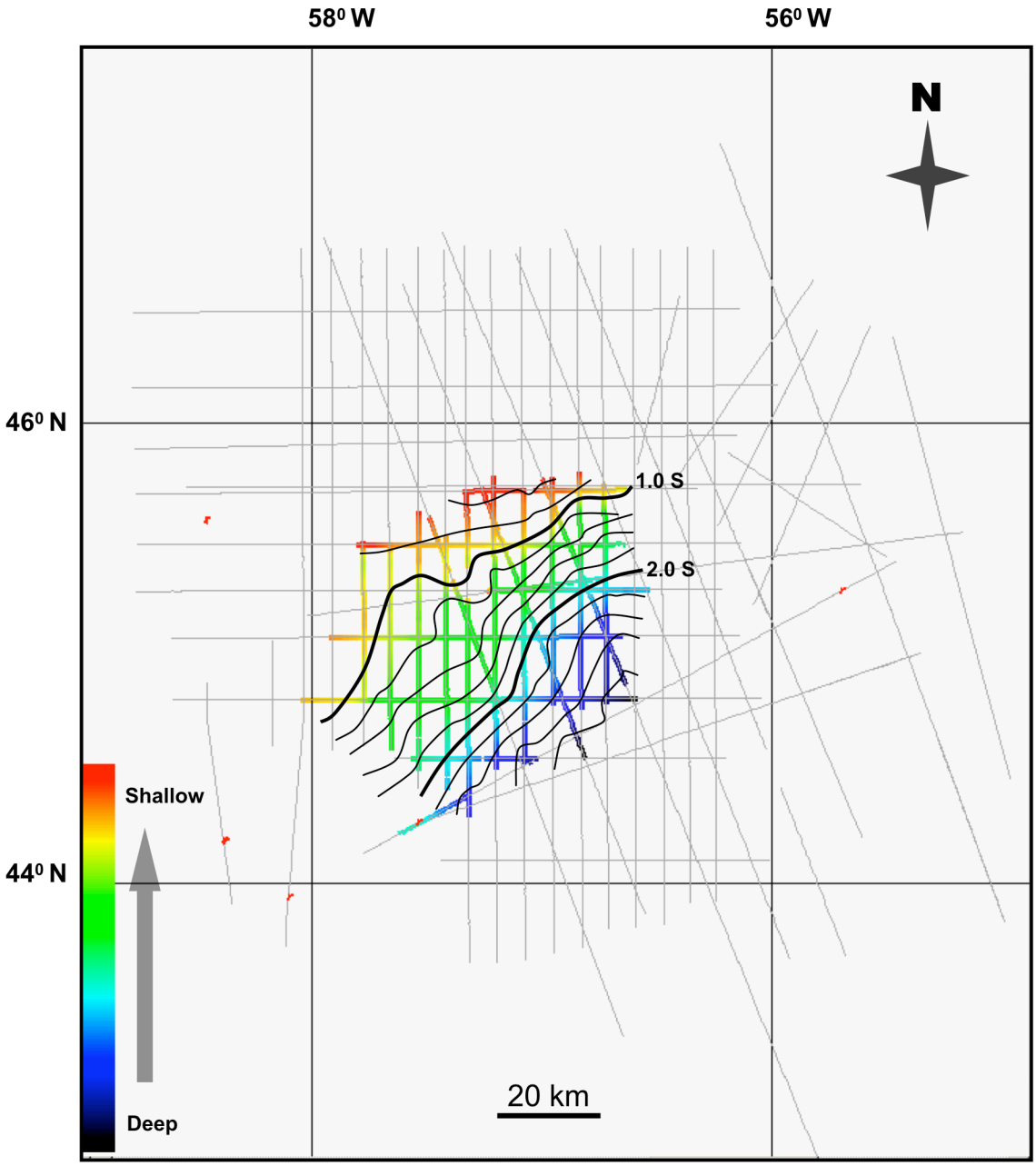

Figure 23. Contour map of Horizon N5. The contours (black lines) represent two-way-travel time. The contour interval is 0.2 second. Horizon N5 exists in the center part of the study area. Horizon N5 deepens toward the southeast.

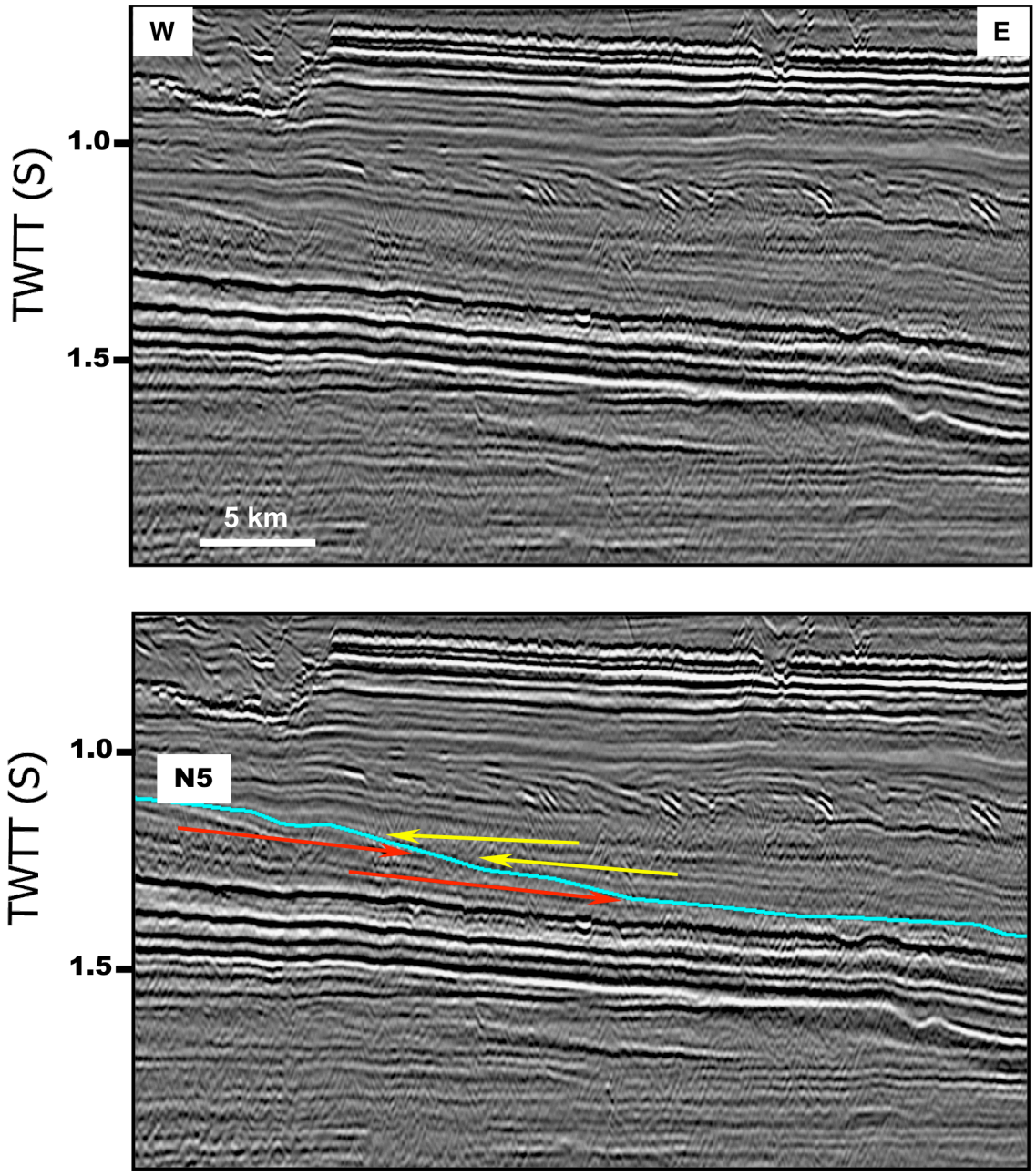

Figure 24. Seismic line C, uninterpreted (top) and interpreted (bottom). Erosional truncations and onlapping terminations show that Horizon N5 is a potential sequence boundary. See Figure 14 for location of seismic line.

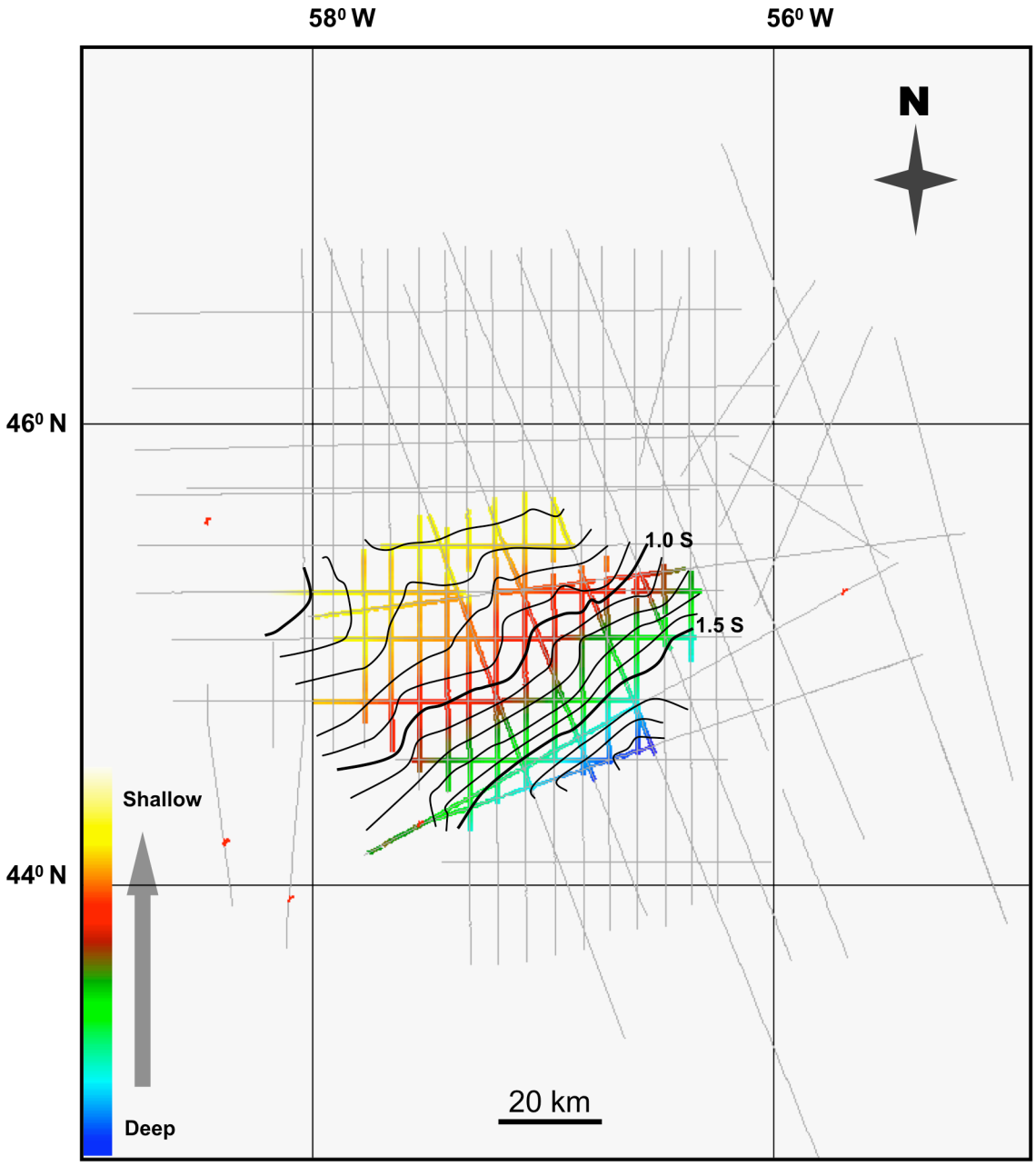

Figure 25. Contour map of Horizon N6. The contours (black lines) represent two-way-travel time. The contour interval is 0.1 second. Horizon N6 exists in the center part of the study area. Horizon N6 deepens toward the southeast.

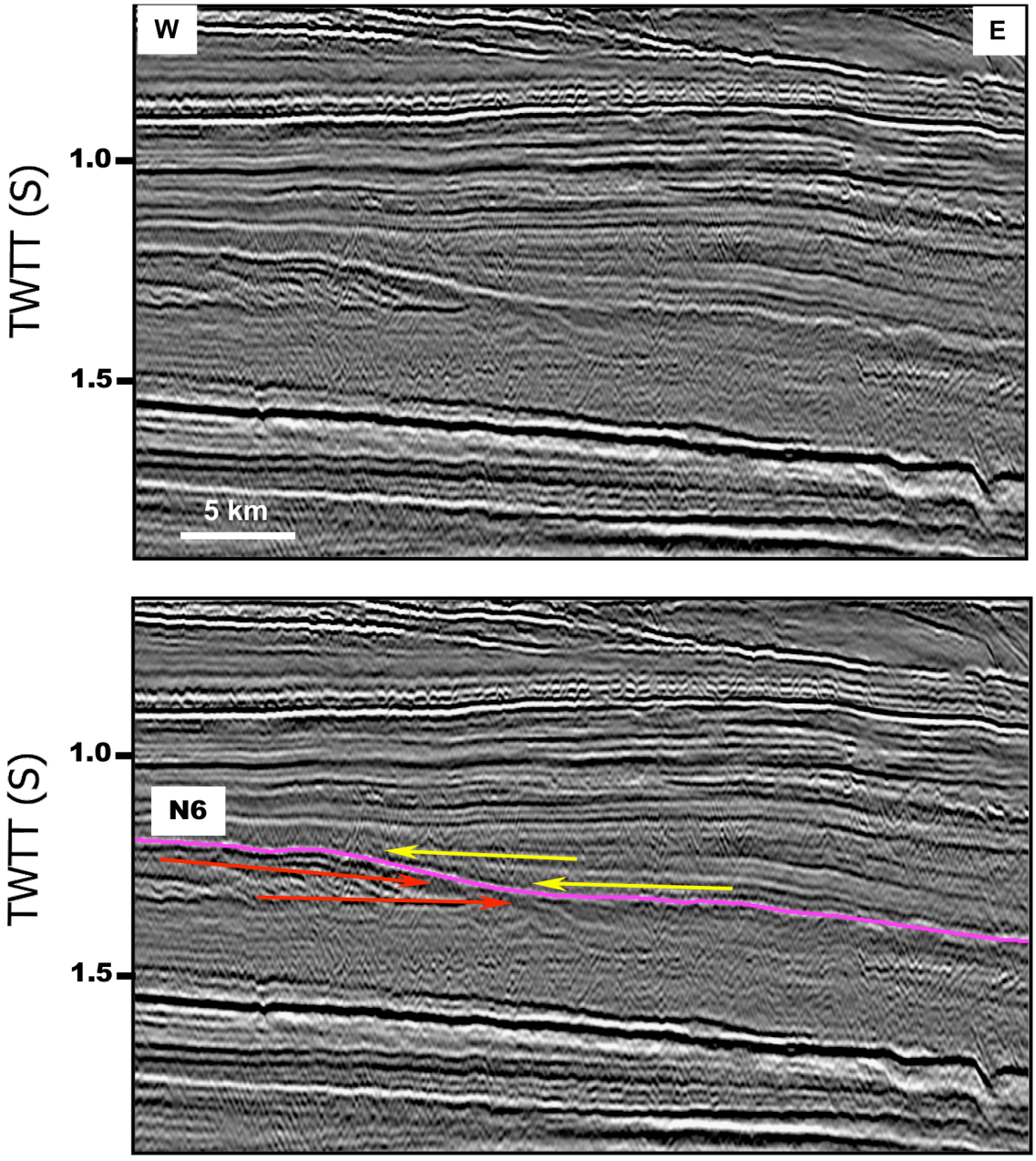

Figure 26. Seismic line B, uninterpreted (top) and interpreted (bottom). Erosional truncations and onlapping terminations show that Horizon N6 is a potential sequence boundary. See Figure 14 for location of seismic line.

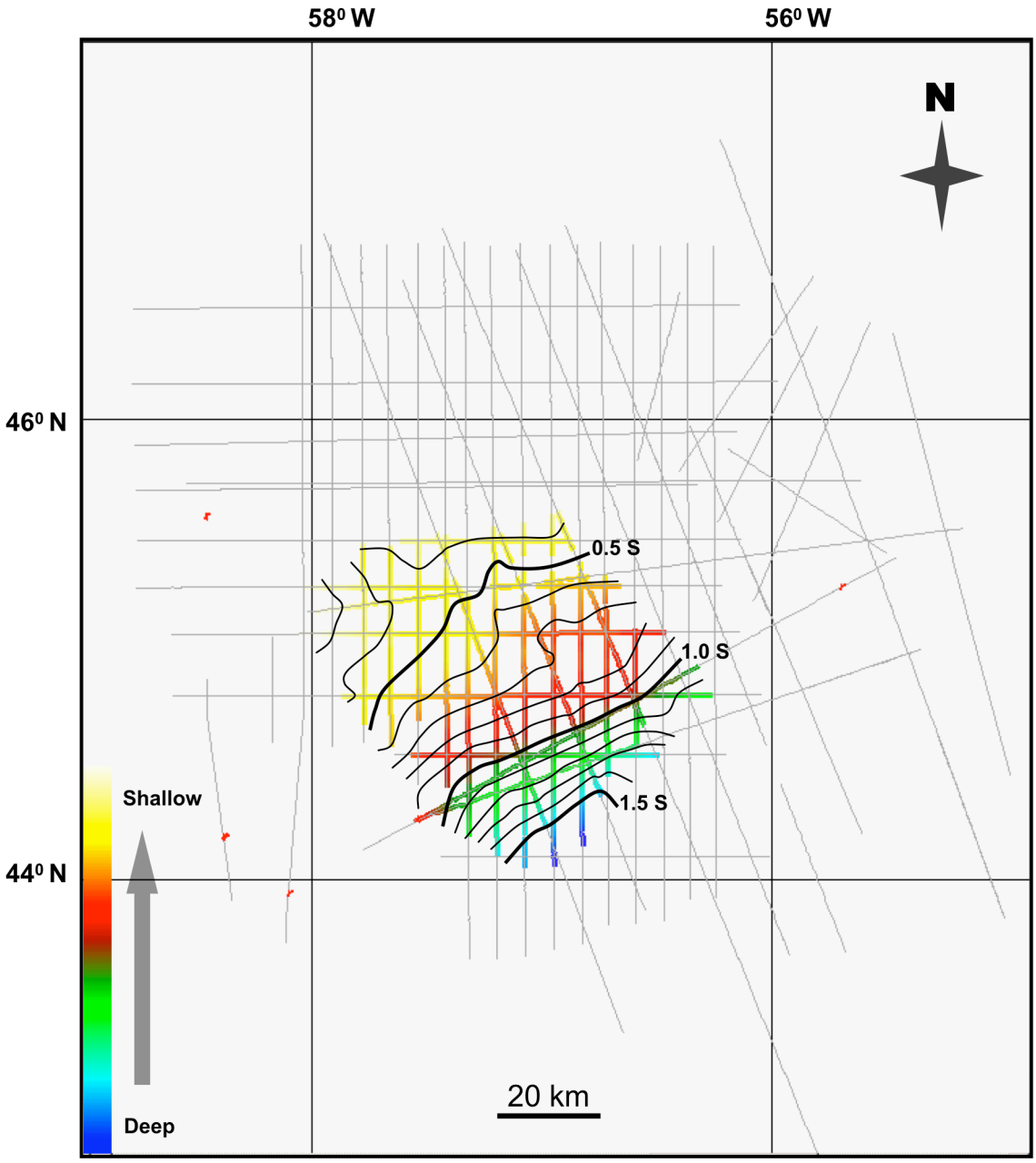

Figure 27. Contour map of Horizon N7. The contours (black lines) represent two-way-travel time. The contour interval is 0.1 second. Horizon N7 exists in the center part of the study area. Horizon N7 deepens toward the southeast.

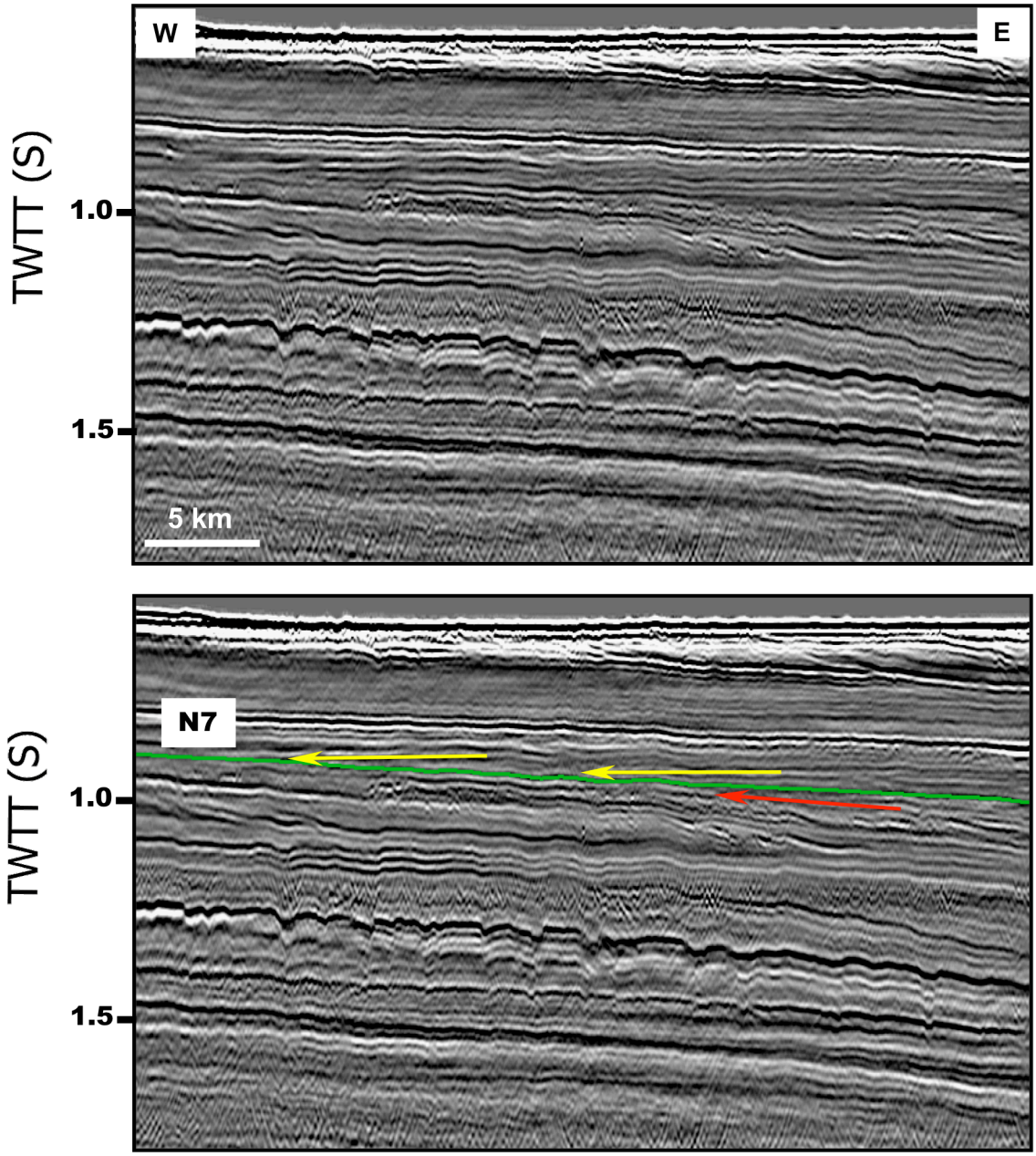

Figure 28. Seismic line A, uninterpreted (top) and interpreted (bottom). Erosional truncations and onlapping terminations show that horizon N7 is a potential sequence boundary. See Figure 14 for location of seismic line.

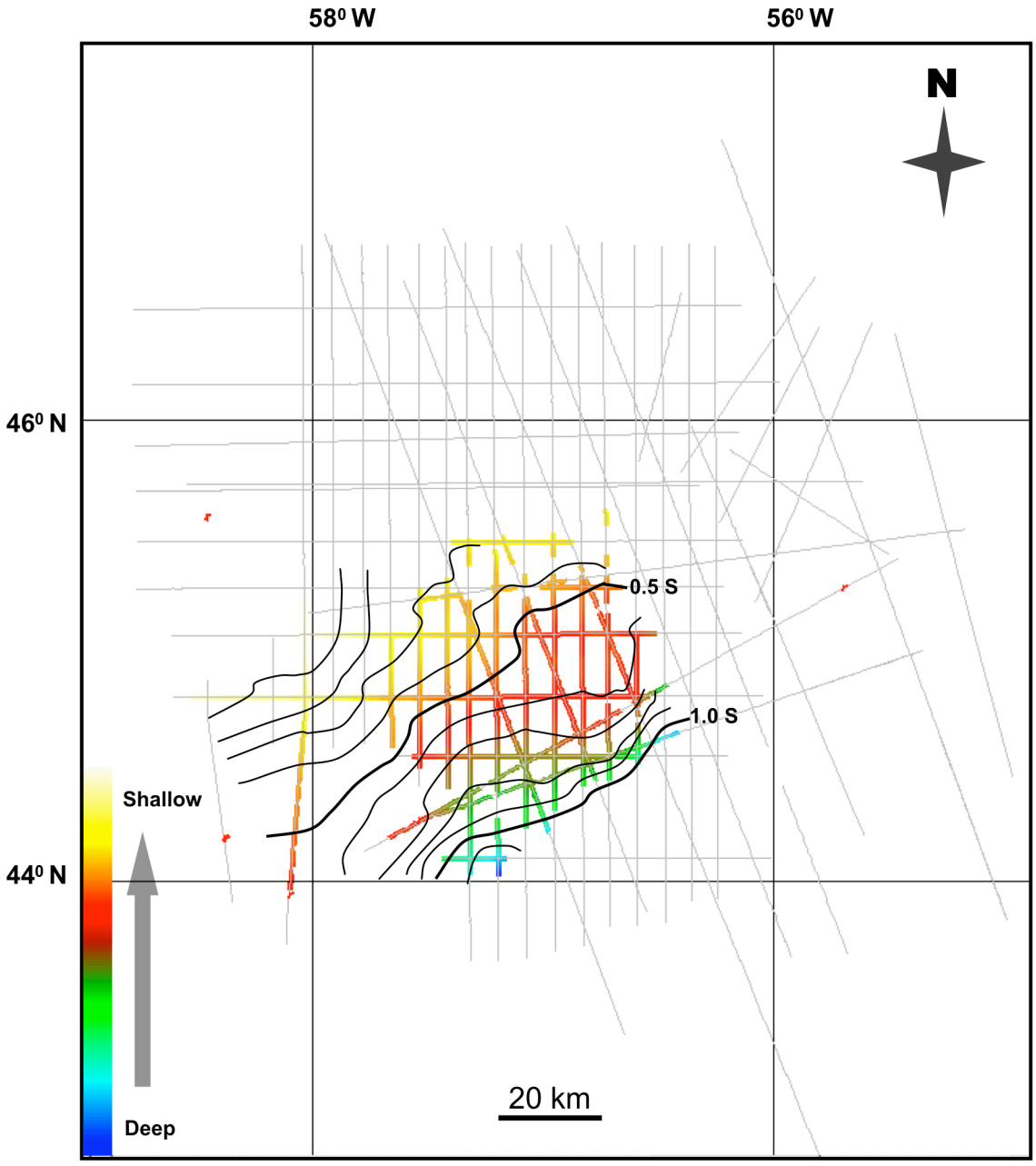

Figure 29. Contour map of Horizon N8. The contours (black lines) represent two-way-travel time. The contour interval is 0.1 second. Horizon N8 exists in the southwest part of the study area. Horizon N8 deepens toward the southeast.

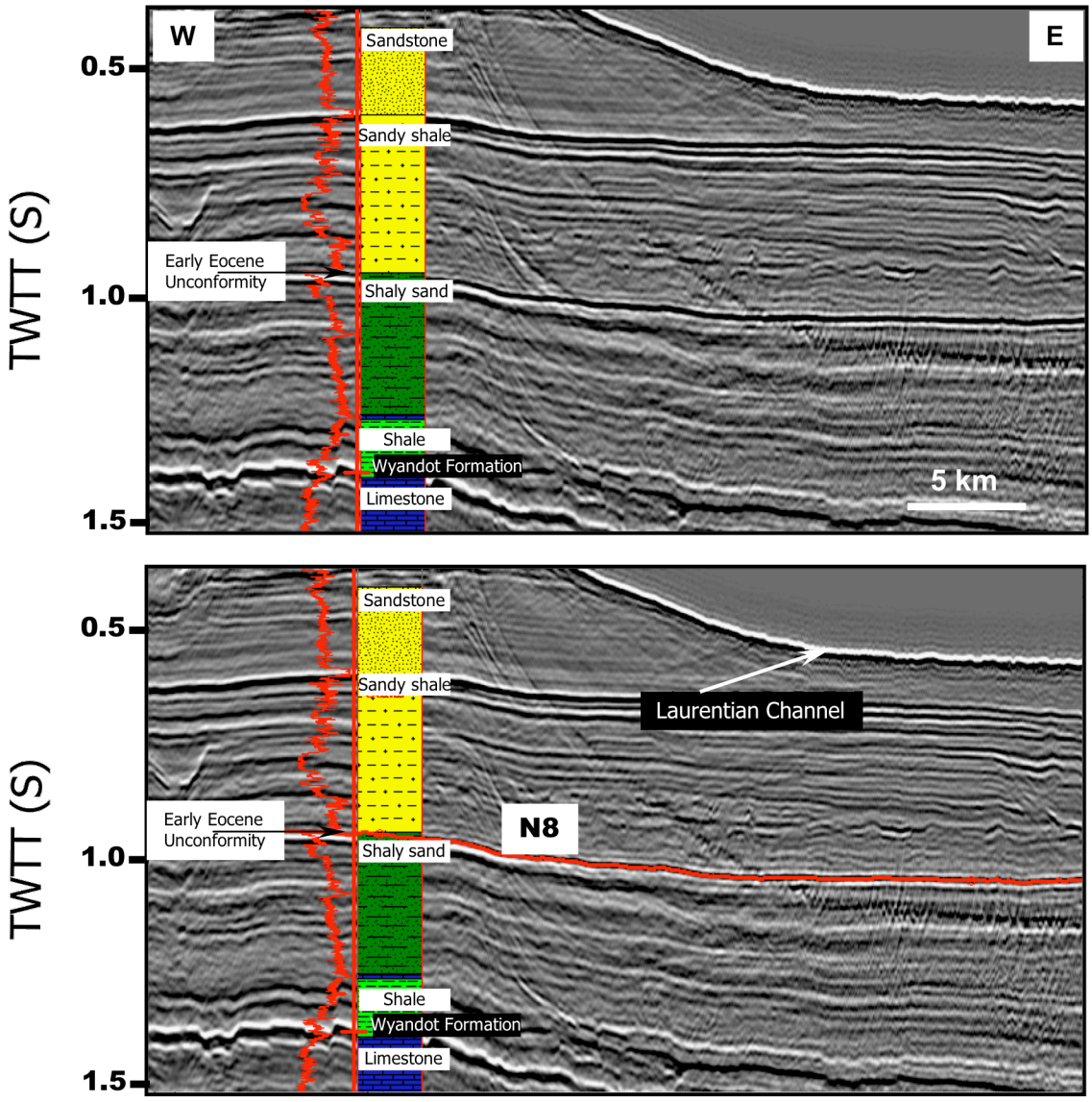

Figure 30. Seismic line X correlating with Dauntless D-35 well, uninterpreted (top) and interpreted (bottom). Horizon N8 is a strong-to-moderate-amplitude reflection associated with an Early Eocene unconformity (based on the Dauntless D-35 well). See Figure 14 for location of seismic line.

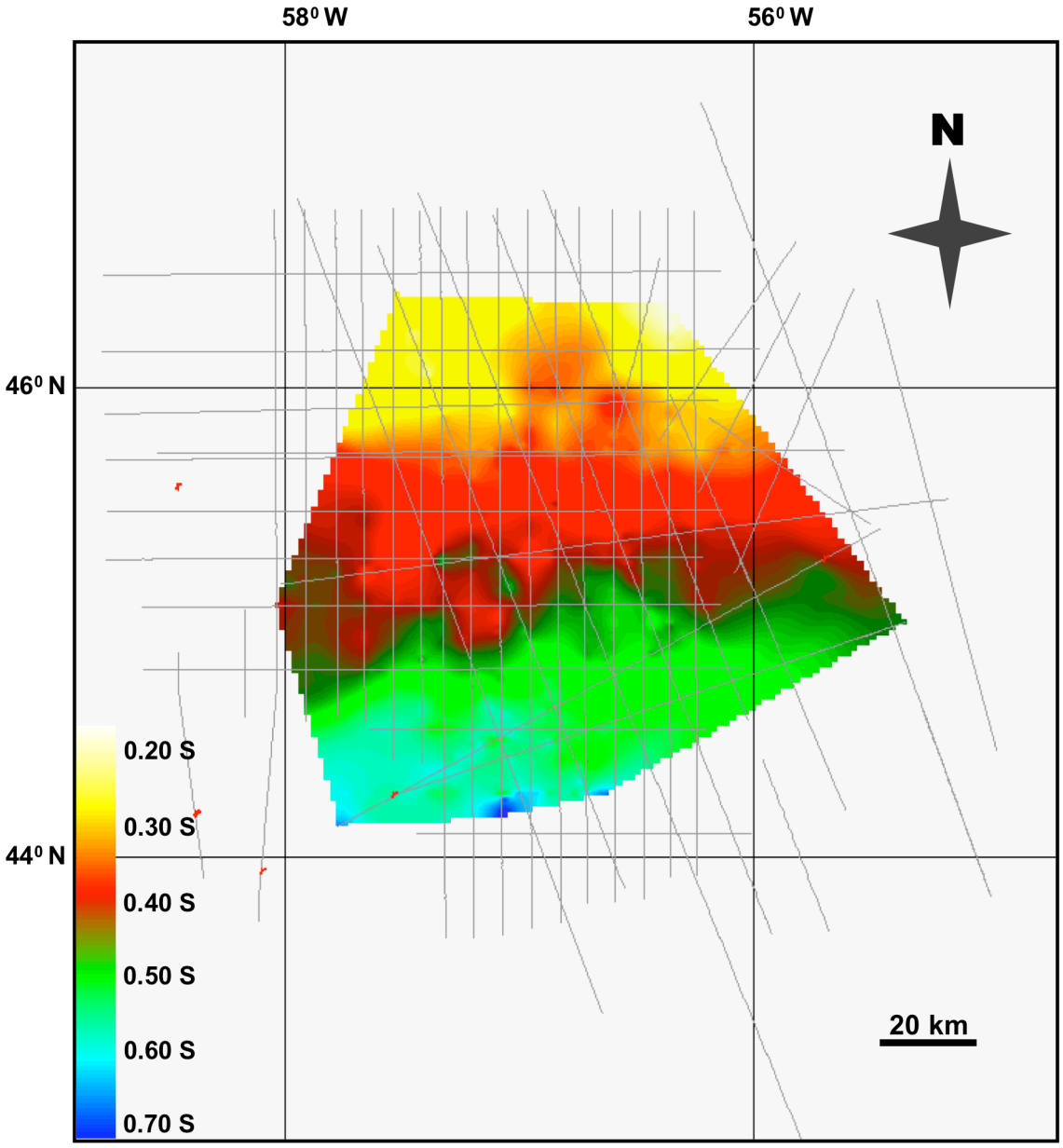

Figure 31. Isochron map of Sequence-1. Sequence-1 thickens toward the south.

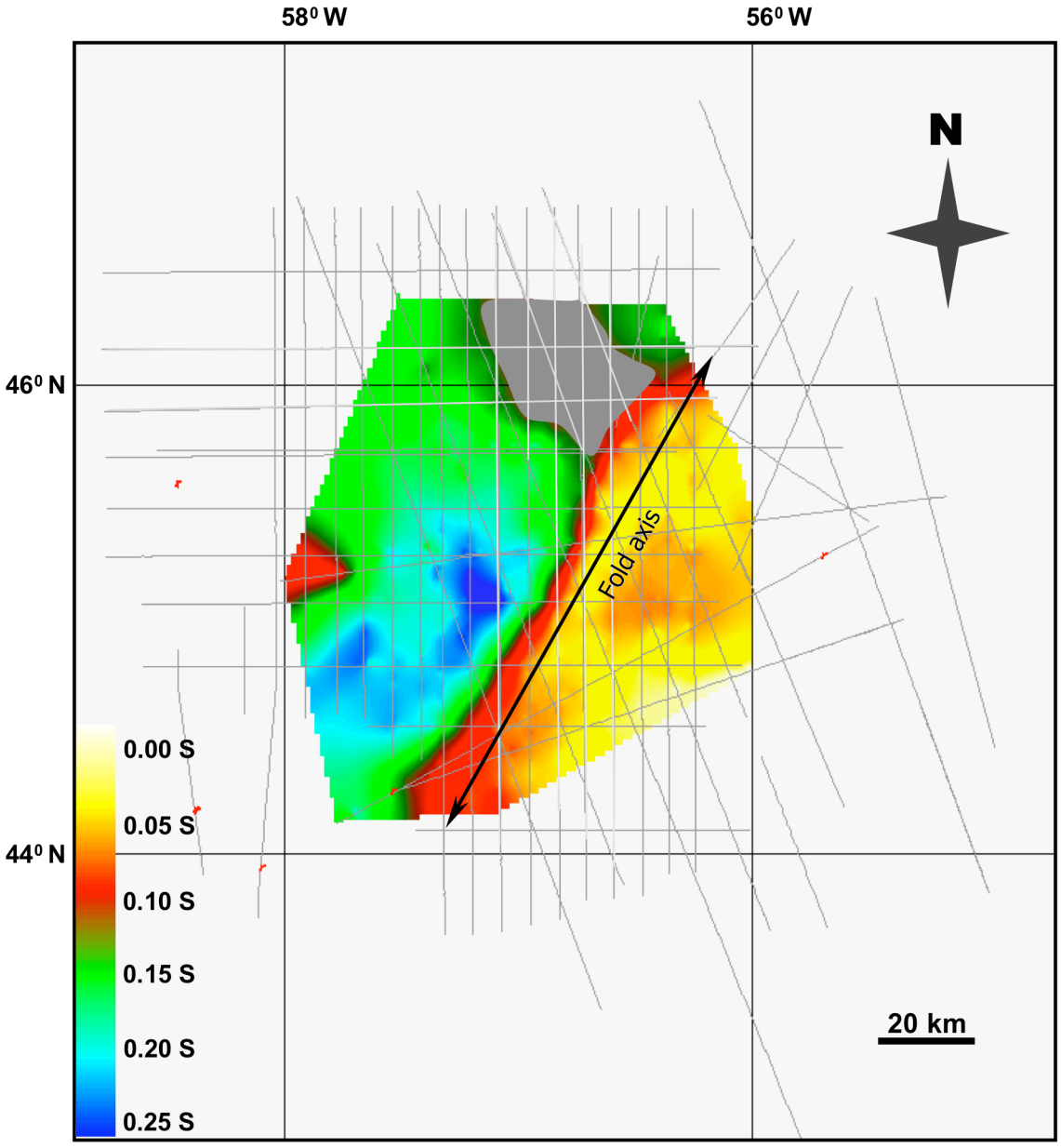

Figure 32. Isochron map of Sequence-2. Sequence-2 thins abruptly toward the southeast indicating the folding in the study area. Black line indicates the fold axis. Grey area indicates missing section of Sequence-2 because salt structures obscure the interpretation in this area.

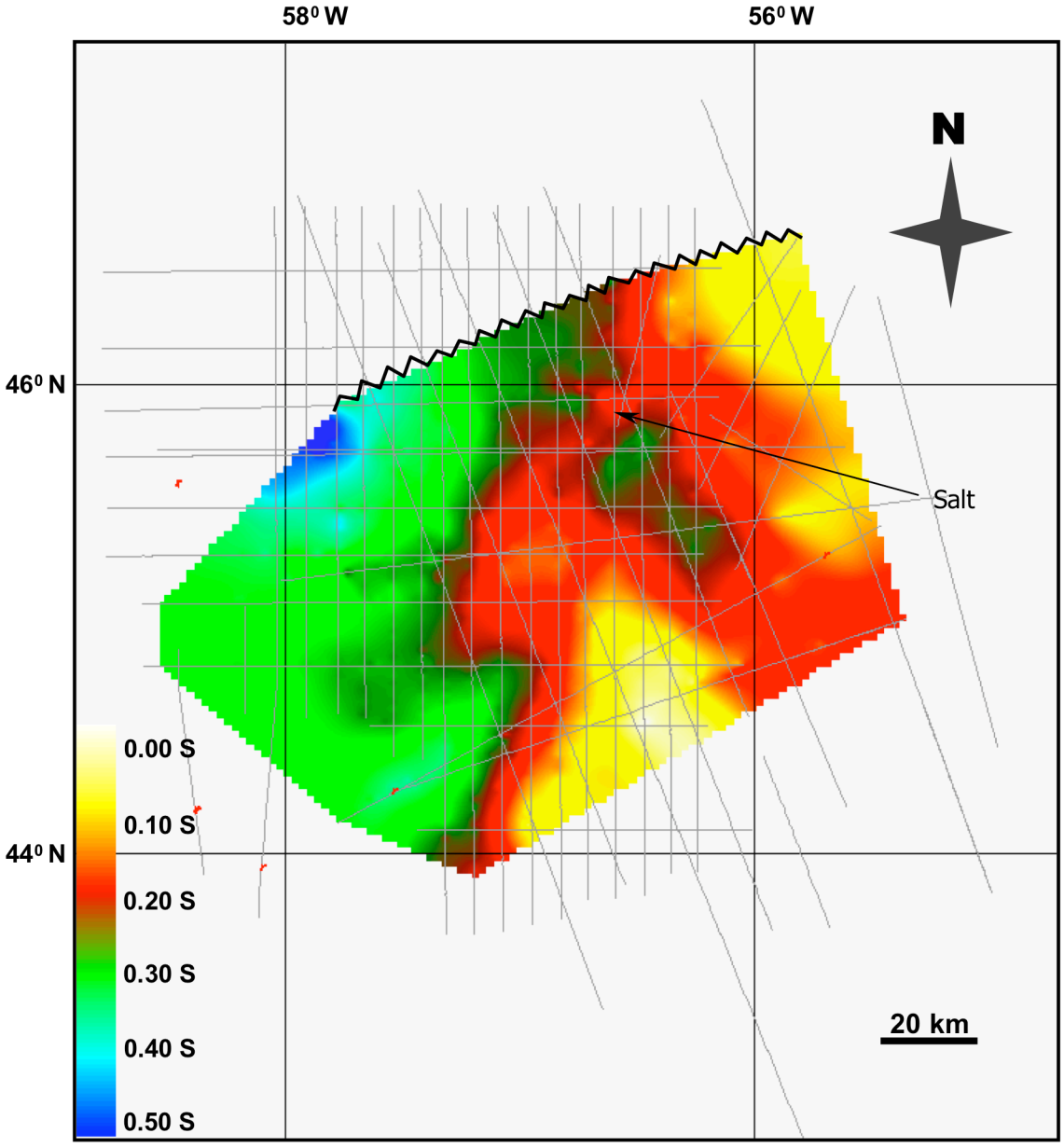

Figure 33. Isochron map of Sequence-3. Sequence-3 generally thickens from east to west. Thickness variations in the northeast part of the study area are likely associated with underlying salt movement. The black zigzag line indicates the erosional limit of Horizon N3.

Figure 34. Seismic line STP-7, uninterpreted (above) and interpreted (below). The changing thickness of Sequence-3 and onlapping terminations show that salt movement occurred during the deposition of Sequence-3. Sequence boundaries are cut by faults; red lines show faults with normal separation. Line drawings of seismic profiles are displayed at approximately 4:1, assuming an average velocity of 3 km/s. See Figure 5 for line location.

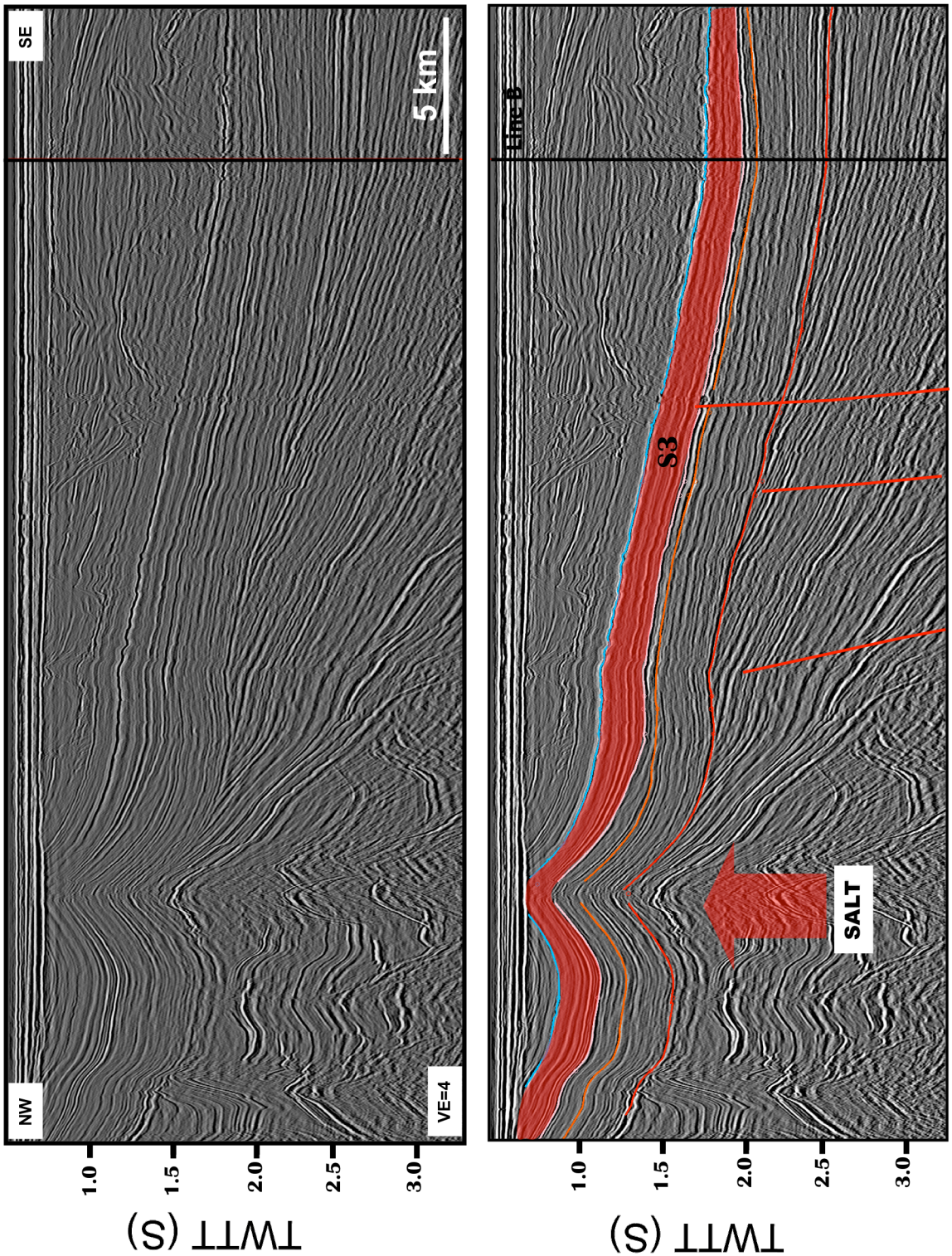
NW
SE
VE=4
5 km
TWTT (S)
1.0
1.5
2.0
2.5
3.0
Line B
S3
SALT
TWTT (S)
1.0
1.5
2.0
2.5
3.0

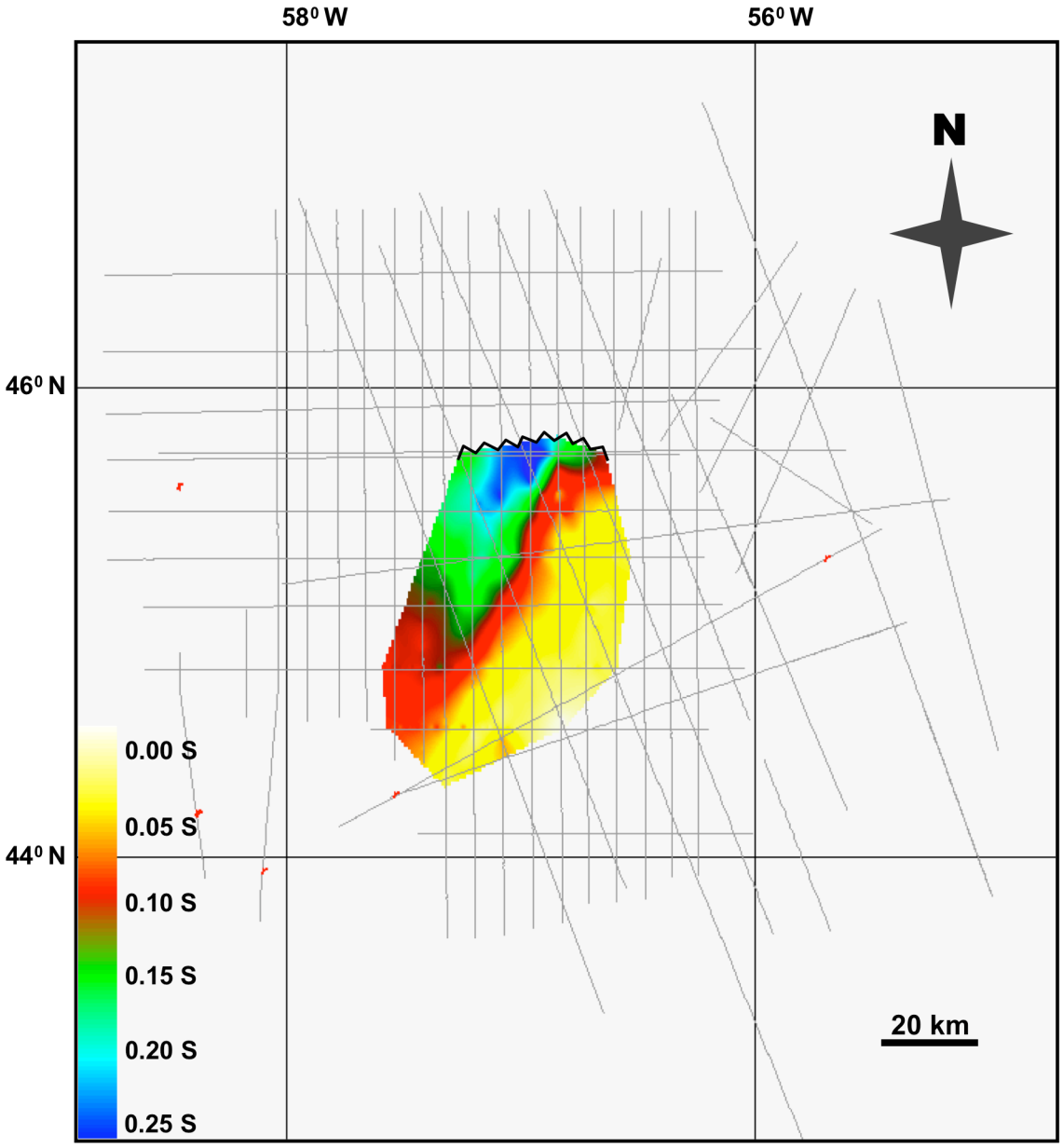

Figure 35. Isochron map of Sequence-4. Sequence-4 exists only in the central part of the study area. Sequence-4 generally thins toward the southeast. The black zigzag line indicates the erosional limit for Horizon N4.

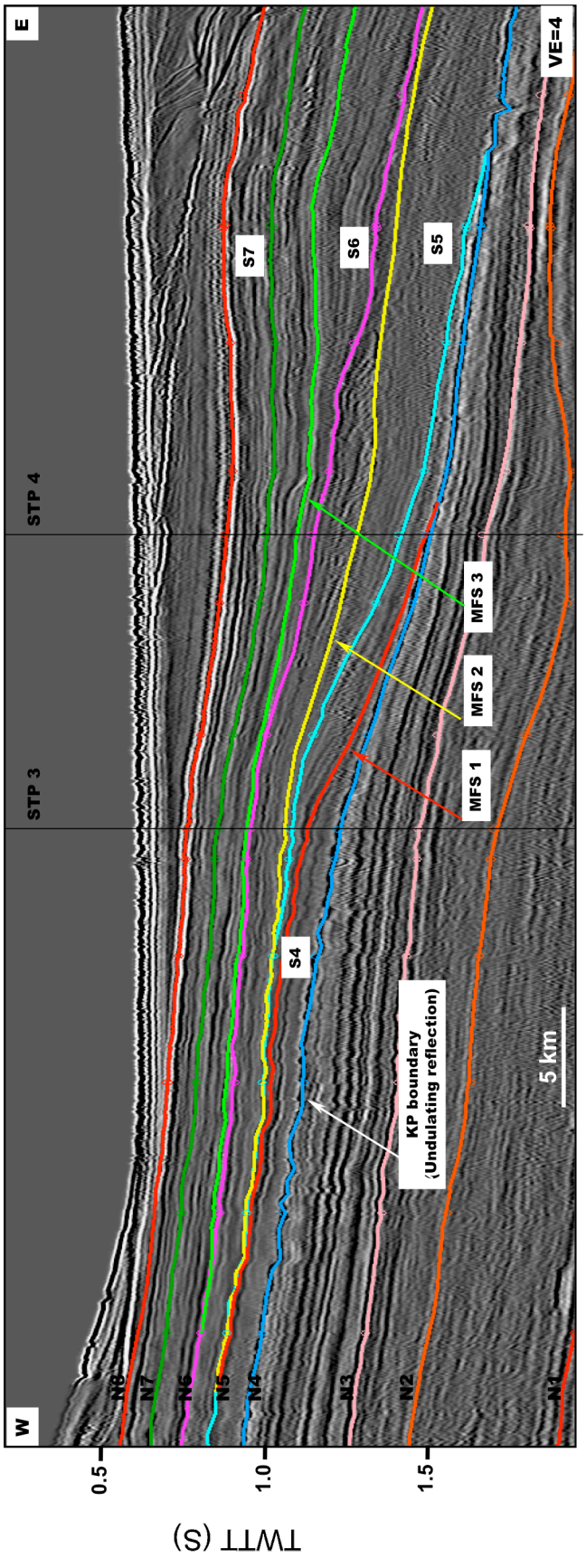

Figure 36. Identified system tracts in the Paleogene sedimentary rocks on seismic line B. N1-N8 are the interpreted horizons in this study. N4 is the Cretaceous/Paleogene boundary unconformity. The red, yellow and green lines are the maximum flooding surfaces (MFS) that separate the lowstand system tracts beneath and the highstand system tracts above. Line drawings of seismic profiles are displayed at approximately 4:1, assuming an average velocity of 3 km/s.

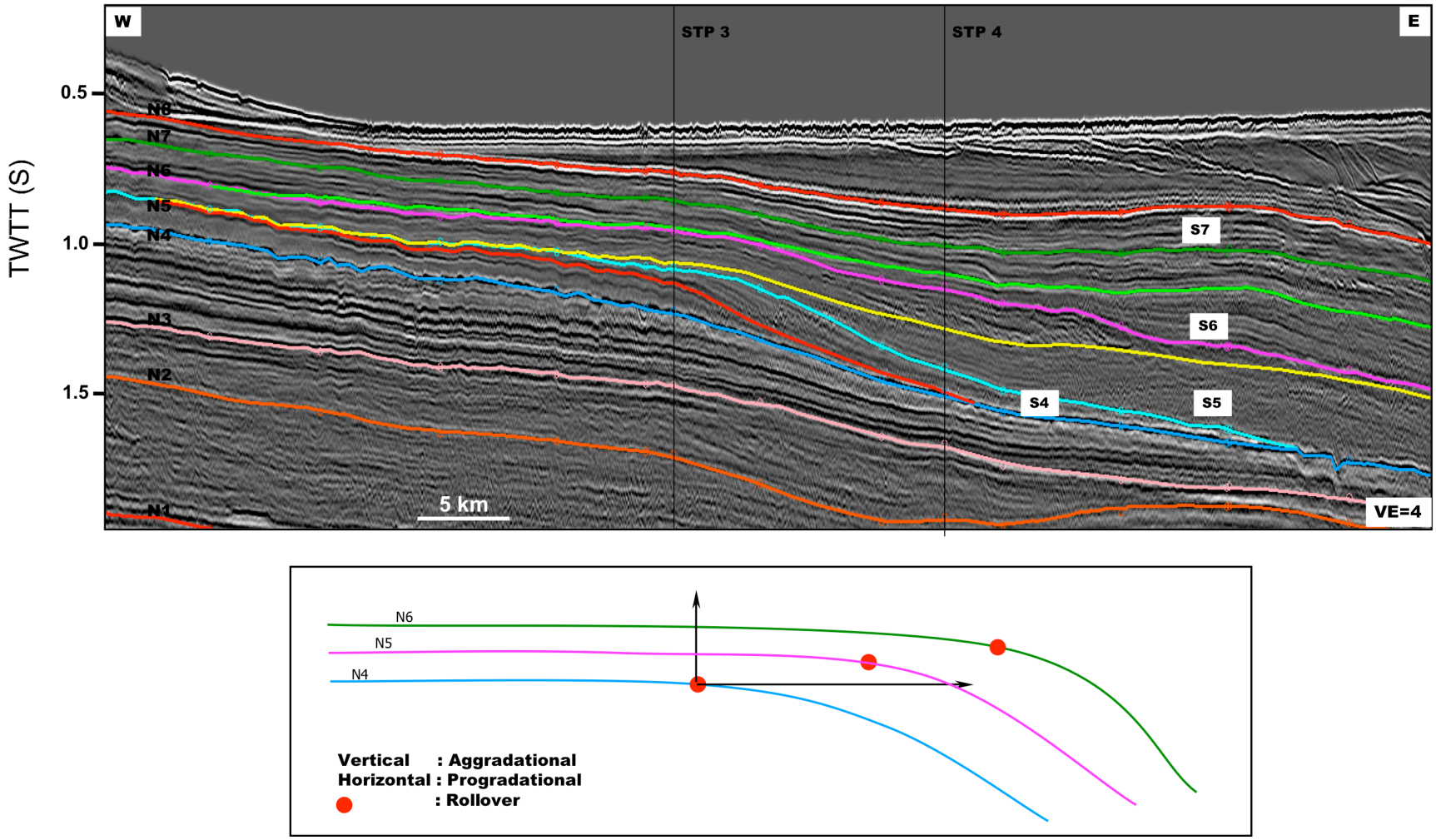

Figure 37. Seismic line B with interpreted system tract (top) and cartoon of clinoform rollover showing aggradational and progradational patterns. Line drawings of seismic profile is displayed at approximately 4:1, assuming an average velocity of 3 km/s.

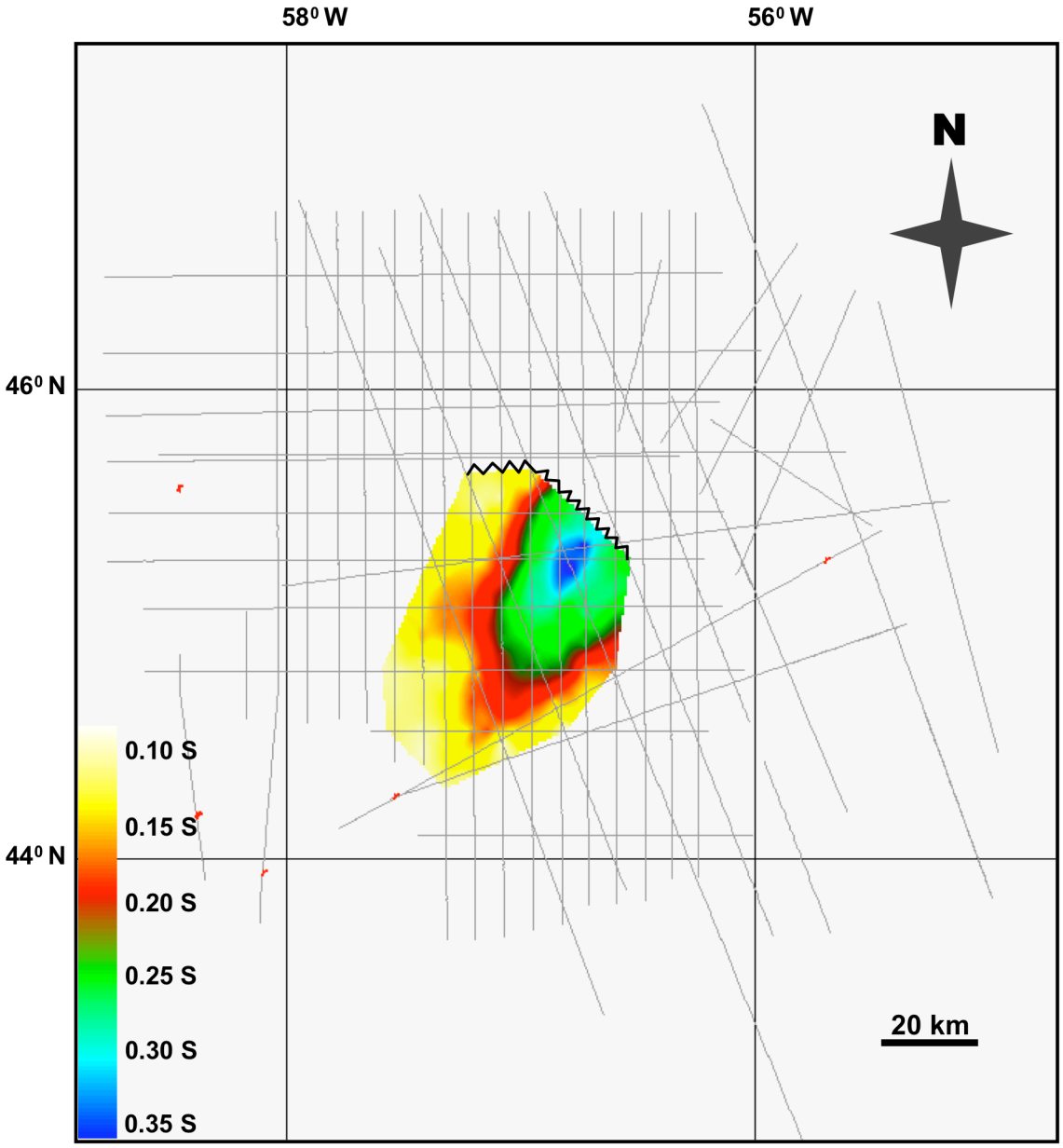

Figure 38. Isochron map of Sequence-5. Sequence-5 exists only in the central part of the study area. Sequence-5 is thin in the northwest, thickens to the southeast, and then thins in the southeast. The black zigzag line indicates the erosional limit for Horizon N5.

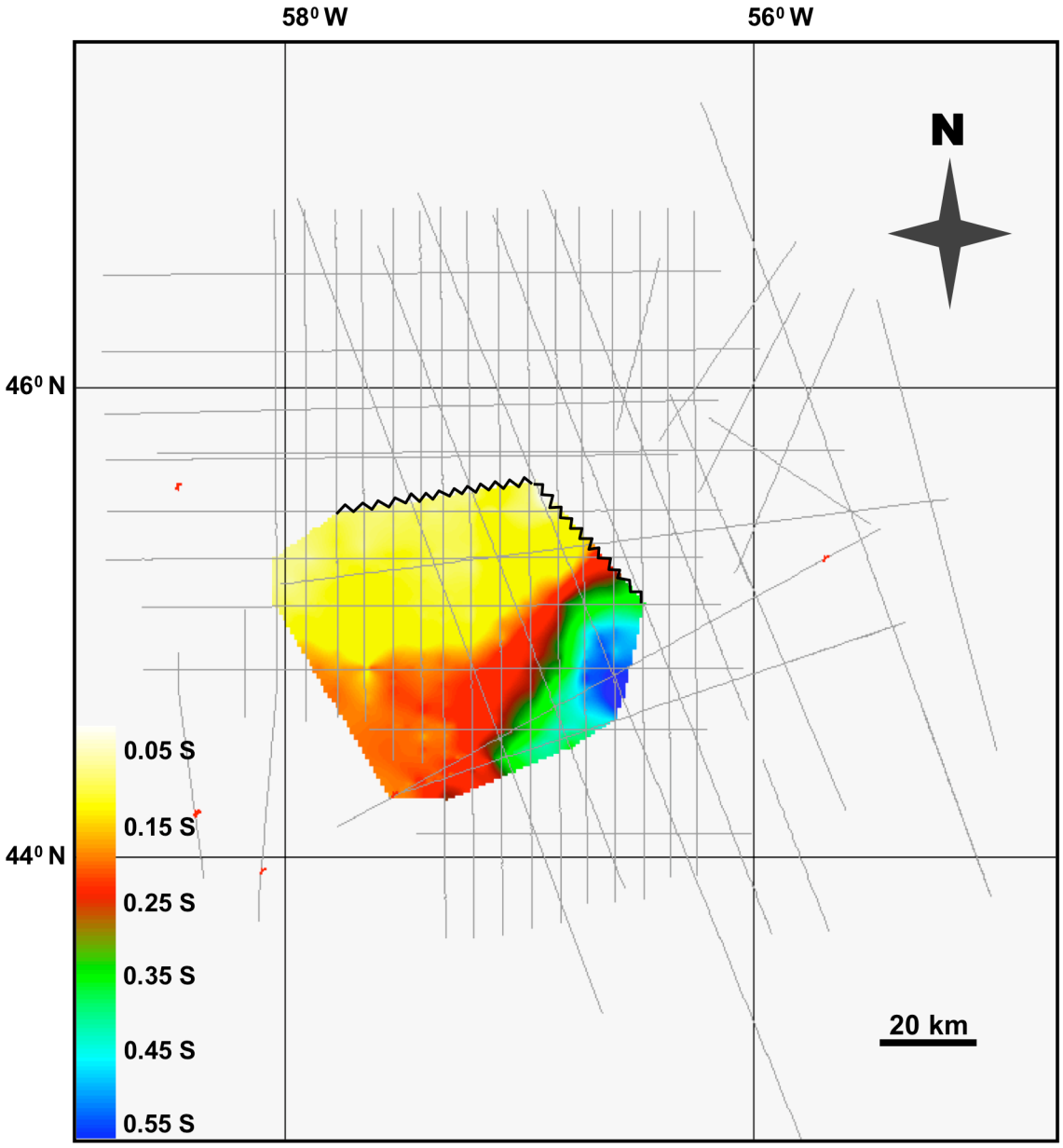

Figure 39. Isochron map of Sequence-6. Sequence-6 exists only in the central part of the study area. Sequence-6 generally thickens toward the southeast. The black zigzag line indicates the erosional limit for Horizon N6.

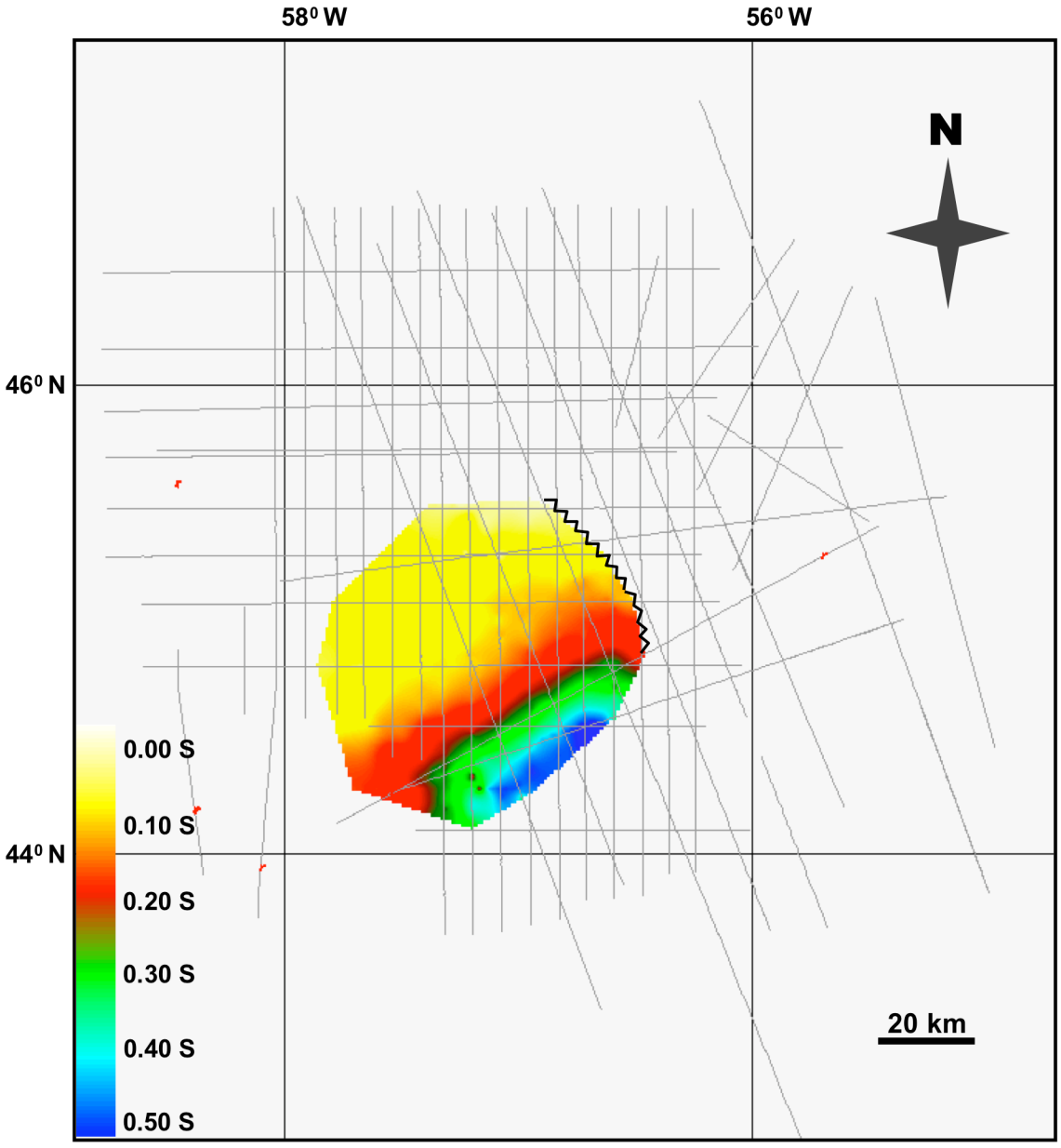

Figure 40. Isochron map of Sequence-7. Sequence-7 exists only in the central part of the study area. Sequence-7 generally thickens toward the southeast. The black zigzag line indicates the erosional limit for Horizon N7.

Figure 41. Seismic line B flattened on top of Sequence-2, uninterpreted (top) and interpreted (bottom). N1-N3 are the interpreted horizons. S-1 and S-2 are the Cretaceous sequences identified in this study. Onlapping terminations are evidence of folding prior to the deposition of Sequence-2. Progradation-downlapping terminations indicate the direction of sediment supply in the Sequence-2. Line drawings of seismic profiles are displayed at approximately 4:1, assuming an average velocity of 3 km/s. See Figure 5 for line location.

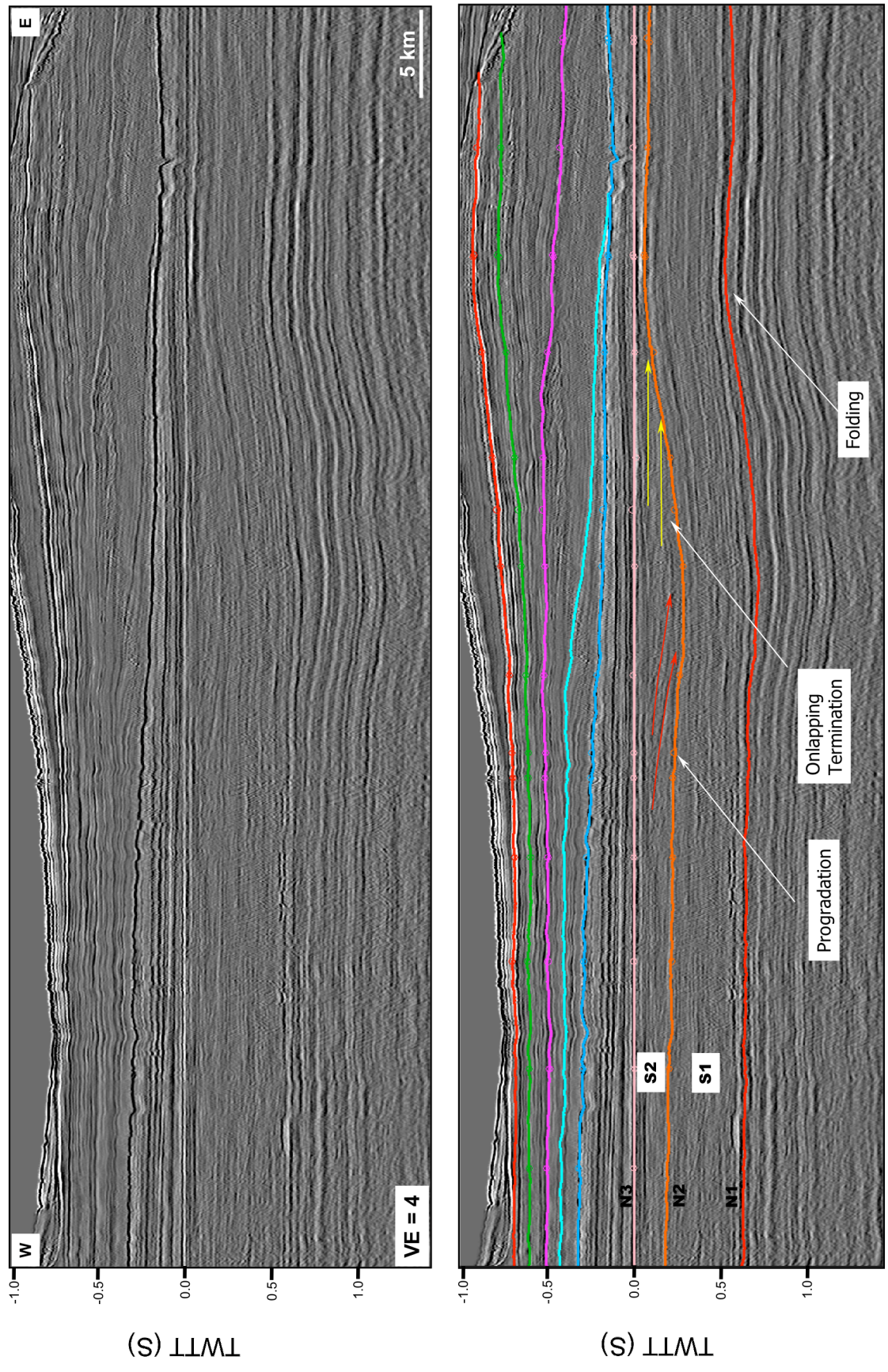
W
E
5 km
VE = 4
TWTT (S)
-1.0
-0.5
0.0
0.5
1.0
N3
N2
N1
S2
S1
Onlapping Termination
Progradation
Folding

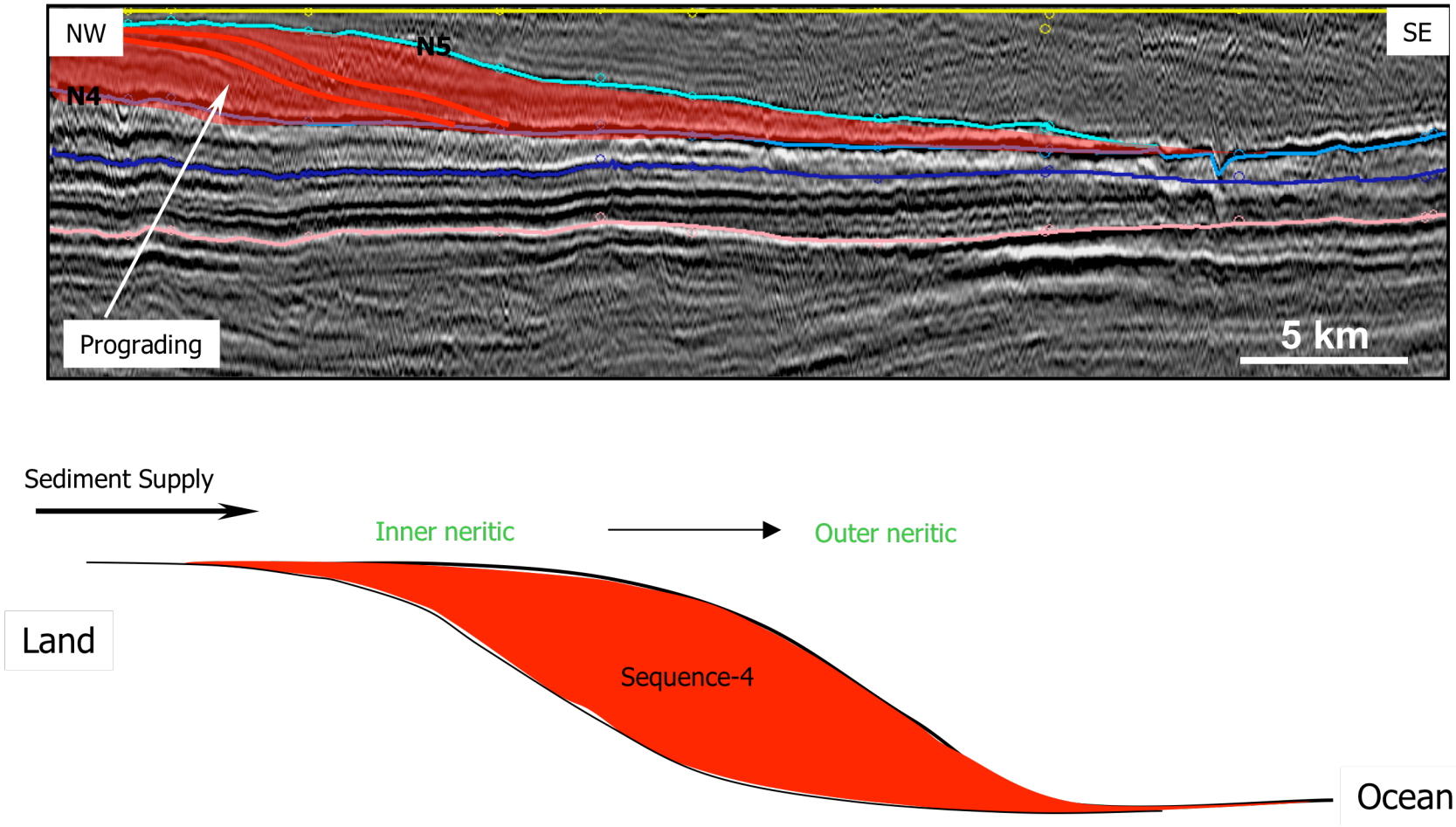

Figure 42. Seismic line STP-4 flattened on MFS 2 (maximum flooding surface-2). Progradational-downlapping terminations indicate the sediment supply direction. The cartoon shows the interpretation of the paleoenvironment. Based on well information, the paleoenvironment during the deposition of Sequence-4 was inner neritic to outer neritic.

Figure 43. Identified direction of sediment supply on isochron maps of Sequence-4 and Sequence-5. V1 is the vector of direction sediment supply from west to east, and V2 is the vector of direction sediment supply from northwest to southeast. Cartoon indicates the deltaic environment and shows the expected distribution of sediment. Based on well information, the paleoenvironment during the deposition of Sequence-4 and Sequence-5 was inner neritic to outer neritic.

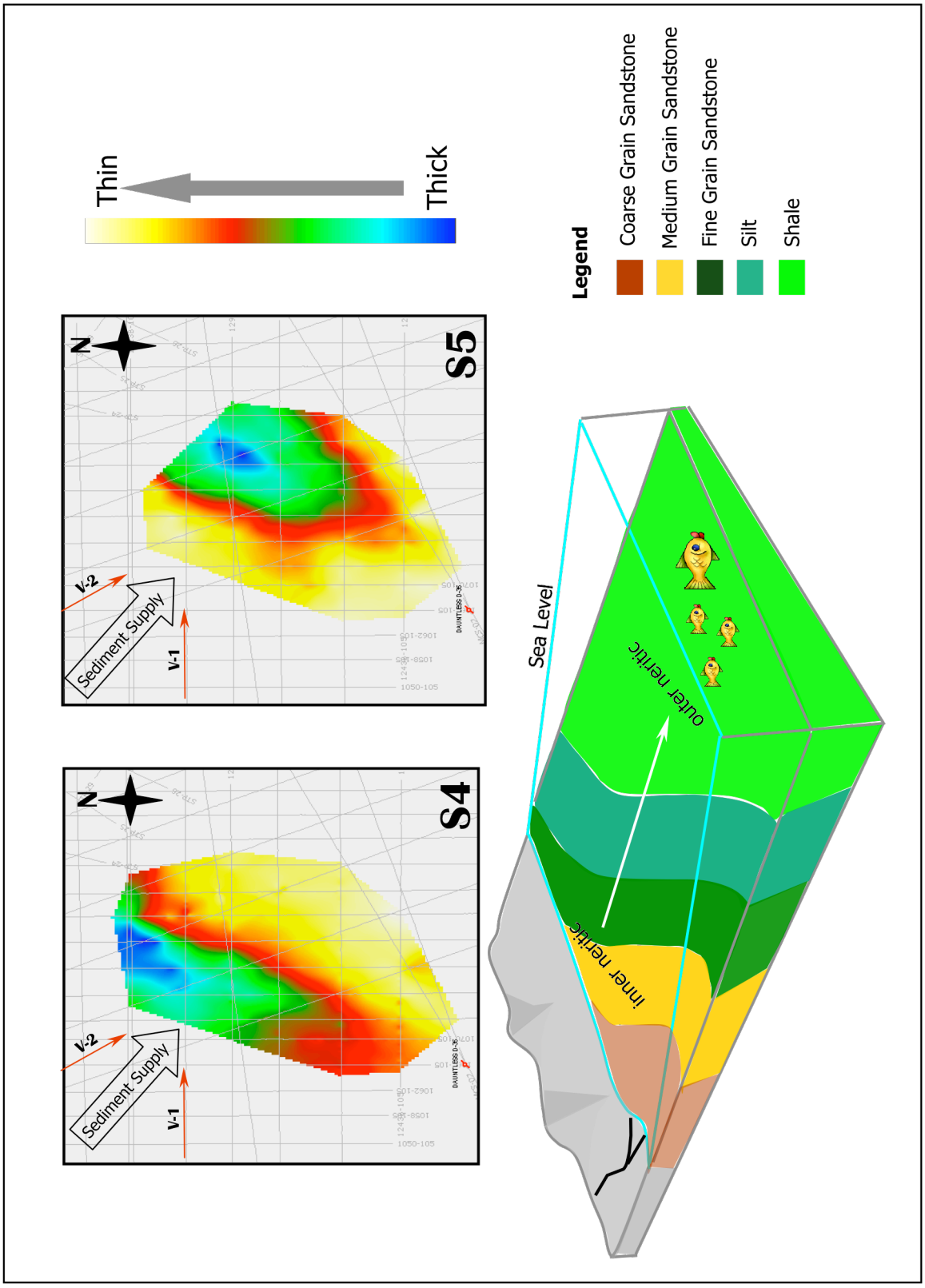
Thin
Thick
Legend
Coarse Grain Sandstone
Medium Grain Sandstone
Fine Grain Sandstone
Silt
Shale
S5
S4
N
V-2
V-1
Sediment Supply
Sea Level
inner neritic
outer neritic

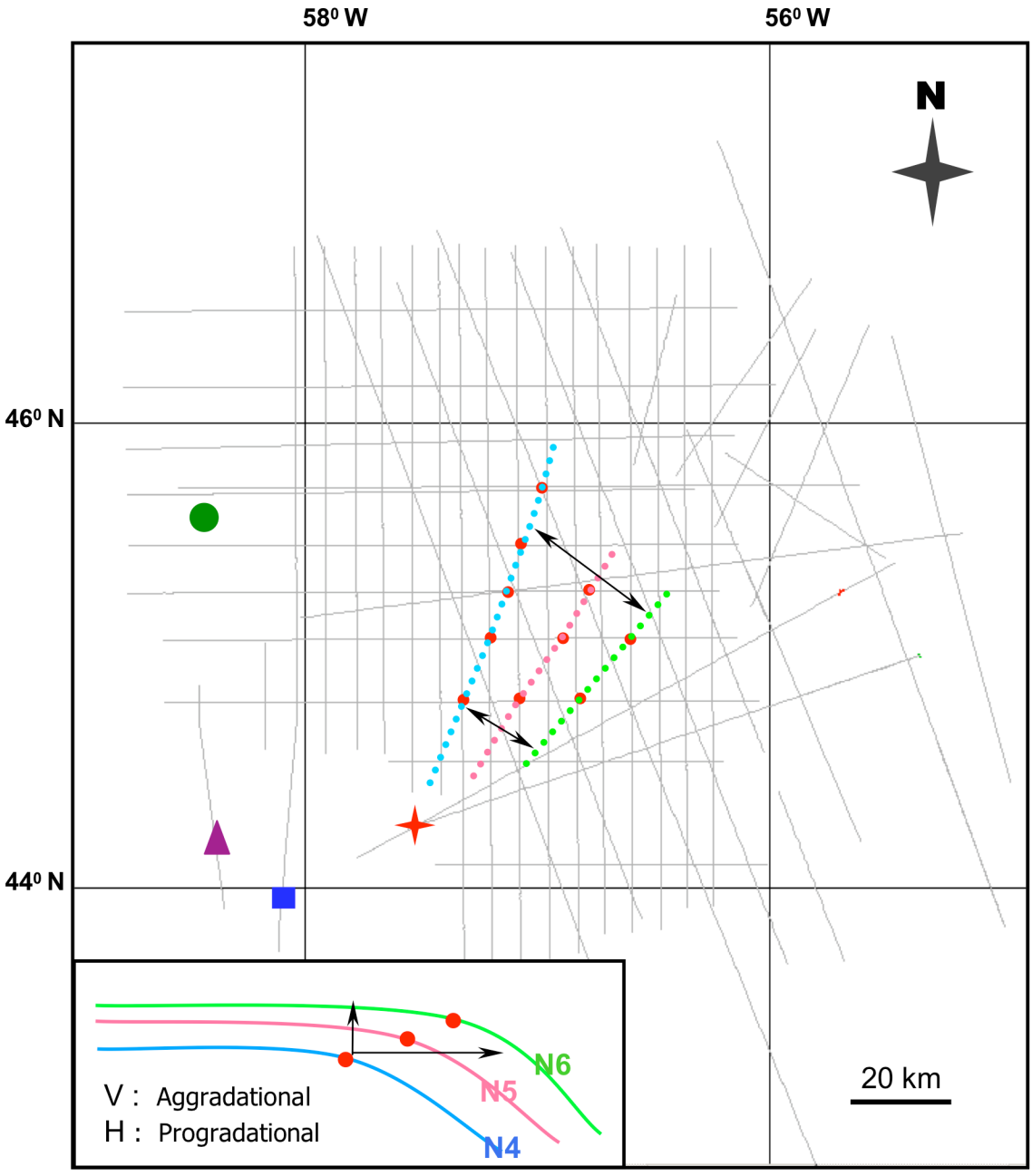

Figure 44. Clinoform rollover map of Paleogene sedimentary rocks. Location of Dauntless D-35 well (red star), Sachem D-76 (blue rectangle), Hesper I-52 (purple triangle), Adventure F-80 (green circle). The blue dot lines indicate the clinoform rollover for Horizon N4, the red dot lines indicate the clinoform rollover for Horizon N5, and the green dot lines indicate the clinoform rollover for Horizon N6. Inset cartoon shows the interpretation of clinoform rollovers indicating the aggradational-progradational patter.

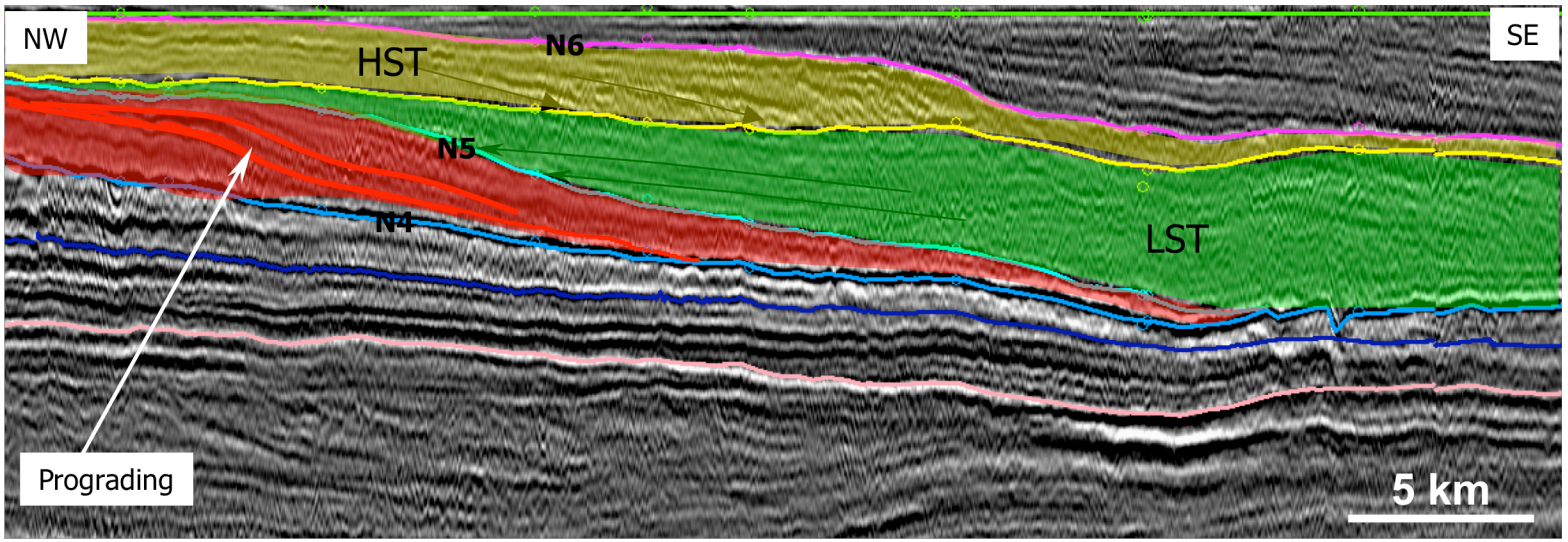

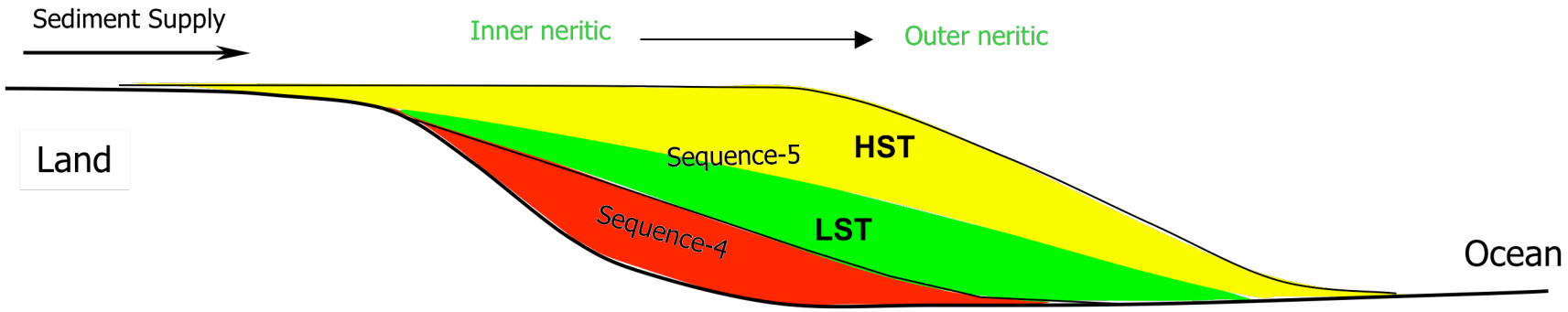

Figure 45. Seismic line STP-4 flattened on MFS 3 (maximum flooding surface-3). Progradational-downlapping terminations indicate the sediment supply direction. The cartoon shows the interpretation of the paleoenvironment and system tracts (LST and HST). Based on well-information, the paleoenvironment during the deposition of Sequence-5 was inner neritic to outer neritic.

Figure 46. Identified direction of sediment supply on isochron map of Sequence-6 and Sequence-7. V1 is the vector of direction sediment supply from west to east and V2 is the vector of direction sediment supply from northwest to southeast. Cartoon indicates the deltaic environment and shows the expected distribution of sediment. Based on well information, the paleoenvironment during the deposition of Sequence-6 and Sequence-7 was inner neritic to outer neritic.

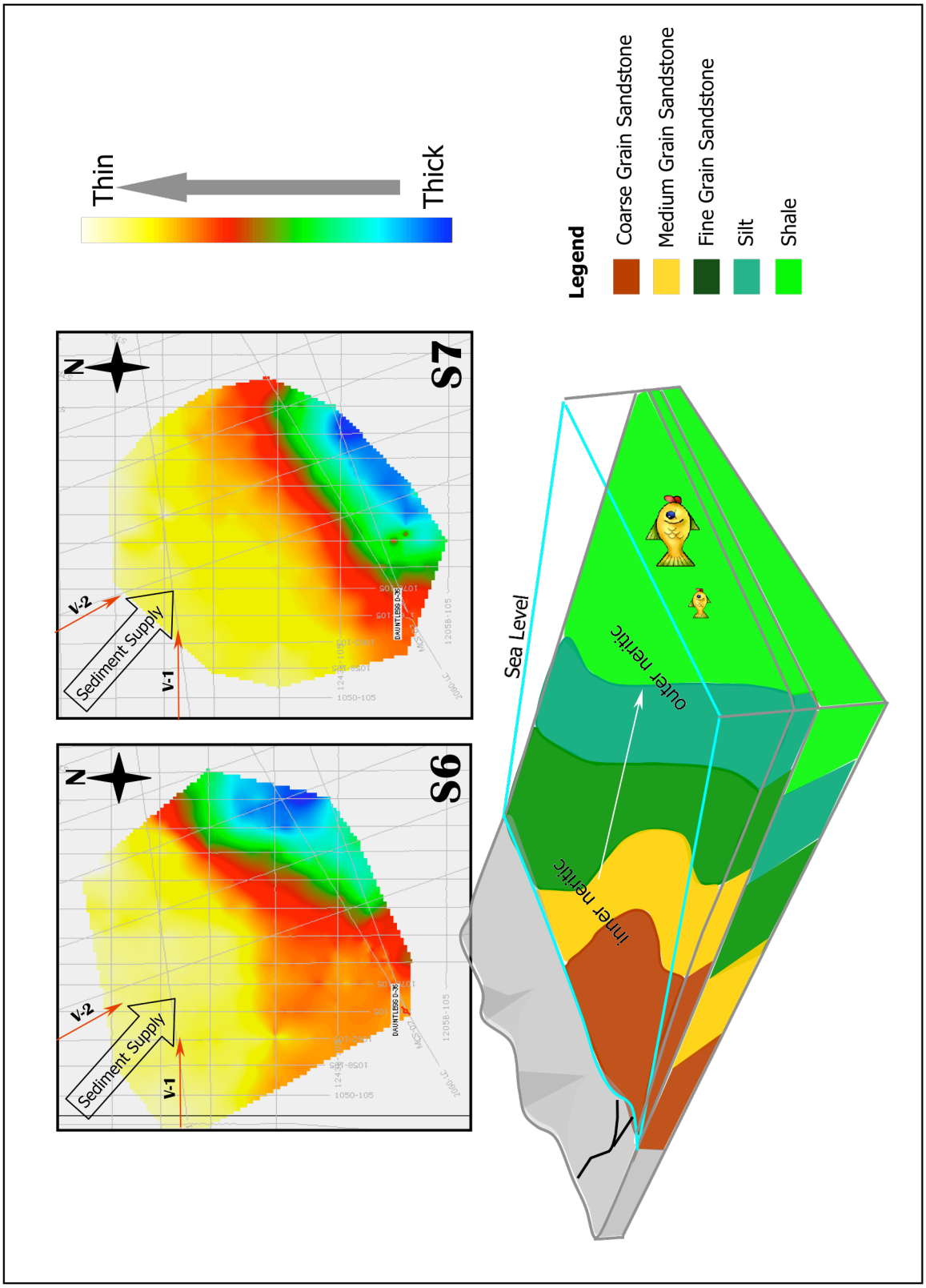
Thin
Thick
Legend
Coarse Grain Sandstone
Medium Grain Sandstone
Fine Grain Sandstone
Silt
Shale
S7
S6
N
V-2
V-1
Sediment Supply
Sea Level
Outer neritic
Inner neritic

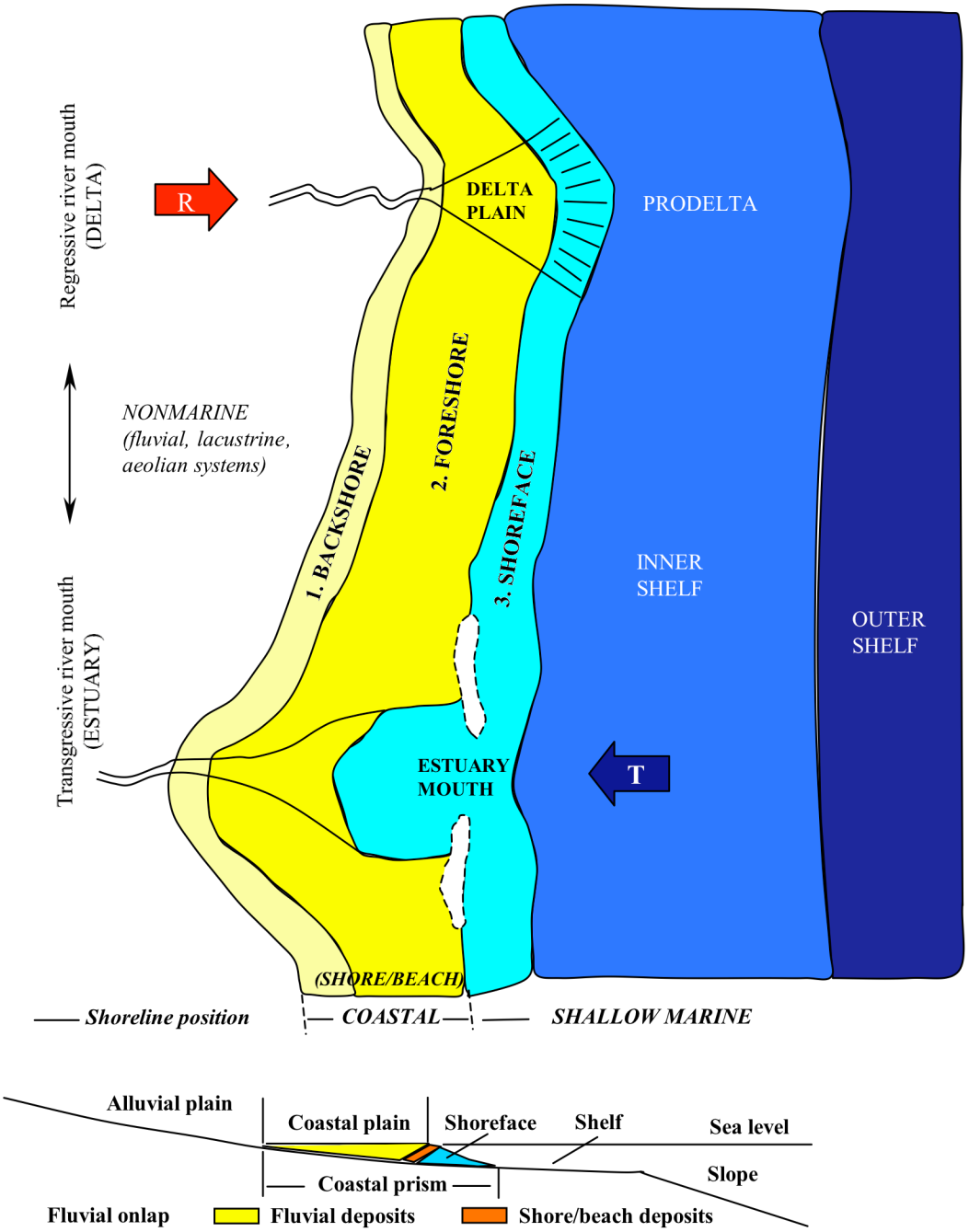

Figure 47. Generalized illustration of the main geomorphic and depositional settings on a continental shelf: alluvial plain, coastal plain, and shallow marine environments. R is regression and T is transgression (from Catuneanu, 2006).

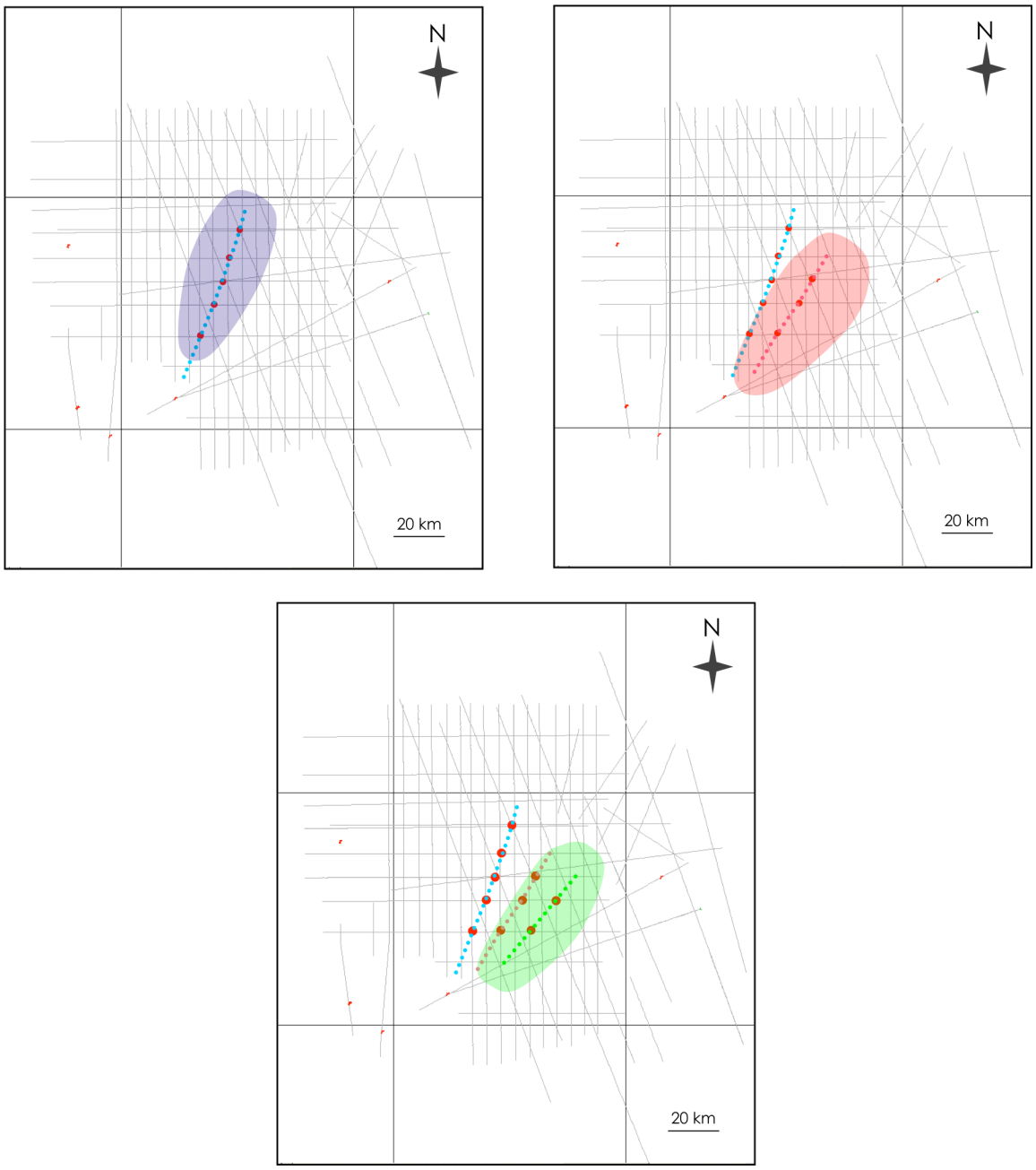

Figure 48. Depocenters migrations during Paleogene deposition. The dark blue color indicates the depocenter of Sequence-4, the red color indicates the depocenter of Sequence-5, and the green color indicates the depocenter of Sequence-6.

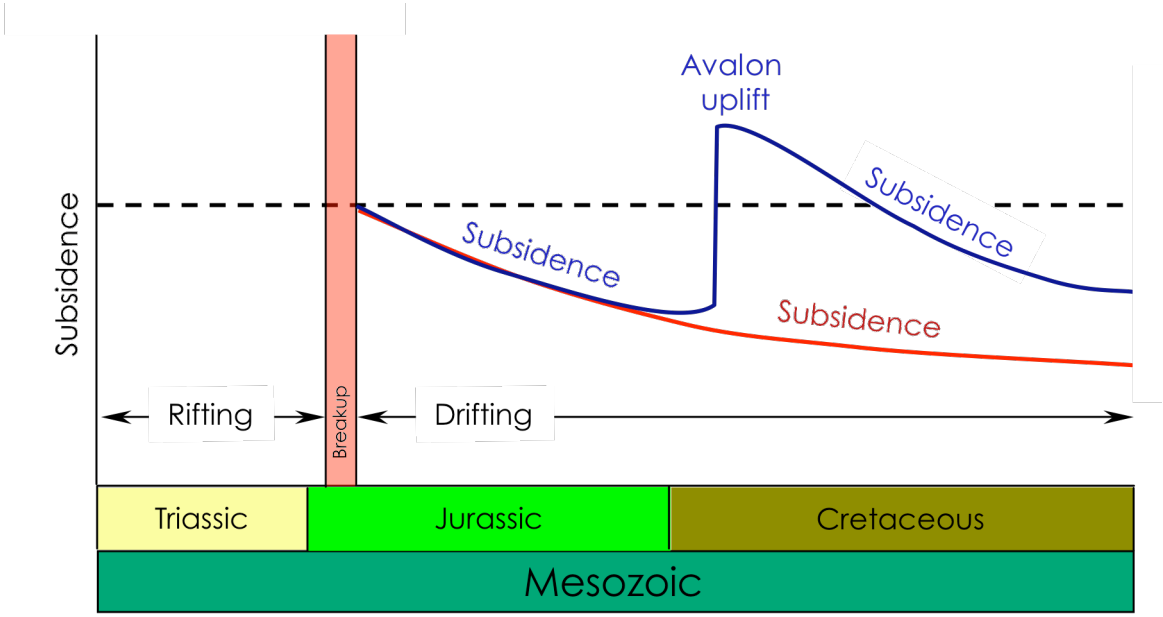

Figure 49. Schematic diagram showing subsidence in the Baltimore Canyon Trough and the Laurentian Subbasin. Red shows the subsidence in the Baltimore Canon Trough (New Jersey passive margin) indicating a typical passive margin (modified from Steckler and Watts, 1978). Blue indicates subsidence in the Laurentian Subbasin with the Avalon uplift occurring in the Late Jurassic/Early Cretaceous (Wade and MacLean, 1990; MacLean and Wade, 1992).

Figure 50. Stratigraphic interpretation of USG multichannel seismic line 25 in the Baltimore Canyon Trough (above) (Poag, 1987) and interpretation of seismic line STP-4 in the Laurentian Subbasin (below). The Jurassic and Cretaceous boundary in the Baltimore Canyon Trough is a disconformity separating parallel beds above and below the unconformity (Poag, 1987). The Jurassic-Cretaceous boundary or Avalon unconformity in the Laurentian Subbasin is an angular unconformity separating relatively flat and undeformed Cretaceous rocks above from folded and tilted Jurassic rocks below.

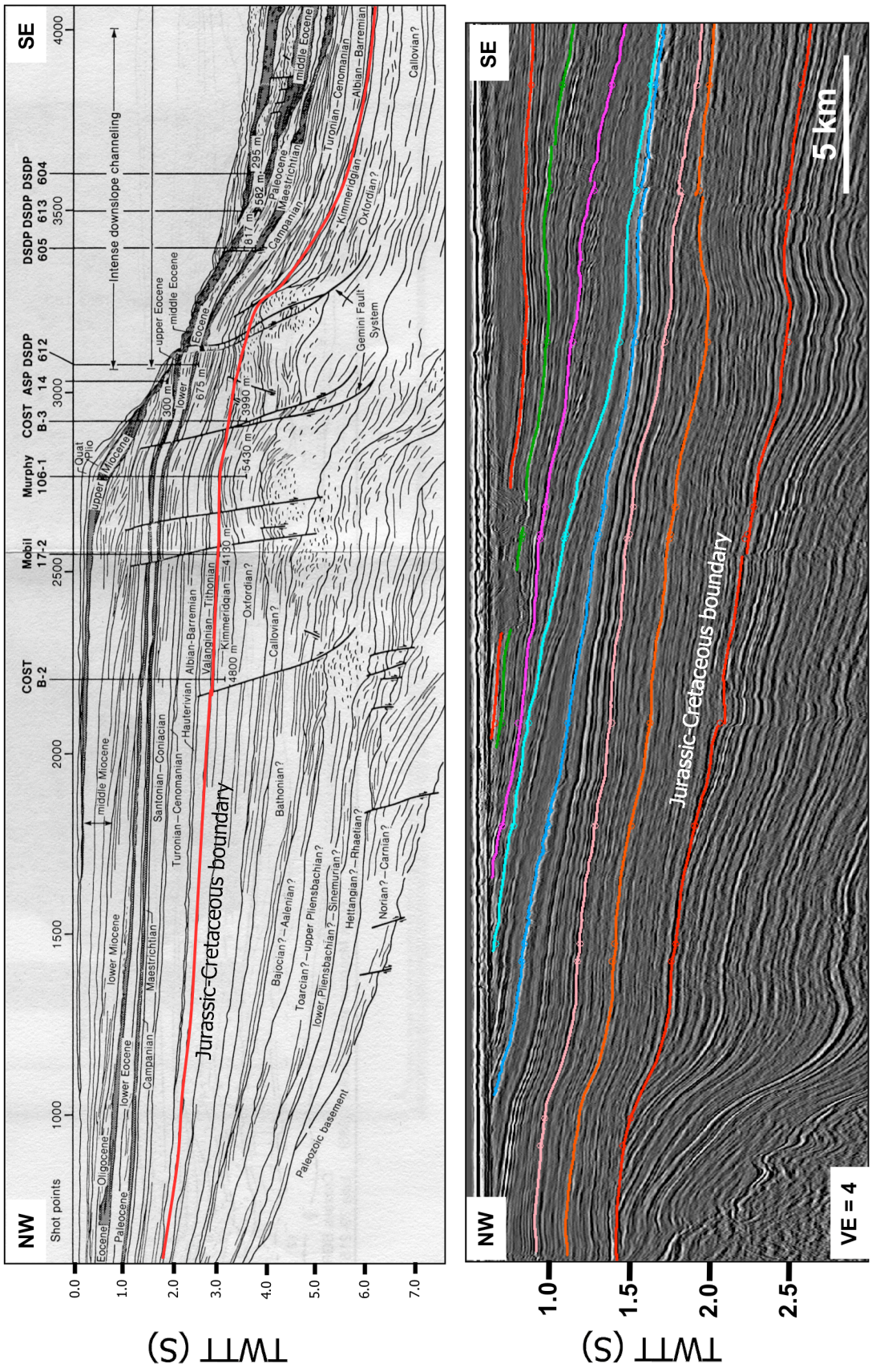
NW
SE
Shot points
COST B-2
Mobil 17-2
Murphy 106-1
COST B-3
ASP 14
DSDP 612
DSDP 605
DSDP 613
DSDP 604
Intense downslope channeling
Jurassic-Cretaceous boundary
Gemini Fault System
TWTT (S)
5 km
VE = 4

Figure 51. USGS line 14 showing salt structure interpreted in the Baltimore Canyon Trough (Grow et al., 1988) (above). Seismic line D from the Laurentian Subbasin showing the salt structures on the Laurentian Subbasin (below).

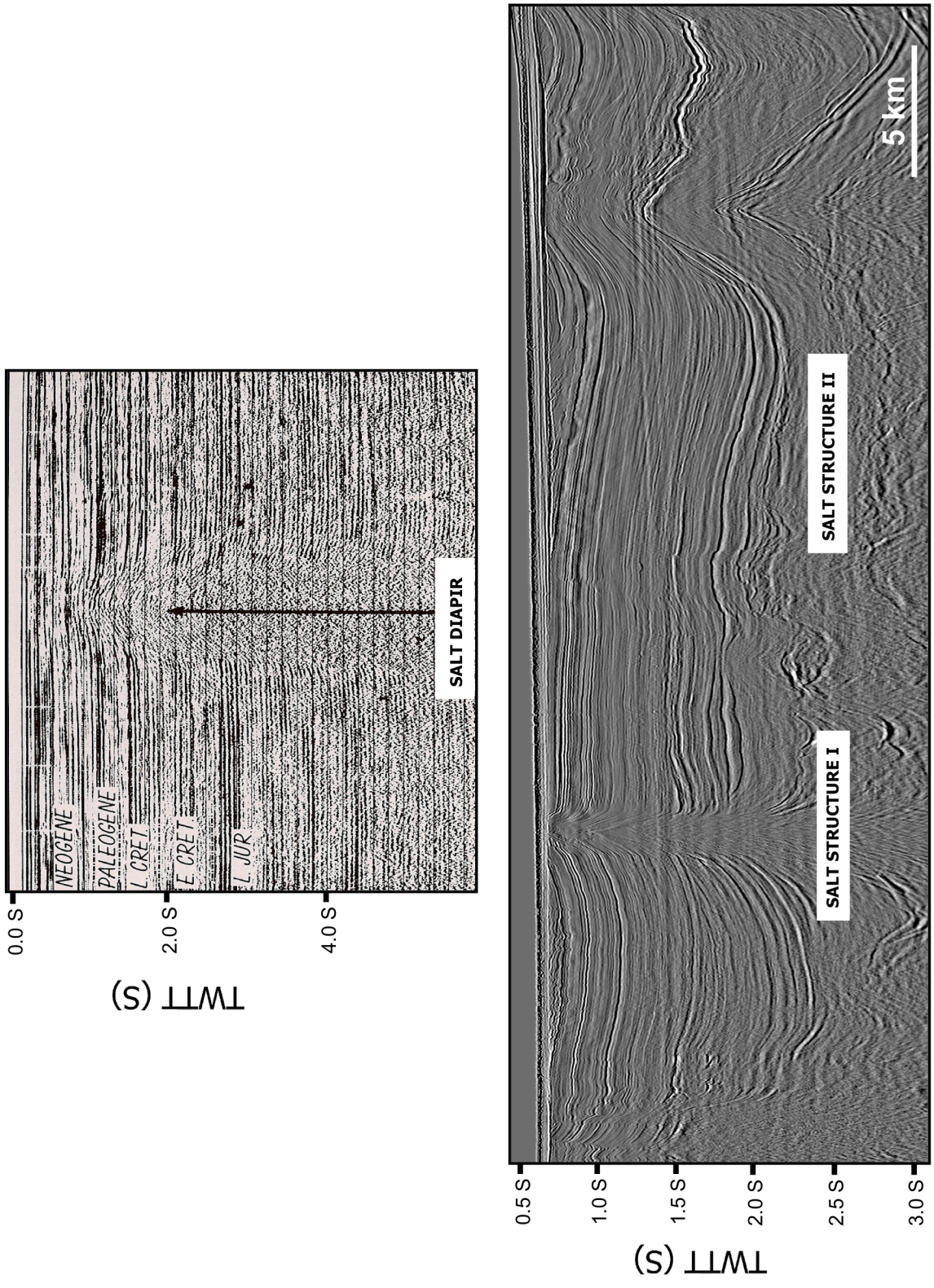
NEOGENE
PALEOGENE
L. CRET
E. CRET
L. JUR
SALT DIAPIR
0.0 S
2.0 S
4.0 S
TWTT (S)
SALT STRUCTURE I
SALT STRUCTURE II
5 km
0.5 S
1.0 S
1.5 S
2.0 S
2.5 S
3.0 S
TWTT (S)

Figure 52. Interpretation of EW9009 line 1003 on the Baltimore Canyon Trough (Mountain, 1994) (above) and interpretation of seismic line STP-4 on the Laurentian Subbasin. The clinoform geometries are present on both passive margins suggesting that margin growth in both areas had aggradational and progradational stratigraphic patterns.

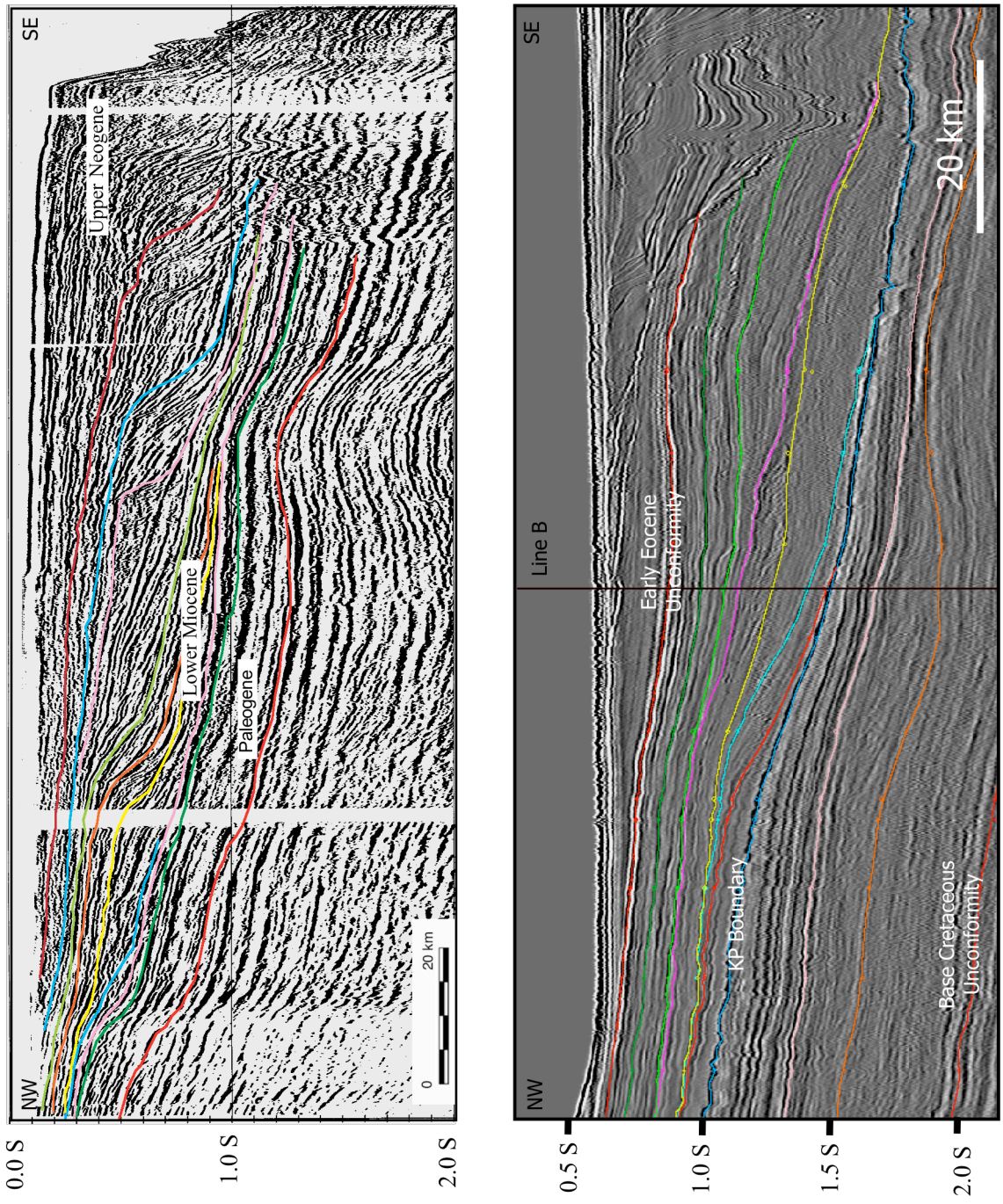
NW
SE
Upper Neogene
Lower Miocene
Paleogene
0
20 km
0.0 S
1.0 S
2.0 S
TWTT (S)
NW
Line B
SE
Early Eocene
Unconformity
KP Boundary
Base Cretaceous
Unconformity
20 km
0.5 S
1.0 S
1.5 S
2.0 S
TWTT (S)

Appendix 1

Lithostratigraphy Pick of Dauntless D35

Year	Author	Depth Type	Top	Bottom	Units	Formation
1993	MACLEAN,B.C. & WADE,J.A.	MD		4700	FT	BANQUEREAU FM
			4700	6002		WYANDOT FM
			6002	7090		DAWSON CANYON FM
			6470	6515		PETREL MB
			7090	9630		LOGAN CANYON FM
			7090	7225		MARMORA MB
			7225	7576		SABLE MB
			7576	9012		CREE MB
			9012	9630		NASKAPI MB
			9630	12165		MISSISAUGA FM
			9630	10770		MISSISAUGA UPPER MB
			10440	10770		("O" MARKER)
			10770	12165		MISSISAUGA MIDDLE MB
			11882	11882		(BASE CRETACEOUS UNCONFORMITY)
			12165	15555		MIC MAC FM
1990	WADE,J.A & MACLEAN,B.C.			4700		BANQUEREAU FM
			4700	6002		WYANDOT FM
			6002	7090		DAWSON CANYON FM
			6470	6515		PETREL MB
			7090	9630		LOGAN CANYON FM
			7225	7576		SABLE MB
			9012	9630		NASKAPI MB
			9630	12165		MISSISAUGA FM

			12165	15555		ABENAKI FM
			12165	15555		BACCARO MB
1982	JANSA,L.F.		800	4700		BANQUEREAU FM
			4700	6516		WYANDOT FM
			6516	7088		DAWSON CANYON FM
			7088	9630		LOGAN CANYON FM
			9012	9630		NASKAPI MB
			9630	12165		MISSISAUGA FM
			10826	11522		VERRILL CANYON FM
			12165	15555		ABENAKI FM
1975	HARDY,I.A.			4700		BANQUEREAU FM
				4700		MASKONOMET BEDS
			4700	6508		WYANDOT FM
			6508	7090		DAWSON CANYON FM
			7090			LOGAN CANYON FM
	.		1180	1750		ESPERANTO BEDS
			1750	3070		MANHASSET BEDS
			3070	4330		NASHWAUK BEDS
			4330	4690		WINDSOR GP

Lithostratigraphy Pick of Sachem D-76

Year	Author	Depth Type	Top	Bottom	Units	Formation
1993	MACLEAN,B.C. & WADE,J.A.	MD		4530	FT	BANQUEREAU FM
			4530	5810		WYANDOT FM
			5810	5810		(UNCONFORMITY ?)
			5810	6766		DAWSON CANYON FM
			6766	9764		LOGAN CANYON FM
			6766	6966		MARMORA MB
			6966	7337		SABLE MB
			7337	9164		CREE MB
			9164	9764		NASKAPI MB
			9764	13033		MISSISAUGA FM
			9764	10890		MISSISAUGA UPPER MB
			10600	10890		("O" MARKER)
			10890	13033		MISSISAUGA MIDDLE MB
			13033	16006		MIC MAC FM
1990	WADE,J.A. & MACLEAN,B.C			4530		BANQUEREAU FM
			4530	5810		WYANDOT FM
			5810	6766		DAWSON CANYON FM
			6766	9764		LOGAN CANYON FM
			6966	7337		SABLE MB
			9164	9764		NASKAPI MB
			9764	12530		MISSISAUGA FM
			12530	13033		MIC MAC FM
			13033	16006		ABENAKI FM

			13033	16006		BACCARO MB
1975	HARDY,I.A.			4530		BANQUEREAU FM
				4530		MASKONOMET BEDS
			4530	5808		WYANDOT FM
			5808	6165		DAWSON CANYON FM
			6165			LOGAN CANYON FM

Lithostratigraphy Pick of Adventure F-80

Year	Author	Depth Type	Top	Bottom	Units	Formation
1993	MACLEAN,B.C. & WADE,J.A.	MD		1302	FT	BANQUEREAU FM
			1302	1706		WYANDOT FM
			1706	2786		DAWSON CANYON FM
			2402	2448		PETREL MB
			2786	3256		LOGAN CANYON FM
			3256	3256		(UNCONFORMITY)
			3256	3393		(CAPROCK)
			3393	6559		ARGO FM
1990	WADE,J.A. & MACLEAN,B.C.		1302	1706		WYANDOT FM
			1706	2786		DAWSON CANYON FM
			2402	2448		PETREL MB
			2786	3256		LOGAN CANYON FM
			3256	3393		IROQUOIS/CAPROCK
			3393	6559		ARGO FM
1982	JANSA,L.F.		422	1302		BANQUEREAU FM
			1302	1706		WYANDOT FM
			1706	2708		DAWSON CANYON FM
			2402	2449		PETREL MB ?
			2708	3160		LOGAN CANYON FM
			3160	3160		(UNCONFORMITY)
			3160	3342		(CAPROCK ?)
			3342	6559		ARGO FM

Appendix 2

Biostratigraphy of Dauntless D35

Year	Author	Top	Bottom	Units	Age	Method	Paleoenvironment
1990	ASCOLI,P.	1030	1900	FT	N/A	MICROPALEO	INNER-OUTER NERITIC
		1900	3060		N/A	MICROPALEO	OUTER NERITIC
		3060	3160		N/A	MICROPALEO	OUTER NERITIC-UPPER BATHYAL
		3160	4380		N/A	MICROPALEO	INNER-OUTER NERITIC
		4380	4660		N/A	MICROPALEO	INNER NERITIC
		4660	5140		N/A	MICROPALEO	UPPER-LOWER BATHYAL
		5140	6540		N/A	MICROPALEO	OUTER NERITIC-UPPER BATHYAL
		6540	6640		N/A	MICROPALEO	INNER-OUTER NERITIC
		6640	7440		N/A	MICROPALEO	OUTER NERITIC
		7440	9080		N/A	MICROPALEO	INNER-OUTER NERITIC
		9080	12770		N/A	MICROPALEO	INNER NERITIC
		12770	15555		N/A	MICROPALEO	TRANSITIONAL-INNER NERITIC
		1030	1200		(NOT DATABLE)	MICROPALEO	
		1230			MIOCENE	CALC BENTH FORAMS	
		1900			L OLIGOCENE	CALC BENTH FORAMS	
		2080			OLIGOCENE	PLANKTONIC FORAMS	
		3060	3060		(UNCONFORMITY)	MICROPALEO	
		3060			EOCENE	PLANKTONIC FORAMS	
		3160			L PALEOCENE	PLANKTONIC FORAMS	
		4380	4660		PALEOCENE	PLANKTONIC FORAMS	
		4660			MAASTRICHTIAN	PLANKTONIC FORAMS	

		5140			CAMPANIAN	PLANKTONIC FORAMS
		5770			SANTONIAN	PLANKTONIC FORAMS
		6140			CONIACIAN	PLANKTONIC FORAMS
		6540			TURONIAN	PLANKTONIC FORAMS
		6640			CENOMANIAN	PLANKTONIC FORAMS
		7254			CENOMANIAN	PLANKTONIC FORAMS
		7440			ALBIAN	PLANKTONIC FORAMS
		9080			ALBIAN	CALC BENTH FORAMS
		9310			APTIAN	CALC BENTH FORAMS
		10200			BARREMIAN	AREN BENTH FORAMS
		10800			HAUTERIVIAN	CALC BENTH FORAMS
		11890			BERRIASIAN	CALC/AREN BENTH FORAMS
		12570			L OXFORDIAN	CALC BENTH FORAMS
		15000			OXFORDIAN	CALC BENTH FORAMS
		3624	3831		BERRIASIAN	CALC BENTH FORAMS
1976	ASCOLI,P.	1260	1900		MIOCENE	CALC BENTH FORAMS
		1900	2080		L OLIGOCENE	PLANKTONIC FORAMS
		1900	2080		MIOCENE	CALC BENTH FORAMS
		2080	3060		OLIGOCENE	CALC BENTH FORAMS
		2080	3060		OLIGOCENE	PLANKTONIC FORAMS
		3060	3160		EOCENE	CALC BENTH FORAMS
		3060	3160		EOCENE	PLANKTONIC FORAMS
		3160	4380		PALEOCENE	PLANKTONIC FORAMS
		3160	4690		PALEOCENE-E EOCENE	AREN BENTH FORAMS
		3160	4660		PALEOCENE-E EOCENE	CALC BENTH FORAMS
		4380	4660		PALEOCENE	PLANKTONIC FORAMS
		4660	5140		MAASTRICHTIAN	CALC BENTH FORAMS

		4660	5140		MAASTRICHTIAN	OSTRACODS	
		4660	5140		MAASTRICHTIAN	PLANKTONIC FORAMS	
		4690	5170		L CAMPANIAN	AREN BENTH FORAMS	
		5140	5770		CAMPANIAN	CALC BENTH FORAMS	
		5140	5770		CAMPANIAN	OSTRACODS	
		5140	5770		CAMPANIAN	PLANKTONIC FORAMS	

Biostratigraphy of Sachem D-76

Year	Author	Top	Bottom	Units	Age	Method	Paleoenvironment
1990	ASCOLI,P.	4526	4610	FT	MAASTRICHTIAN	MICROPALEO	OUTER NERITIC-BATHYAL
		4650	5220		CAMPANIAN		OUTER NERITIC-BATHYAL
		5280	5580		SANTONIAN		OUTER NERITIC-BATHYAL
		5640	5770		CONIACIAN		OUTER NERITIC-BATHYAL
		5818	6150		CENOMANIAN		NERITIC
		6180	8820		L ALBIAN-E CENOMANIAN		MOSTLY INNER NERITIC
		8910	9600		ALBIAN		INNER NERITIC-LITTORAL
		9660	10440		APTIAN		MOSTLY INNER NERITIC
		10500	11280		BARREMIAN		INNER NERITIC-LITTORAL
		11340	11820		HAUTERIVIAN		INNER NERITIC-LITTORAL
		11880	12270		BERRIASIAN-VALANGINIAN		MOSTLY INNER NERITIC
		12330	12900		L KIMMERIDGIAN-TITHONIAN		INNER NERITIC
		12960	13800		L OXFORDIAN-E KIMMERIDGIAN		INNER NERITIC
		13860	14970		OXFORDIAN		INNER NERITIC
		15030	16000		CALLOVIAN		INNER NERITIC
1980	DOEVEN,P.	5690	5690		SANTONIAN	NANNOFOSS	
		5770	5770		CONIACIAN-E SANTONIAN		
		5802	5802		CONIACIAN		
		5818	5818		CENOMANIAN		
		5862	5862		L CENOMANIAN		
		6022	6022		CENOMANIAN		
1976	MOBIL OIL CANADA	0	1560		PLIOCENE-PLEISTOCENE	MICROPALEO	
		1560	2160		MIOCENE-PLIOCENE		

		2160	2654		MIOCENE			
		2654	3015		MIOCENE			
		3015	4500		PALEOCENE			
		4500	4680		MAASTRICHTIAN			
		4680	5340		CAMPANIAN			
		5340	5690		SANTONIAN			
		5690	5818		CONIACIAN			
		5818	6800		CENOMANIAN			
		6800	10050		ALBIAN			
		10050	10525		APTIAN			
		10525	11000		BARREMIAN (PROBABLE)			
		11000			HAUTERIVIAN (PROBABLE)			
		12330			TITHONIAN-BERRIASIAN			
		14720	16000		OXFORDIAN			
		900	3300		CENOZOIC (NEOGENE)	PALYNOLOGY	(UNKNOWN)	
		3300	4500		PALEOCENE		MARINE	
		4500	5600		CAMPANIAN		MARINE	
		5600	5800		SANTONIAN (LOWER CONIACIAN)		MARINE	
		5800	6000		TURONIAN-CONIACIAN		MARINE	
		6000	6800		CENOMANIAN		MARINE	
		6800	9700		ALBIAN		MARINE	
		9700	10700		APTIAN		MARINE	
		10700	11100		BARREMIAN		MARINE	
		11100	11700		HAUTERIVIAN		MARINE	
		11700	12800		BERRIASIAN-VALANGINIAN		MARINE	
		12800	14100		KIMMERIDGIAN		MARINE	

Appendix 3

Time to Depth Conversion of Dauntless D-35

TWT(s)	Depth (m)
0.51	457.20
0.90	853.44
0.95	914.40
1.01	991.21
1.21	1219.20
1.38	1429.51
1.45	1524.00
1.64	1828.80
1.73	1975.10
1.84	2133.60
1.97	2339.34
2.02	2438.40
2.08	2530.45
2.19	2743.20
2.37	3048.00
2.47	3276.60
2.63	3657.60
2.72	3855.72
2.82	4114.80
2.88	4267.20
3.03	4663.44

Time to Depth Conversion of Sachem D-76

TWT (S)	Depth (m)
0.08	58.52
0.26	205.44
0.42	370.03
0.55	505.05
0.72	671.17
0.94	884.53
1.13	1097.89
1.35	1350.87
1.48	1555.09
1.61	1737.97
1.76	1951.33
1.89	2164.69
2.00	2347.57
2.13	2560.93
2.25	2777.34
2.34	2944.98
2.51	3292.45
2.64	3551.53
2.74	3787.75
2.82	3941.67
2.94	4237.33
3.06	4542.13

Time to Depth Conversion of Hesper P-52

TWT (S)	Depth (m)
0	40.50
0.29	316.64
0.47	475.45
0.63	628.76
0.78	771.11
0.92	928.08
1.05	1077.43
1.19	1229.83
1.26	1261.50
1.29	1383.75
1.39	1534.63
1.49	1687.03
1.60	1839.43
1.70	1991.83
1.80	2144.23
1.89	2296.63
1.98	2449.03
2.06	2601.43
2.14	2753.83
2.18	2807.17
2.36	3063.50
2.58	3599.50

Appendix 4

Detailed Processing Parameters for Canadian Government Seismic Data

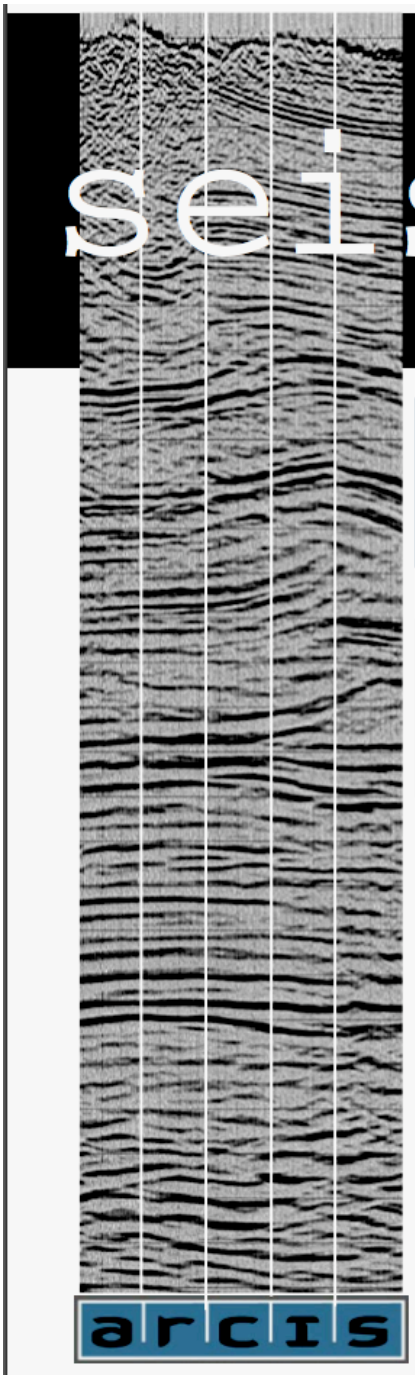

seismic

Final Processing Report

St. Pierre
Laurentian Sub Basin of the
Grand Banks of Newfoundland

Prepared For:

CANADA 1842 GEOLOGICAL SURVEY - COMMISSION GÉOLOGIQUE

Natural Resources Canada | Ressources naturelles Canada

March 2006

arcis

1. INTRODUCTION

This report describes the 2D marine processing sequence of the St. Pierre – Offshore Nova Scotia seismic data acquired in 1984 and 1985 by Western Geophysical and GSI.

There were 29 lines originally representing 3,098.29 km, but line STP-07 has been split into 2 parts (A & B), due to 394 missing shot points, resulting a total of 30 lines.

2. DATA ACQUISITION

Two different datasets were acquired over the area in 1984 and 1985.

2.1. GSI LINES

These lines are: STP-01, 02, 24, 25, 26, 27, 28 and 29.

Acquisition parameters:

Contractor: GSI
Shot for: MINISTER OF ENERGY
Vessel: M/V FRED AGNICH

Source:
- Depth: 7 m
- Array Volume: 4075 cu.in.
- Pressure: 2000 PSI
- Shot Interval: 25 m
- Airgun Delay: 51.2 ms

Streamer:
- Channels: 120
- Group Interval: 25 m
- Streamer Depth: 13

Physical Offsets:
- Center of Source to Center of Near Channel: Varies 198 to 246 m
- Streamer Length: 3000 m

Instruments:
- Model: DFS V
- Record Length: 8 sec
- Sample Rate: 4 msec
- Tape Format: SEG-B

Low Cut Filter: 5.3 Hz
High Cut Filter: 90 Hz

2.2. WESTERN LINES

These lines are: STP-03, 04, 05, 06, 07A, 07B, 08, 09, 10, 11, 12, 13, 14, 15, 16, 17, 18, 19, 20, 21, 22 and 23.

Acquisition parameters:

Contractor: Western Geophysical
Shot for: A.G.C.
Vessel: Party # 123

Source:
- Depth: 7 m
- Array Volume: 1590 cu.in.
- Shot Interval: 26.67 m
- Airgun Delay: 0 ms

Streamer:
- Channels: 120
- Group Interval: 26.67 m
- Streamer Depth: 10

Physical Offsets:
- Center of Source to Center of Near Channel: 190 m
- Streamer Length: 3200 m

Instruments:
- Model: LITTON 16
- Record Length: 8 sec
- Sample Rate: 2 msec
- Tape Format: SEG-D
- Low Cut Filter: 12Hz
- High Cut Filter: 180 Hz

Appendix 5

Detailed Processing Parameters for TGS/Nopec Seismic Data

TGS

CANADA
LC-105 & NS-103
NON-EXCLUSIVE 2-D SURVEY

ACQUISITION PARAMETERS

Acquisition Date:	**May 2002-October 2002**
Data Acquired By:	**GSI, M/V Admiral**
Recording Instrument:	**I/O MSX**
Filter settings:	**Low: 2Hz – 6 dB/octave**
	High: 206Hz – 264 dB/octave
Airgun Source Volume	**5240 cubic inch**
Gun Depth:	**6 meters**
Shotpoint Interval:	**37.5 meters**
Group Interval:	**12.5 meters**
Streamer type:	**I/O MSX**
Streamer Depth:	**9 meters**
Recording channels:	**640**
Streamer Length:	**8000 meters**
Record Length:	**14336 ms**
Sample Interval:	**2 milliseconds**
Nominal Fold:	**106**

PROCESSING SEQUENCE

- **LC-105 Processing performed by Spectrum - Processing completed April 2003**
- **NS-103 Processing performed by TGS-NOPEC - Processing completed March 2003**
- **Resample 2ms to 4ms**
- **Edit bad traces and shots**
- **Merge seismic trace headers with navigation**
- **FK anti-alias filter and trace drop - 640 channels to 320 - output NAV-MERGE - *NS-103 only***
- **2:1 adjacent trace sum - 640 channels to 320 - output NAV-MERGE – *LC-105 only***
- **Spherical divergence correction**
- **Deconvolution – single design gate, 280ms operator, 16ms gap**
- **Water velocity Radon**
- **Velocity analysis every 2km**
- **Primary velocity Radon- output RADON**
- **Migration velocity analysis every 1km**
- **Kirchhoff pre stack time migration- output PSTM-GATHERS**
- **Residual velocity analysis every 1km – output PSTM-GATHERS+NMO**
- **Stack - Output RAW MIG**
- **Filter and scaling - output PROC-MIG**

AVAILABLE DELIVERABLES

- **Raw field data/shot ordered**
- **Field data with navigation in trace headers/shot ordered**
- **Radon de-multiple CDP gathers**
- **Pre stack time migrated CDP gathers without NMO correction**
- **Pre stack time migrated CDP gathers with NMO correction**
- **Raw migration**
- **Processed migration**
- **Stacking velocities (ASCII)**
- **Migration velocities (ASCII)**
- **Processed source-receiver navigation – UKOOA**
- **Post stack navigation – UKOOA**
- **Workstation-ready tapes available in SMT, Landmark, and Geoquest**

TGS

Laurentian Channel
NON-EXCLUSIVE 2-D CANADA SURVEY

ACQUISITION PARAMETERS

Acquisition Date:	**August 1999**
Data Acquired By:	**Geco-Prakla**
Kilometers:	**4,495.800 kilometers**
Shooting Orientation:	**North-South/East-West**
Recording Instrument:	**Nessie 3**
Streamer Type:	**Geco-Prakla Nessie 4**
Streamer Positioning:	**Compass / RGPS**
Airgun Source:	**7918 cubic inches**
Gun Depth:	**7.5 meters +/-1 meter**
Shotpoint Interval:	**37.5 meters**
Group Interval:	**25 meters**
Recording Channels:	**320**
Streamer Depth:	**9 meters +/-1.5 meters**
Streamer Length:	**8000 meters**
Record Length:	**14.336 seconds**
Sample Interval:	**2 milliseconds**
Nominal Fold:	**106**

PROCESSING SEQUENCE

- **Data processing performed by: CGG Canada Services Ltd.**
- **Processing completed January 2000**
- **Swell noise removal**
- **Spherical divergence correction**
- **Shot domain F-K filter**
- **Convert source signature to minimum phase equivalent**
- **Deconvolution – single gate, shot average, 250 ms operator, 4 ms gap**
- **Predictive deconvolution – 240 ms operator, 24 ms gap**
- **Trace to trace editing**
- **Resample to 4ms - record length 11000 ms**
- **Velocity analysis- 2000 m**
- **Radon demultiple – 0-3000 ms**
- **FK demultiple - 2000-11000 ms**
- **Wave equation modeling demultiple – on selected lines**
- **2D Kirchhoff DMO**
- **Velocity analysis - 500 m**
- **Spectral whitening**
- **Stack**
- **Peg leg multiple removal – on selected lines**
- **FX migration (steep dip)**
- **FX deconvolution and AGC**

AVAILABLE DELIVERABLES

- **Raw field data/shot ordered**
- **Raw stack**
- **Raw migration**
- **Processed stack**
- **Processed migration**
- **Stacking velocities (ASCII)**
- **Migration velocities (ASCII)**
- **Post stack navigation –UKOOA**
- **Workstation-ready tapes available in SMT, Landmark, and Geoquest**